THE INFLUENCE OF THE NN^* CHANNEL ON ELASTIC NN SCATTERING

Thesis by

Harvey Kenneth Shepard

In Partial Fulfillment of the Requirements

For the Degree of

Doctor of Philosophy

California Institute of Technology

Pasadena, California

1966

(Submitted December 14, 1965)

ACKNOWLEDGEMENTS

I wish to thank Professor Steven Frautschi for suggesting the study of this topic and for his continuing encouragement and gentle guidance during the course of this work. Among the many others who have been of help in some aspect of this research are E. Abers, L. Balazs, J. Blue, Y. Dothan, R. Gerbracht, R. Griffith, Y. Hara, B. Kayser, R.S. McKean, A. Scotti, W.G. Wagner, and G. Zweig. I am deeply grateful to the National Science Foundation for their financial support as an NSF Predoctoral Fellow during part of this work, and I am also indebted to the U.S. Atomic Energy Commission for providing funds to cover computing costs.

Finally, however inadequately, I must thank my wife Nancy for her understanding and loving support.

ABSTRACT

The problem of two channels, NN and NN^*, coupled through unitarity, is studied to see whether sizable peaks can be produced in elastic nucleon-nucleon scattering due to the opening of a strongly coupled inelastic channel. One-pion-exchange (OPE) interactions are calculated to estimate the $NN^* \longrightarrow NN^*$ and $NN \longrightarrow NN^*$ amplitudes. The OPE production amplitudes are used as the sole dynamical input to drive the multichannel ND^{-1} equations in the determinental approximation, and the effect on the $J = 2+ \ (^1D_2)$ elastic NN scattering amplitude is studied as the width of the unstable N^* and strength of coupling to the inelastic channel are varied. A cusp-type enhancement appears in the NN channel near the NN^* threshold but for the known value of the N^* width the cusp is so "wooly" that any resulting elastic peak is likely to be too broad and diminished in height to be experimentally prominent. A brief survey of current experimental knowledge of the real part of the $^1D_2$ NN phase shift near the NN^* threshold is given, and the values are found to be much smaller than the nearly "resonant" phase shifts predicted by the coupled channel model.

TABLE OF CONTENTS

I. INTRODUCTION

After much work in single channel dynamical calculations, there has been increasing effort within the last four years to study the effects of higher channels which are coupled through unitarity to the lower energy elastic scattering processes. The most ambitious attempts have been in the πN problem where the $\pi\pi N$ channel has been included, usually in some approximate way via a pseudo-two-particle ρN or πN^* channel[1-8]. Although the calculations are not quantitatively convincing it does seem clear that inclusion of these higher channels may help to explain the second and third pion-nucleon resonances. From this work and other simple models which have been studied it is evident that the existence of such inelastic channels may act to produce an enhancement in the elastic scattering amplitudes (and cross-section) at energies near and even below the threshold where the inelastic scattering can physically occur. Experimentally, many resonances are found to lie close to the threshold for an inelastic process. Even if this association with thresholds proves accidental, one can speculate that the succession of resonances seen in the πN and $\pi\pi$ systems as higher energies are explored can be explained by including more and more of the inelastic channels which becomes accessible as the energy is increased.

Let us list briefly some of the ways a higher energy channel can cause an enhancement in a lower coupled channel[9]:

1. Threshold Effects (Cusps, Ball-Frazer mechanism)[3,4,10,11 12]. Here

the effect is primarily kinematical and occurs very near to the energy where the inelastic channel opens up. If the inelastic channel contains an unstable particle (and thus the channel is really a three- or more-particle channel, the cusp can become rounded (a so-called "wooly" cusp) and the enhancement smeared over a broader region. Cusps are most prominent when the particles in the inelastic channel are produced in a low orbital angular momentum state (viz. $\ell = 0$).* The prominence of the cusp (i.e., whether it is observable or not) is also dependent on the strength of the coupling between the elastic and inelastic channels. The Ball-Frazer peak is associated with the rapid rise of an inelastic cross-section to its unitarity limit.

2. Strong Inelastic Forces (Cook-Lee Mechanism):[1] If the coupling between channels is strong enough a resonance may appear in the lower elastic channel below the inelastic threshold. Loosely speaking, there is an attraction produced due to a virtual transition from the elastic to the inelastic channel and back again. The system oscillates in a resonance like configuration. By including unitarity in our calculations we allow such a strongly coupled inelastic channel to produce its effect in the elastic channel below the inelastic threshold. Above the inelastic threshold unitarity acts to severely damp the elastic amplitude.

---

* A good example now seems to be available: an S-wave cusp in elastic πN scattering at the ηN threshold. This can be seen in the analysis of P. Auvil and C. Lovelace, Nuovo Cimento 33, 473 (1964).

3. Virtual Bound State Resonance: (Dalitz, Sakurai)[13,14,9]. Here the higher channel, if isolated, contains enough attraction to produce a bound state. But because of the existence of a lower energy channel the "virtual" bound state produced in the higher elastic channel decays and is seen as a resonance in the lower channel, usually not too far below the inelastic threshold*). For this mechanism to operate a fairly weak coupling between channels seems necessary in order to partially isolate the higher channel.

The question naturally arises whether the existence of higher channels in the NN system can produce any effects such as those listed above.

In the present work we shall consider one specific higher channel, the πNN channel, which we shall treat as a pseudo-two-particle state consisting of an N and an N^*, where the N^* is the I = 3/2, $J = 3/2^+$ 1238 MeV πN resonance. Via this isobar model[1,2] we consider only that part of the πNN state in which two of the final particles are produced in a resonant state**). This model of NN^* production has been successful in explaining many of the features of pion production in NN collisions (e.g., momentum spectra of the pion and recoil nucleon, angular correlations between pions and nucleons, etc.) below a couple of BeV[15]. In our actual dynamical calculations we shall partially include the true three-body nature of the state by use of a phase space factor which allows for the width(and hence instability)

---

* An example of this type of resonance is the interpretation of the $\pi\Lambda$ (Y_1^*) resonance as a bound state of the $\bar{K}N$ channel. See, for example, reference 13.

** We will ignore the error introduced by not anti-symmetrizing with respect to the two nucleons in the final state.

of the N^* [11]. Most of the formalism we shall use has been fully discussed in references 1 and 2.

Besides the fact that NN^* production is prominent experimentally this particular inelastic channel was chosen for study for several other reasons. Because of the sizable width of the N^*, approximately 125 MeV full width at half-maximum, one expects that "force" diagrams such as Figures 1(a) and 1(b) below

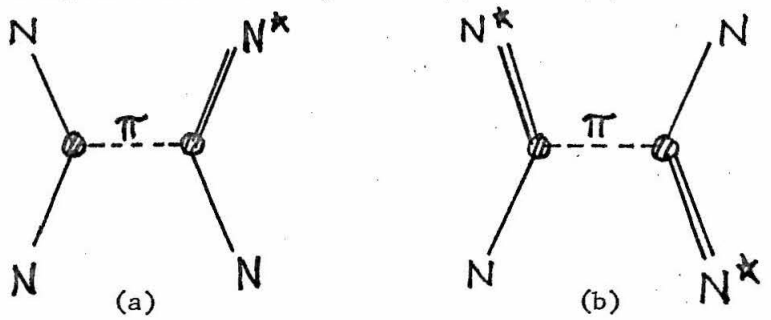

One Pion Exchange (OPE) Interactions in
(a) $N + N \rightarrow N + N^*$ and (b) $N + N^* \rightarrow N + N^*$

Figure 1

would make a large contribution due to the large coupling at the πNN^* vertex. (A large coupling between channels might suggest that mechanism (2) discussed above could produce an enhancement in the elastic NN channel.)

Diagram 1(b) also contains a cut in the physical region [running from $S = 2(M^{*2} + M^2) - \mu^2$ to $S = (M^{*2} - M^2)^2/\mu^2$, where M = nucleon mass = 938 MeV, $M^* = N^*$ mass = 1238 MeV, μ = pion mass = = 139 MeV] which, as noted by Peierls[16] can sometimes produce peaks in elastic cross-sections*). However, such a peak is usually not

---

* A more careful examination of specific cases has shown that these peaks may not be present. See, for example, C. Goebel, Phys. Rev. Letters 13, 143 (1964).

confined to a single J, P, I state and has a shape and an asymmetry different than a resonance-like Breit-Wigner distribution.

Experimentally, there are no known resonances in NN scattering. (There is, of course, a bound state - the deuteron.) Neither the total nor the differential cross-sections show any strong peaking below 1 BeV. However, several of those who have attempted to phenomenologically describe the data find some enhancement in the I = 1 state near a lab energy of 600 MeV. For example, in Fig. 2 below, we have plotted $\frac{p^2}{(\hbar c)^2}\frac{d\sigma}{d\Omega}$ $(\theta_{CM} = \pi/2)$ vs. lab kinetic energy for the case of proton-proton scattering (which is pure I = 1). The data is taken from Table A2 in Wilson's book on the NN interaction[17]. Although the 90^o (CM) scattering does diminish the contribution from some odd ℓ states both even and odd orbital angular momenta contribute, and we cannot simply isolate the enhancement to a specific state of angular momentum and parity*). The proposed enhancement occurs at an energy near or slightly below the threshold for the inelastic process $N + N \rightarrow N + N^*$ (a strong reason for studying this channel). This reaction only can occur in the I = 1 state (where the N^* is the I = 3/2 isobar).

---

* In spinless scattering since $P_\ell(\pi/2) = 0$ for odd ℓ's, only even ℓ's are present at $\theta_{CM} = \pi/2$. But for pp scattering, using the notation of reference 18, although $M_{11}(\pi/2) = 0$, $M_{1-1}(\pi/2) = 0$, $M_{00}(\pi/2) = 0$ both $M_{10}(\pi/2)$ and $M_{01}(\pi/2)$ are non zero and contain odd ℓ states.

Figure 2

$p^2 \frac{d\sigma}{d\Omega}$ for proton-proton scattering at 90^o c.m.

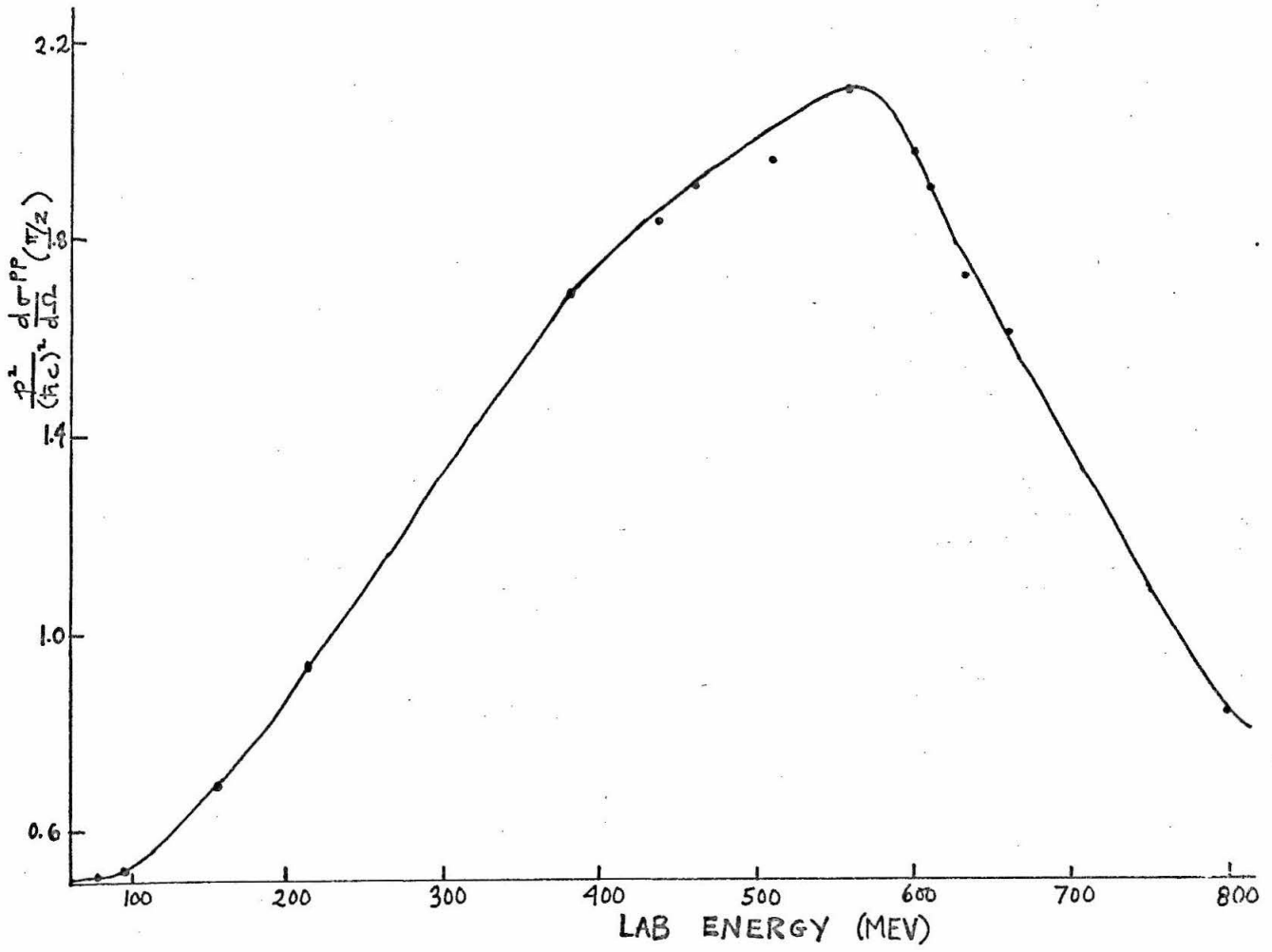
2.2
1.8
1.4
1.0
0.6
$\frac{p^2}{(\hbar c)^2}\frac{d\sigma^{pp}}{d\Omega}(\pi/2)$
100
200
300
400
500
600
700
800
LAB ENERGY (MEV)

Our ideas on cusps also encourage us to look for states in which the new channel is in a low angular momentum configuration, preferably L = 0. The nucleon has $J^P = 1/2^+$; the three-three resonance treated as an unstable particle has $J^P = 3/2^+$. Therefore, putting the NN^* in an L = 0 state requires $|NN^*\rangle$ be in a P = +, total J = 1 or 2 state. To couple to $|NN\rangle$ with I = 1, P = +, the generalized Pauli principle forces the NN state to have S = 0, L = 2 and thus J = 2.

So with $L_{NN^*} = 0$ the pertinent channel spin-parity is $J^P = 2^+$, I = 1 with the NN in a $^1D_2$ state. Although we shall briefly examine some of the forces in other J^P states by looking at the OPE Born amplitudes, we shall ultimately perform detailed dynamical calculations only in this one state.

Above 400 MeV a phase shift analysis of proton-proton scattering is greatly complicated by the presence of inelastic scattering which causes the phase shifts to become complex; i.e., not purely real. Most of the work done in the 600 MeV region has been performed in the U.S.S.R. using the 6-meter synchrocyclotron in Dubna. For pp, neglecting inelasticity and using the requirement of unitarity, five independent experiments*) performed at all angles are sufficient

---

* Briefly, we can list the kinds of experiments from which to choose.
1. Single scattering experiments to measure the unpolarized differential cross-section.
2. Double scattering experiments to measure the polarization P.
3. Triple scattering experiments to measure R (related to the rotation of the polarization vector in the plane of the second scattering), A, D (describes the extent to which the second scattering depolarizes an initially polarized beam), or spin correlation experiments in which one measures the polarizations of the recoiling target usually in correlation with the polarization of the outgoing nucleon. At one energy and angle there are nine independent quantities which can be measured. For more details, see refs. 17, 18, and 19.

to determine M the scattering matrix at all angles[18]. This however, is only academic interest even aside from inelasticity, for in practice, one takes a number of pieces of (hopefully reliable) experimental data and attempts to fit with several (often variable) parameters and then uses some goodness of fit criteria (commonly chi-square) to search for acceptable solutions. Usually several such solutions are found and other types of data (e.g., data on $p + p \rightarrow \pi^+ + d$) or auxiliary requirements must be used to reduce the number of satisfactory solutions.[18]

In the so-called modified phase shift analysis the use of the one-pion exchange (OPE) contribution for high angular momentum states allows one to get as good chi-squares using many fewer parameters (for example at 310 MeV one can get the same χ^2 using nine parameters and OPE as using fourteen parameters with no OPE)[19].

In making a phase shift analysis of pp scattering at 657 MeV, Azhgirei et al.[20] assume one meson exchange for $\ell \geq 5$ states. They assume the phase shifts are complex ($\Delta = \delta + i\gamma$) and use absorption coefficients (averaged over J) for the $^3P_{0,1,2}$, $^3F_{2,3}$, and $^1D_2$ states which are obtained from the experimental cross-sections for the inelastic processes $p + p \rightarrow \pi^+ + d$, $p + p \rightarrow \pi^+ + n + p$, $p + p \rightarrow \pi^0 + p + p$. They used 45 experimental quantities and determined twelve parameters, nine phase shifts ($\ell \leq 4$) and three absorption coefficients. With a $\chi^2 = 36.7$ (For a good fit χ^2 = number of data points - number of parameters) they find

$$\delta_{real}(^1D_2) = 11.7^\circ \pm 2.2, \; r_2 = .668 \; (e^{-2\gamma} = r).$$

Using new data on the parameter A they modified their values to $\delta = 8.7 \pm 4.9$, $r_2 = .678$.

Similar analyses (Golovin[21], Zul'karneev and Silin[22], Dzhelepov[23]) also find that Re $\delta_{^1D_2} \approx 10^o$ for lab energies near 600 MeV.

It thus seems reasonably safe to conclude from these analyses, although they are not yet completely satisfactory, that no true resonance exists in the $^1D_2$ pp state. The enhancement which may be present seems more likely to be what we have classed as a threshold or cusp effect.

In this paper we shall study the coupled processes $N + N \to N + N$, $N + N \leftrightarrow N + N^*$, $N + N^* \to N + N^*$ in the isobar approximation treating the N^* as an unstable particle. Ultimately in our dynamical calculations (using the determinental approximation to the multichannel ND^{-1} method) we shall ignore all forces but those due to the inelastic process $N + N \to N + N^*$. And only the longest range part of this interaction, the OPE diagram Fig. 1(a) will be kept. Besides providing the longest range interaction, pion exchange leads to cuts in the partial wave amplitudes lying nearest the physical region . Other particle exchanges were neglected for simplicity and because the relevant effective coupling constants (e.g., for the ρNN^*, ωNN^*, ηNN^* vertices) are not well known, though we could use the SU_6 symmetry scheme to estimate them. It is the inelastic OPE amplitudes which shall drive the system of coupled equations. Our work is clearly related to the strip approximation diagram for NN scattering shown in Figure 3. This diagram would

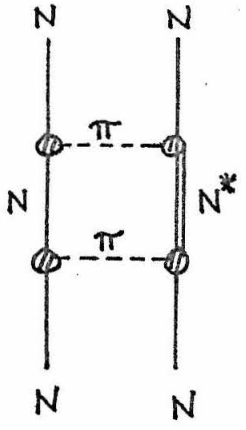

A Strip Approximation Diagram for Nucleon-Nucleon Scattering

Figure 3

correspond to the lowest order term in the solution to the set of coupled unitarity equations.

The elastic forces from the processes $N + N \to N + N$ (e.g., forces due to exchange of π, ρ, ω, η,[24]) and $N + N^* \to N + N^*$ (exchange of π, ρ, ...) will be ignored in our dynamical calculations for several reasons.

As we shall see in Sec. II the $NN^* \to NN^*$ elastic forces, at least those given by the diagram of Fig. 1(b), do not seem to contain either very much attraction or repulsion where this is estimated by studying the sign and (non zero) magnitudes of the amplitudes (with momenta divided out) at or near threshold. For this reason, and because of a need to restrict the size and complexity of the problem these NN^* elastic forces were omitted. As will be discussed in Sec. I, to describe elastic $NN^* \to NN^*$ scattering in a state of definite J, P, and I requires in general, a 4 x 4 matrix (i.e., ten independent

amplitudes)*). Since elastic NN scattering in a state of definite J, P, I requires a 2 x 2 matrix (involving two eigenphases and a mixing parameter) for triplet scattering (but only a single amplitude for the S = 0 case), the most general coupled NN, NN^* problem would involve 6 x 6 matrices. Thus, the "two" channel NN, NN^* system really consists of six coupled channels.

Besides the limit on complexity, perhaps the strongest reason for ignoring all elastic forces is just the desire to isolate and study the effect of a production process on an elastic channel coupled to it via the unitarity relations. We thus can study the mechanisms (1) and (2) described above in their purest form without any complications. As Cook and Lee have noted[25] "it is likely in many processes that the "elastic" forces contribute very little to the structure of the elastic amplitude near the thresholds of inelastic channels. It is rather the particular form of the coupling between the amplitudes; i.e., the unitarity relations, which is responsible for the structure."

We shall find that our coupled channel model does predict a cusp type enhancement near the NN^* threshold. However, because of the broad width of the N^*, we find that the cusp in the elastic amplitude becomes rounded and flattened, and diminished in height by the presence of sizable inelasticity. Thus, the peaks predicted by our model would not be very prominent experimentally. However, our model does predict real phase shifts close to 90° and thus disagrees with the experimental

* For small J's (< 2) fewer amplitudes are required. (J = 0 requires 1 and J = 1 requires 6).

data we have cited. We therefore must conclude that important repulsive forces have been omitted from our model.

The influence of the NN^* channel on NN scattering has also been considered by Leung[26] and Coulter et al.,[27] and we shall compare their work and approach with ours in Sec. VII.

The organization of this paper is as follows:

In Section II we describe some general features of the NN, NN^* system; especially the restriction on the number of independent amplitudes imposed by angular momentum, parity, and isotopic spin conservation and time-reversal invariance. Section III contains the calculation of the OPE amplitudes for the diagrams of Fig. 1. The properties of the spin 3/2 N^* state and the πNN^* vertex are reviewed. We then project out partial wave helicity amplitudes and form amplitudes of definite parity. The problem of off-mass-shell terms in the partial wave amplitudes is briefly discussed. The high energy and threshold behavior of the amplitudes are examined. Signs and relative magnitudes of forces in different J^P states are estimated. The analytic structure of the $NN \to NN^*$ partial wave amplitudes is described and the appearance of complex singularities is noted.

In Section IV we state the unitarity relations for partial wave amplitudes in the isobar approximation and give the solution in the form of the multichannel ND^{-1} equations.

Next, (in Section V) we choose proper phase space factors to eliminate kinematical singularities (at least those close to the physical region) and guarantee that our resultant "unitarized" amplitude will have the correct threshold behavior. We discuss and

illustrate the modified phase space factor that we use for the NN^* state. This pseudo-three particle phase-space factor is compared with the approximate form suggested by Nauenberg and Pais[11] in their discussion of wooly cusps. Also in this section we perform the continuation of the $NN \to NN^*$ Born amplitudes to the region between the NN and NN^* thresholds since this will be needed for the dynamical calculations.

In Section VI, we discuss the approximations to be made in our determinental calculation. Detailed questions concerning the choice of subtraction point, the convergence of integrals, the use of a cutoff, and the handling of principal value integrals are explained. Some general properties of the solution are also discussed.

Section VII contains the numerical results of our computer calculations. We examine and plot graphically the dependence of the NN elastic scattering amplitude on the magnitude of the coupling between channels (the size of the inelastic amplitude), the width of the N^*, the choice of subtraction point and the cutoff. The problem of ghosts is briefly discussed. Finally, we summarize the results of our work.

In Section VIII we briefly discuss some possible SU_3 implications of our coupled channel model.

Appendix A summarizes the symbols, notations and relevant kinematics we use, and Appendix B gives many details needed for projecting out the OPE partial wave helicity amplitudes. In Appendix C the problem of complex singularities and anomalous thresholds is examined further.

II. GENERAL FEATURES OF THE NN AND NN^* CHANNELS

In the center of mass the NN threshold is at 1.876 BeV and the NN^* threshold at 2.176 BeV.*). (Later when including the N^* width we shall effectively be allowing the threshold to extend to lower energies.) In terms of T_{lab} the lab kinetic energy of the incident nucleon we have

$$T_{lab} = \frac{W_{CM}^2 - 4M^2}{2M} \qquad \text{(II.1)}$$

and also

$$P_{CM}^2 = \frac{M\, T_{lab}}{2} \qquad \text{(II.2)}$$

where we are using energy units (c = 1). With W_{CM} = 2.176 BeV we find the NN^* threshold occurs at $T_{lab} \cong 646$ MeV.

The general kinematical features of nucleon-nucleon scattering are well-known[28]. Assuming charge independence, parity conservation and time reversal invariance, five independent amplitudes are required for a complete characterization of nucleon-nucleon (or $N\bar{N}$) scattering. The NN state can have either isotopic spin 0 or 1. For a given value of total angular momentum J the two-nucleon system can be in an S = 0 or S = 1 state. Because of the Pauli principle there can be no transitions between the two spin states. For the singlet state (S = 0) we have only L = J and one amplitude characterizes the scattering.

---

* In Appendix A we have summarized the notation and conventions we will be using in our calculations and given a brief review of the kinematics of the reactions $N + N^* \to N + N^*$ and $N + N \to N + N^*$.

If $S = 1$ we have $L = J$ or $L = J \pm 1$. (If $J = 0$ clearly $L = J - 1$ is not present.) For $L = J$, again one amplitude is sufficient since parity conservation forbids transitions to $L = J \pm 1$. If $L = J \pm 1$ we need three amplitudes to describe the transitions $L = J - 1 \rightarrow L = J - 1$, $J + 1 \rightarrow J + 1$, $J - 1 \rightarrow J + 1$ (which is equal to the amplitude for $J + 1 \rightarrow J - 1$ by time-reversal invariance). Hence a total of five independent amplitudes (for $J > 0$) are needed.

The generalized Pauli principle implies that for allowed transitions in N-N scattering $(-1)^{I + L + S} = -1$, and thus for example, fixing the parity and isospin determines the allowed S. Using the relations between amplitudes implied by P, T, and I conservation the same kind of counting procedure as above can also be carried out in the helicity representation[28,29].

Now consider $N + N^* \rightarrow N + N^*$ scattering. Here, the total I is 1 or 2 and hence only the $I = 1$ part of NN^* can couple to an NN state. With a fixed J, we have either $S = 1$ or 2, and because the N and N^* are not identical particles, there can be transitions between the different spin states. And specifying I places no restrictions on allowed values of L or S as it did for the antisymmetrized NN state. With $S = 1$ we can have $L = J$, $J \pm 1$ (assuming $J > 0$), and for $S = 2$, $L = J$, $J \pm 1$, $J \pm 2$ ($J > 1$) are all possible. Hence the states $|S = 1, L = J\rangle$, $|S = 2, L = J\rangle$, $|S = 2, L = J + 2\rangle$, and $|S = 2, L = J - 2\rangle$ all have parity $(-1)^J$ and there may be transitions between any of them. Using time-reversal invariance (e.g., amplitude for $J + 2 \rightarrow J - 2$ equals amplitude for $J - 2 \rightarrow J + 2$) we find we need

ten independent amplitudes to describe elastic NN^* scattering for $P = (-1)^J$. Similarly $|S = 1, L = J + 1\rangle$, $|S = 1, L = J - 1\rangle$, $|S = 2, L = J + 1\rangle$, $|S = 2, L = J - 1\rangle$ all have parity $(-1)^{J-1}$ and again ten independent amplitudes are needed to describe scattering with this parity. So for $J > 1$, a total of twenty independent amplitudes would be needed for a complete characterization of elastic NN^* scattering in a given isotopic spin state. (It is easy to see that for $J = 0$ only $|S = 1, L = 1\rangle$ and $|S = 2, L = 2\rangle$ are allowed, thus requiring one amplitude for each parity; while for $J = 1$ there are six independent amplitudes for each parity.)

Let us perform the same counting of independent amplitudes in terms of a helicity description of each two-particle state (we are talking about the N^* as if it were a stable particle).

Define the partial wave helicity amplitudes $\langle \lambda_4\ \lambda_3 | T^J(W) | \lambda_1\ \lambda_2 \rangle$ for the process $1(N) + 2(N^*) \to 3(N^*) + 4(N)$ by the relations*)

$$d\sigma = \left| f_{\lambda_4\ \lambda_3;\ \lambda_1\ \lambda_2}(\theta,\varphi) \right|^2 d\Omega \qquad \text{(II.3)}$$

$$f_{\lambda_4\ \lambda_3;\ \lambda_1\ \lambda_2}(\theta,\varphi) = \frac{1}{p} \sum_J (2J + 1) \langle \lambda_4\ \lambda_3 | T^J(W) | \lambda_1\ \lambda_2 \rangle \cdot$$

$$\cdot\ e^{i(\lambda-\mu)\varphi}\ d^J_{\lambda\mu}(\theta) \qquad \text{(II.4)}$$

$$(\lambda = \lambda_1 - \lambda_2,\ \mu = \lambda_4 - \lambda_3),$$

---

* See Appendix B and Reference 29 for more details on the helicity formalism.

and in the case of elastic scattering (1 = 4, 2 = 3)

$$\langle \lambda_4\ \lambda_3 | S^J(W) | \lambda_1\ \lambda_2 \rangle = \delta_{\lambda_1\lambda_4}\delta_{\lambda_2\lambda_3} + 2i\langle \lambda_4\ \lambda_3 | T^J(W) | \lambda_1\ \lambda_2 \rangle . \qquad \text{(II.5)}$$

Parity conservation implies

$$\langle -\lambda_4, -\lambda_3 | T^J | -\lambda_1, -\lambda_2 \rangle = \eta_g \langle \lambda_4\ \lambda_3 | T^J | \lambda_1\ \lambda_2 \rangle \qquad \text{(II.6)}$$

$$\text{with } \eta_g = \frac{\eta_3\ \eta_4}{\eta_1\ \eta_2} \quad (-1)^{S_3 + S_4 - S_1 - S_2}$$

where η_i is the intrinsic parity of particle i and S_i its intrinsic spin. Hence, for $NN^* \to NN^*$ we have $\eta_1 = \eta_2 = \eta_3 = \eta_4 = +$ and $S_1 = S_4 = 1/2$, $S_2 = S_3 = 3/2$ and thus $\eta_g = +$.

Time-reversal invariance requires

$$\langle \lambda_4\ \lambda_3 | T^J | \lambda_1\ \lambda_2 \rangle = \langle \lambda_1\ \lambda_2 | T^J | \lambda_4\ \lambda_3 \rangle . \qquad \text{(II.7)}$$

It is now easy to see that between the eight initial states $|1/2\ 3/2\rangle$, $|1/2\ 1/2\rangle$, $|1/2\ -1/2\rangle$, $|1/2\ -3/2\rangle$, $|-1/2\ 3/2\rangle$, $|-1/2\ 1/2\rangle$, $|-1/2\ -1/2\rangle$, $|-1/2\ -3/2\rangle$ and similar eight final states (just replace the ket by a bra vector) only twenty independent amplitudes may be formed which we have defined in the following matrix.

	$\|1/2\ 3/2\rangle$	$\|1/2\ 1/2\rangle$	$\|1/2\ -1/2\rangle$	$\|1/2\ -3/2\rangle$	$\|-1/2\ 3/2\rangle$	$\|-1/2\ 1/2\rangle$	$\|-1/2\ -1/2\rangle$	$\|-1/2\ -3/2\rangle$
$\langle 1/2\ 3/2\|$	T^J_1	T^J_2	T^J_3	T^J_4	T^J_5	T^J_6	T^J_7	T^J_8
$\langle 1/2\ 1/2\|$	T^J_2	T^J_9	T^J_{10}	T^J_{11}	T^J_{12}	T^J_{13}	T^J_{14}	T^J_7
$\langle 1/2\ -1/2\|$	T^J_3	T^J_{10}	T^J_{15}	T^J_{16}	T^J_{17}	T^J_{18}	T^J_{13}	T^J_6
$\langle 1/2\ -3/2\|$	T^J_4	T^J_{11}	T^J_{16}	T^J_{19}	T^J_{20}	T^J_{17}	T^J_{12}	T^J_5
$\langle -1/2\ 3/2\|$	T^J_5	T^J_{12}	T^J_{17}	T^J_{20}	T^J_{19}	T^J_{16}	T^J_{11}	T^J_4
$\langle -1/2\ 1/2\|$	T^J_6	T^J_{13}	T^J_{18}	T^J_{17}	T^J_{16}	T^J_{15}	T^J_{10}	T^J_3
$\langle -1/2\ -1/2\|$	T^J_7	T^J_{14}	T^J_{13}	T^J_{12}	T^J_{11}	T^J_{10}	T^J_9	T^J_2
$\langle -1/2\ -3/2\|$	T^J_8	T^J_7	T^J_6	T^J_5	T^J_4	T^J_3	T^J_2	T^J_1

On the sides of the matrix we have listed the initial and final helicity states.

To form helicity amplitudes with a definite parity we follow reference 29 and use the relation

$$P|JM;\ \lambda_a\ \lambda_b\rangle = \eta_a\eta_b\ (-1)^{J-S_a-S_b}\ |JM;\ -\lambda_a,\ -\lambda_b\rangle\ . \qquad \text{(II.8)}$$

Thus, we construct normalized NN^* states $\frac{1}{\sqrt{2}}\ (|\lambda_a\ \lambda_b\rangle \pm |-\lambda_a,\ -\lambda_b\rangle)$ which have parity $\pm\ (-1)^J$.

Now, we can form scattering matrices for elastic NN^* scattering in states of definite parity (we have used Eqs. (II.6) and (II.7) and the definitions in the last matrix.

	$\frac{1}{\sqrt{2}}(\lvert 1/2\ 3/2\rangle + \lvert -1/2\ -3/2\rangle)$	$\frac{1}{\sqrt{2}}(\lvert 1/2\ 1/2\rangle + \lvert -1/2\ -1/2\rangle)$	$\frac{1}{\sqrt{2}}(\lvert 1/2\ -1/2\rangle + \lvert -1/2\ 1/2\rangle)$	$\frac{1}{\sqrt{2}}(\lvert 1/2\ -3/2\rangle + \lvert -1/2\ 3/2\rangle)$
$\frac{1}{\sqrt{2}}(\langle 1/2\ 3/2\rvert + \langle -1/2\ -3/2\rvert)$	$T_1^J + T_8^J$	$T_2^J + T_7^J$	$T_3^J + T_6^J$	$T_4^J + T_5^J$
$\frac{1}{\sqrt{2}}(\langle 1/2\ 1/2\rvert + \langle -1/2\ -1/2\rvert)$	$T_2^J + T_7^J$	$T_9^J + T_{14}^J$	$T_{10}^J + T_{13}^J$	$T_{11}^J + T_{12}^J$
$\frac{1}{\sqrt{2}}(\langle 1/2\ -1/2\rvert + \langle -1/2\ 1/2\rvert)$	$T_3^J + T_6^J$	$T_{10}^J + T_{13}^J$	$T_{15}^J + T_{18}^J$	$T_{16}^J + T_{17}^J$
$\frac{1}{\sqrt{2}}(\langle 1/2\ -3/2\rvert + \langle -1/2\ 3/2\rvert)$	$T_4^J + T_5^J$	$T_{11}^J + T_{12}^J$	$T_{16}^J + T_{17}^J$	$T_{19}^J + T_{20}^J$

all of which have parity $+ (-1)^J$

	$\frac{1}{\sqrt{2}}(\lvert 1/2\ 3/2\rangle - \lvert -1/2\ -3/2\rangle)$	$\frac{1}{\sqrt{2}}(\lvert 1/2\ 1/2\rangle - \lvert -1/2\ -1/2\rangle)$	$\frac{1}{\sqrt{2}}(\lvert 1/2\ -1/2\rangle - \lvert -1/2\ 1/2\rangle)$	$\frac{1}{\sqrt{2}}(\lvert 1/2\ -3/2\rangle - \lvert -1/2\ 3/2\rangle)$
$\frac{1}{\sqrt{2}}(\langle 1/2\ 3/2\rvert - \langle -1/2\ -3/2\rvert)$	$T_1^J - T_8^J$	$T_2^J - T_7^J$	$T_3^J - T_6^J$	$T_4^J - T_5^J$
$\frac{1}{\sqrt{2}}(\langle 1/2\ 1/2\rvert - \langle -1/2\ -1/2\rvert)$	$T_2^J - T_7^J$	$T_9^J - T_{14}^J$	$T_{10}^J - T_{13}^J$	$T_{11}^J - T_{12}^J$
$\frac{1}{\sqrt{2}}(\langle 1/2\ -1/2\rvert - \langle -1/2\ 1/2\rvert)$	$T_3^J - T_6^J$	$T_{10}^J - T_{13}^J$	$T_{15}^J - T_{18}^J$	$T_{16}^J - T_{17}^J$
$\frac{1}{\sqrt{2}}(\langle 1/2\ -3/2\rvert - \langle -1/2\ 3/2\rvert)$	$T_4^J - T_5^J$	$T_{11}^J - T_{12}^J$	$T_{16}^J - T_{17}^J$	$T_{19}^J - T_{20}^J$

all of which have parity - $(-1)^J$.

So we verify again that there are ten independent amplitudes required to describe scattering in a state of given J, P, and I.

Now consider $N + N \to N + N^*$ scattering. Time-reversal invariance will relate this process to the reaction $N + N^* \to N + N$ but will not affect our counting of the independent amplitudes in $N + N \to N + N^*$. The channels couple only in the I = 1 state. Hence, the NN system must have L even (P = +) and S = 0 or L odd (P = -) and S = 1 to satisfy the Pauli principle.

In an I = 1 state of given J we have the following possibilities:

With P = +, $|S = 0, L = J\rangle_{NN}$ can couple to the NN^* states $|S = 1, L = J\rangle$, $|S = 2, L = J\rangle$, $|S = 2, L = J + 2\rangle$ and, $|S = 2, L = J - 2\rangle$ so four independent amplitudes are needed (assuming $J > 1$). Note that for even parity all odd J amplitudes will vanish. With P = - and J odd, the NN states $|S = 1, L = J\rangle$, can couple to $|NN^*\rangle$ with $|S = 1, L = J\rangle$, $|S = 2, L = J\rangle$, $|S = 2, L = J + 2\rangle$ and $|S = 2, L = J - 2\rangle$. This again requires four amplitudes (for $J > 1$) or with P = - and J even, the NN states $|S = 1, L = J - 1\rangle$ and $|S = 1, L = J + 1\rangle$ will couple to NN^* states with $|S = 1, L = J - 1\rangle$, $|S = 1, L = J + 1\rangle$, $|S = 2, L = J + 1\rangle$ and $|S = 2, L = J - 1\rangle$. For this latter case, there will be eight independent amplitudes (for $J > 0$). Hence, a total of sixteen independent amplitudes is required for a complete characterization of $N + N \to N + N^*$ (or $N + N^* \to N + N$) scattering (for $J \geq 2$).

In terms of helicity amplitudes for the process $1(N) + 2(N) \to 3(N) + 4(N^*)$ conservation of parity implies (cf Eq. (II.6)

$$\langle -\lambda_3, -\lambda_4 | t^J | -\lambda_1, -\lambda_2 \rangle = - \langle \lambda_3 \lambda_4 | t^J | \lambda_1 \lambda_2 \rangle \qquad \text{(II.9)}$$

and we can form the matrix of scattering amplitudes

$\langle NN^* \vert \diagdown \vert NN \rangle$	$\vert 1/2\ 1/2 \rangle$	$\vert 1/2\ -1/2 \rangle$	$\vert -1/2\ 1/2 \rangle$	$\vert -1/2\ -1/2 \rangle$
$\langle 1/2\ 3/2 \vert$	t_1^J	t_2^J	t_3^J	t_4^J
$\langle 1/2\ 1/2 \vert$	t_5^J	t_6^J	t_7^J	t_8^J
$\langle 1/2\ -1/2 \vert$	t_9^J	t_{10}^J	t_{11}^J	t_{12}^J
$\langle 1/2\ -3/2 \vert$	t_{13}^J	t_{14}^J	t_{15}^J	t_{16}^J
$\langle -1/2\ 3/2 \vert$	$-t_{16}^J$	$-t_{15}^J$	$-t_{14}^J$	$-t_{13}^J$
$\langle -1/2\ 1/2 \vert$	$-t_{12}^J$	$-t_{11}^J$	$-t_{10}^J$	$-t_9^J$
$\langle -1/2\ -1/2 \vert$	$-t_8^J$	$-t_7^J$	$-t_6^J$	$-t_5^J$
$\langle -1/2\ -3/2 \vert$	$-t_4^J$	$-t_3^J$	$-t_2^J$	$-t_1^J$

or in terms of amplitudes of definite parity we have

A. For $P = + (-1)^J = - (-1)^{J-1}$

$\langle NN^* \vert \diagdown \vert NN\rangle$	$\frac{1}{\sqrt{2}}(\vert 1/2\ 1/2\rangle - \vert -1/2\ -1/2\rangle)$	$\frac{1}{\sqrt{2}}(\vert 1/2\ -1/2\ - \vert -1/2\ 1/2\rangle)$
$\frac{1}{\sqrt{2}}(\langle 1/2\ 3/2\vert + \langle -1/2\ -3/2\vert)$	$t_1^J - t_4^J$	$t_2^J - t_3^J$
$\frac{1}{\sqrt{2}}(\langle 1/2\ 1/2\vert + \langle -1/2\ -1/2\vert)$	$t_5^J - t_8^J$	$t_6^J - t_7^J$
$\frac{1}{\sqrt{2}}(\langle 1/2\ -1/2 + \langle -1/2\ 1/2\vert)$	$t_9^J - t_{12}^J$	$t_{10}^J - t_{11}^J$
$\frac{1}{\sqrt{2}}(\langle 1/2\ -3/2\vert + \langle -1/2\ 3/2\vert)$	$t_{13}^J - t_{16}^J$	$t_{14}^J - t_{15}^J$

and B. for $P = - (-1)^J = + (-1)^{J-1}$

$\langle NN^* \vert \diagdown \vert NN\rangle$	$\frac{1}{\sqrt{2}}(\vert 1/2\ 1/2\rangle + \vert -1/2\ -1/2\rangle)$	$\frac{1}{\sqrt{2}}(\vert 1/2\ -1/2\rangle + \vert -1/2\ 1/2\rangle)$
$\frac{1}{\sqrt{2}}(\langle 1/2\ 3/2\vert - \langle -1/2\ -3/2\vert)$	$t_1^J + t_4^J$	$t_2^J + t_3^J$
$\frac{1}{\sqrt{2}}(\langle 1/2\ 1/2\ \vert - \langle -1/2\ -1/2\vert)$	$t_5^J + t_8^J$	$t_6^J + t_7^J$
$\frac{1}{\sqrt{2}}(\langle 1/2\ -1/2\vert - \langle -1/2\ 1/2\vert)$	$t_9^J + t_{12}^J$	$t_{10}^J + t_{11}^J$
$\frac{1}{\sqrt{2}}(\langle 1/2\ -3/2\vert - \langle -1/2\ 3/2\vert)$	$t_{13}^J + t_{16}^J$	$t_{14}^J + t_{15}^J$

For P = + the only allowed NN state with the proper symmetry is $\frac{1}{\sqrt{2}}$ ($|1/2\ 1/2\rangle$ - $|-1/2\ -1/2\rangle$) and the amplitudes in the second column of case (A) will all vanish leaving only four independent amplitudes. (With I = 1, P = + we must have $S_{NN} = 0$ and it is easy to see physically that $|+1/2\ -1/2\rangle$ and $|-1/2\ 1/2\rangle$ are S = 1 states.) The symmetrization requirement for identical particles also means that for odd J only $\lambda_1 \neq \lambda_2$ is allowed[30]. Thus, for P = -, J odd the first column of case (A) vanishes and we are again left with only four amplitudes as we found earlier by considering allowed L and S values. All of these results will be satisfied by the NN → NN* OPE amplitudes presented in the next section.

Now, we can briefly consider the coupled channel NN, NN* problem. For each parity (and $J \geq 2$) we, in general, have a 6 x 6 scattering matrix, which contains the 2 x 2 elastic NN scattering submatrix and 4 x 4 submatrix for elastic NN* scattering.

$$\begin{array}{c} \\ \langle NN| \\ \langle NN^*| \end{array} \begin{array}{c} \begin{array}{cc} |NN\rangle & |NN^*\rangle \end{array} \\ \begin{pmatrix} NN \to NN & (NN^* \to NN) \\ NN \to NN^* & NN^* \to NN^* \end{pmatrix} \end{array} .$$

For the cases P = +, J even and P = -, J odd (L = J) only one NN state is allowed and the coupled channel scattering matrix reduces to 5 x 5.

To give a little more feeling for the states which couple between the two channels we have shown, in Table I, the angular

momentum states of the NN system which couple to the angular momentum states of the NN^* system for some low lying values of the total angular momentum.

Table I

The NN, NN^* Coupled Angular Momentum States for $J \leq 2$

J^P	NN	NN^*
0^+	$^1S_0$	$^5D_0$
0^-	$^3P_0$	$^3P_0$
1^+	$^3S_1$, $^3D_1$	$^3S_1$, $^3D_1$, $^5D_1$
1^-	$^1P_1$	$^5P_1$, $^5F_1$, $^3P_1$
2^+	$^1D_2$	$^5S_2$, $^5D_2$, $^5G_2$, $^3D_2$
2^-	$^3P_2$, $^3F_2$	$^5P_2$, $^5F_2$, $^3P_2$, $^3F_2$

As discussed in the Introduction we shall ultimately be specializing to scattering in the $J = 2^+$ state and thus we in principle will be working with 5 x 5 matrices, containing four independent inelastic ($NN \rightarrow NN^*$) scattering amplitudes. The actual input (of Born amplitudes) to our dynamical problem will look like

$$\left(\begin{array}{c|cccc} 0 & t^{JP}_{1,4-} & t^{JP}_{5,8-} & t^{JP}_{9,12-} & t^{JP}_{13,16-} \\ \hline t^{JP}_{1,4-} & & & & \\ t^{JP}_{5,8-} & & & & \\ t^{JP}_{9,12-} & & 0 & & \\ t^{JP}_{13,16-} & & & & \end{array}\right)$$

where

$$t^{JP}_{i,k\pm} = t^{J}_{i} \pm t^{J}_{k} \ . \qquad \text{(II.10)}$$

since we will be setting all elastic ($NN \to NN$, $NN^{*} \to NN^{*}$) forces equal to zero.

III. THE OPE AMPLITUDES

In this section we shall calculate the OPE amplitudes for the diagrams of Fig. 1, project out partial wave helicity amplitudes for states of definite parity, discuss the threshold and high-energy behavior of these amplitudes and use the threshold values (the "scattering lengths") to estimate the strength of attraction in different J^P states.

The amplitudes will be calculated using Feynman's rules[31]. This will lead to the appearance of some "off-mass-shell" pieces for low J's, terms which have no dynamical cuts and would not have appeared in a strict S-matrix derivation of the amplitude. These terms lead to some difficulties (for the low J states in which they appear) and one is not certain exactly how to handle them. There seem to be good arguments both for keeping and ignoring them. They make our conclusions for the J = 0 and J = 1 states somewhat unreliable.

Before we can calculate the Feynman Amplitudes we must discuss the field theoretic treatment of the spin 3/2N*[32].

The wave functions for spin 3/2 particles will be written as a set of four four-component spinors ψ_μ, $\mu = 0, 1, 2, 3$; the index μ being a tensor index in space time. The ψ_μ satisfy the equations

$$(\not{p} - M^*)\ \psi_\mu = 0 \qquad \text{(III.1)}$$

$$\gamma_\mu\ \psi_\mu = 0\ . \qquad \text{(III.2)}$$

The second equation is a subsidiary condition which removes the spin 1/2 part in ψ_μ. These equations imply the Lorentz condition

$$p_\mu \psi_\mu = 0 \ . \qquad \text{(III.3)}$$

In terms of plane wave solutions of the spin 3/2 equation we have

$$\psi_\mu(x) = \eta \ u_\mu(\vec{p},\lambda) e^{-ip\cdot x} \qquad \text{(III.4)}$$

with the normalization

$$\bar{u}_\mu \ u_\mu = -1$$

and

$$|\eta|^2 = \frac{1}{V}\frac{M^*}{E} \ . \qquad \text{(III.5)}$$

u_μ and $\bar{u}_\mu$ obey the equations

$$(\not{p} - M^*) \ u_\mu(\vec{p}) = 0 \qquad \text{(III.6)}$$

$$\gamma_\mu \ u_\mu = 0 \qquad \text{(III.7)}$$

$$\bar{u}_\mu(\not{p} - M^*) = 0 \qquad \text{(III.8)}$$

$$\bar{u}_\mu \gamma_\mu = 0 \ . \qquad \text{(III.9)}$$

The state vectors corresponding to different helicity states for the spin 3/2 particle are

$$u_\mu(3/2) = \epsilon_\mu(1) \ u \ (1/2) \qquad \text{(III.10a)}$$

$$u_\mu(1/2) = \sqrt{\frac{2}{3}} \ \epsilon_\mu(0) \ u(1/2) + \sqrt{\frac{1}{3}} \ \epsilon_\mu(1) \ u(-1/2) \qquad \text{(III.10b)}$$

$$u_\mu(-1/2) = \sqrt{\frac{1}{3}} \ \epsilon_\mu(-1) \ u(1/2) + \sqrt{\frac{2}{3}} \ \epsilon_\mu(0) \ u(-1/2) \qquad \text{(III.10c)}$$

$$u_\mu(-3/2) = \epsilon_\mu(-1) \ u(-1/2) \qquad \text{(III.10d)}$$

where we are considering the spin 3/2 states a direct product of spin 1 and spin 1/2 states. Definitions and details regarding $u(\pm 1/2)$ and ϵ_μ are found in Appendix B.

We write the πNN and πNN^* couplings (omitting the isotopic spin part) as

$$g\,\bar{\psi}\,\gamma_5\,\varphi\,\psi \tag{III.11}$$

and

$$\frac{G}{M}\,(\varphi\,\partial_\mu\,\bar{\psi} - \bar{\psi}\,\partial_\mu\,\varphi)\,\psi_\mu + \text{h.c.}, \tag{III.12}$$

respectively, (φ = pion field, ψ = nucleon field).

In momentum space these become

$$g\,\bar{u}\,\gamma_5\,u \tag{III.13}$$

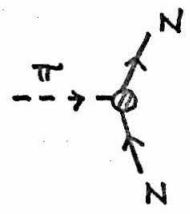

and

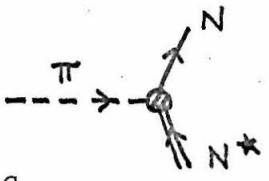

$$\frac{G}{M}\,(p_N + p_\pi)_\mu\,u_\mu\,. \tag{III.14}$$

Using this coupling we determine the effective πNN^* coupling constant, G, by calculating the N^* decay rate (into $N + \pi$) and equating it to the experimental full width at half-maximum, Γ. We find[5]

$$\Gamma = \frac{1}{3\pi}\left(\frac{G}{M}\right)^2 \frac{p_N^{\,3}(E_N + M)}{M^*} \tag{III.15}$$

where

$$E_N = \sqrt{p_N^{\,2} + M^2} \tag{III.16a}$$

$$P_N^2 = \frac{[(M^*)^2 - (M+\mu)^2][(M^*)^2 - (M-\mu)^2]}{4(M^*)^2} . \qquad \text{(III.16b)}$$

Using $M^* = 1238$ MeV, $\Gamma = 125$ MeV, we get

$$\left(\frac{G}{M}\right) = 61.7/\text{BeV}^2 \qquad \text{(III.17)}$$

or

$$G^2 = 54.3.$$

Now, we are ready to calculate the OPE amplitudes (for Fig. 1) using the πNN and πNN^* couplings given in (III.13) and (III.14) above and the conventional rules for Feynman diagrams (as given for example, by Schweber, ref. 31).

First, consider the process $N + N^* \to N + N^*$

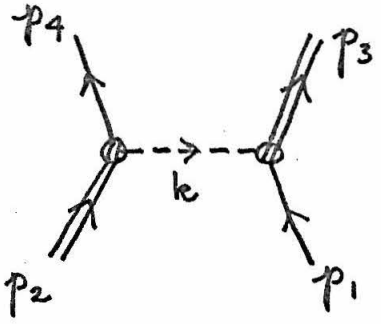

The $N + N^* \to N + N^*$ OPE Interaction

Fig. 4

In momentum space

$$R_{\lambda_4\lambda_3;\lambda_1\lambda_2} = (2\pi)^4 (-i)^2 \, i \frac{M}{E_1} \frac{M^*}{E_3} \left(\frac{G}{M}\right)^2 .$$

$$\cdot \frac{\bar{u}(\vec{p}_4,\lambda_4)\ (k - p_4)_\mu\ u_\mu(\vec{p}_2,\lambda_2)\ \bar{u}_\nu(\vec{p}_3,\lambda_3)(p_1 - k)_\nu\ u(\vec{p}_1,\lambda_1)}{(p_3 - p_1)^2 - \mu^2} \qquad \text{(III.18a)}$$

$$= 4i\ (2\pi)^4 \left(\frac{G}{M}\right)^2 \frac{MM^*}{E_1E_2} \cdot$$

$$\cdot \frac{\bar{u}(\lambda_4)\ (p_4)_\mu\ u_\mu(\lambda_2)\ \bar{u}_\nu(\lambda_3)\ (p_1)_\nu\ u(\lambda_1)}{(p_3 - p_1)^2 - \mu^2} \qquad \text{(III.18b)}$$

where we have used momentum conservation at the vertices and Eq. (B8) to simplify (III.18a). We also have

$$(p_3 - p_1)^2 = M^{*2} + M^2 - 2E_1E_3 - 2q^2 \cos\theta \qquad \text{(III.19)}$$

$$(p_3 - p_1)^2 - \mu^2 = 2q^2 \left(\frac{M^{*2} + M^2 - \mu^2 - 2E_1E_3}{2q^2} - \cos\theta\right)$$

$$\equiv 2q^2\ (A - \cos\theta). \qquad \text{(III.20)}$$

Using equations (III.18b), (III.20), (III.10), (B14,15,16), and (A7 - 12) we may calculate the Feynman amplitude R for any combination of initial and final helicities. (Using parity conservation and time reversal invariance only 20 amplitudes must be calculated. See Section I.)

We next form partial wave helicity amplitudes

$$\langle \lambda_4\ \lambda_3 | R^J | \lambda_1\ \lambda_2 \rangle = \frac{1}{2} \int_{-1}^{1} R^{(x,w)}_{\lambda_4\lambda_3;\lambda_1\lambda_2}\ d^J_{\lambda\mu}(\theta)\ dx \qquad \text{(III.21)}$$

where $x = \cos\theta$ and with our conventions*)

$$\langle \lambda_4\ \lambda_3 | S^J(W) | \lambda_1\ \lambda_2 \rangle = \delta_{\lambda_1\lambda_4}\delta_{\lambda_2\lambda_3} + \frac{2qE_1E_2}{W}\ \frac{1}{(2\pi)^5}\ \langle \lambda_4\ \lambda_3 | R^J | \lambda_1\ \lambda_2 \rangle \tag{III.22}$$

where we are temporarily omitting the isotopic spin part of the amplitude $(\bar{N}^*_k\ \delta_{jk}\ N)\ (\bar{N}\ \delta_{j\ell}\ N^*_\ell)$. Finally, after much tedious calculation, we combine the partial wave helicity amplitudes into amplitudes of definite parity according to the prescription given in Section II. We have listed the results in Appendix B. Only the expressions for T^{JP} when $J \geq 3$ are listed. For smaller J's some of the amplitudes are not present. (We know from Section I that for $J = 0$ there is only one amplitude for each parity and for $J = 1$ there are six amplitudes for each parity.) And when $J < 3$ those partial wave amplitudes which are present contain extra terms, so called off-mass-shell terms**). It would take us too far afield to launch into a thorough

---

*) We may also relate R^J to the T^J of Section I.

$$\langle \lambda_4\ \lambda_3 | T^J | \lambda_1\ \lambda_2 \rangle = \frac{qE_1E_2}{W}\ \frac{-i}{(2\pi)^5}\ \langle \lambda_4\ \lambda_3 | R^J | \lambda_1\ \lambda_2 \rangle .$$

**) In the expressions (writing $t = (p_3 - p_1)^2$)

$$\frac{t}{t - m^2} = \frac{m^2}{t - m^2} + 1$$

$$\frac{t^2}{t - m^2} = \frac{m^4}{t - m^2} + t + m^2 ,$$

etc. Those terms with no denominators on the right-hand side of the equations will produce off-mass-shell terms in the partial wave amplitudes.

discussion of such terms but a few tentative remarks can be made on the basis of some examination of their properties in the present case (no details will be given).

The on-shell ($J \geq 3$) amplitudes are found to have the expected threshold behavior

$$T^{JP} \sim \begin{cases} q^{2(J-2)+1} & P = +(-1)^J \\ q^{2(J-1)+1} & P = -(-1)^J \end{cases}$$

($L = \binom{J-2}{J-1}$ are the lowest orbital momenta which can appear for fixed $J \geq 2$, $P = \pm(-1)^J$ and at threshold $\delta_L \sim q^{2L+1}$.)

Thus, these on-shell amplitudes, if evaluated for $J < 2$, will not have the ordinary $q^{2L_{min}+1}$ threshold behavior, and can even be quite singular at $q = 0$. But the off-shell amplitudes do turn out to have the "proper" threshold behavior (where "proper" includes the fact that for $q^2 = 0$, parity and angular momentum conservation may forbid $L = 0$ in the second order diagram). Another argument in favor of keeping these perturbation theory terms is that they <u>are</u> the result of our field-theoretic calculation (i.e., they are present in the Feynman amplitudes) and, in addition, they often seem to express some physics, at least to second order.

On the other hand, we may argue against keeping the off-mass-shell terms for the following reasons:

1. These terms frequently turn out to have quite divergent high-energy behavior and thus must be damped out anyway before used in a

dynamical calculation.

2. Single particle exchanges generally are a poor approximation for the low partial waves especially when there is absorption present[33].
3. S-matrix theory does not seem to contain such terms and in a dynamical calculation we want to use as our input just the singular part of the interaction.
4. Choosing a different field theoretic coupling for the πNN^* vertex would result in different off-shell terms appearing, so they are ambiguous if nothing else.

Fortunately, in our dynamical calculation we will not be considering a J,P state where such terms are present, but on the basis of the previous arguments one is inclined to favor discarding the off-shell terms when they are present and a dynamical dispersion-theoretic-type calculation is going to be made. In such a calculation, the proper threshold behavior is usually guaranteed by the choice of amplitude or by making suitable subtractions in the dispersion relations.

When we estimate the signs and strengths of forces in the various J, P, I NN^* states by calculating the theoretical values with momentum factors divided out we shall also give the results for the off-shell amplitudes but not take them too seriously.

Before doing this, let us consider the $N + N \rightarrow N + N^*$ OPE amplitudes

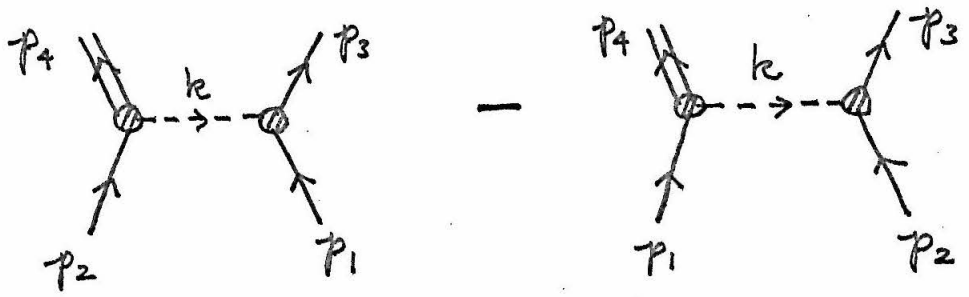

(a) (b)

The $N + N \rightarrow N + N^*$ OPE Interaction

Fig. 5

As the figure symbolically shows, we must form the difference of the amplitudes with particles 1 and 2 interchanged in order to properly antisymmetrize the $NN \rightarrow NN^*$ amplitude.

$$R_{\lambda_3\lambda_4;\lambda_1\lambda_2} = (2\pi)^4 \, (-i)^2 \, i \sqrt{\frac{M^3 M^*}{E_1 E_2 E_3 E_4}} \; g \left(\frac{G}{M}\right) \cdot$$

$$\cdot \left\{ \frac{\bar{u}_\mu(\vec{p}_4,\lambda_4) \; (p_2 + k)_\mu \; u(\vec{p}_2,\lambda_2) \; \bar{u}(\vec{p}_3,\lambda_3) \; \gamma_5 \; u(\vec{p}_1,\lambda_1)}{(p_3 - p_1)^2 - \mu^2} \right.$$

$$\left. - \frac{\bar{u}_\mu(\vec{p}_4,\lambda_4)(p_1 + k)_\mu \; u(\vec{p}_1,\lambda_1) \; \bar{u}(\vec{p}_3,\lambda_3) \; \gamma_5 \; u(\vec{p}_2,\lambda_2)}{(p_3 - p_2)^2 - \mu^2} \right\} \tag{III.23}$$

where

$$(p_3 - p_1)^2 = 2M^2 - 2E_1E_3 - 2pp' \cos\theta \tag{III.24a}$$

$$(p_3 - p_2)^2 = 2M^2 - 2E_1E_3 + 2pp' \cos\theta \tag{III.24b}$$

and

$$(p_3 - p_1)^2 - \mu^2 \equiv 2pp' (z - \cos\theta) \qquad \text{(III.25a)}$$

$$(p_3 - p_2)^2 - \mu^2 \equiv - 2pp' (-z - \cos\theta) \qquad \text{(III.25b)}$$

with

$$z = \left\{ \frac{2M^2 - \mu^2 - 2E_1E_3}{2pp'} \right\} . \qquad \text{(III.26)}$$

Using Eqs. (B-21 - 24) we can calculate R for any set of initial and final helicities and then form partial wave helicity amplitudes according to equation (III.21). Finally, we combine these into amplitudes of definite parity following the description in Sec. I. The results are:

$$t^{JP}_{1,4\pm} = \frac{a}{2\sqrt{2}} \frac{\sqrt{J(J+1)}}{(2J+1)} \frac{1}{p'} \left[Q^{(z)}_{J+1} - Q^{(z)}_{J-1} \right] \left\{ \begin{array}{l} \left[\alpha_1 + \beta_1 z \right] \\ \left[-\beta_1 - \alpha_1 z \right] \end{array} \right. \quad J \text{ even}$$

$$= 0 \quad J \text{ odd.} \qquad \text{(III.27a)}$$

$$t^{JP}_{13,16\pm} = \frac{a}{2\sqrt{2}} \frac{1}{p'} \sqrt{(J-1)(J)(J+1)(J+2)} \left\langle \left[\frac{Q^{(z)}_{J+2}}{(2J+3)(2J+1)} - \frac{2Q^{(z)}_{J}}{(2J+3)(2J-1)} + \right. \right.$$

$$\left. \left. + \frac{Q^{(z)}_{J-2}}{(2J+1)(2J-1)} \right] \left\{ \begin{array}{c} + \beta_2 \\ \alpha_2 \end{array} \right\} \right\rangle \quad J \text{ even}$$

$$= 0 \quad J \text{ odd.} \qquad \text{(III.27b)}$$

$$t^{JP}_{9,12\pm} = - \frac{a}{\sqrt{6}} \frac{\sqrt{J(J+1)}}{(2J+1)} \left[Q^{(z)}_{J+1} - Q^{(z)}_{J-1} \right] \frac{1}{pp'} \quad . \qquad \text{(III.27c)}$$

$$\begin{bmatrix} -\left(\frac{-\beta_2}{M^*}\, p'E_1 + \frac{\alpha_1 p}{2}\right) - z\left(\frac{\beta_1 p}{2} - \frac{\beta_2 pE_4}{M^*}\right) \\ \left(\frac{\alpha_2 p'E_1}{M^*} + \frac{\beta_1 p}{2}\right) + z\left(\frac{\alpha_1 p}{2} + \frac{\alpha_2 pE_4}{M^*}\right) \end{bmatrix} \qquad J \text{ even} \qquad \text{(III.27c)}$$

$= 0 \quad J$ odd .

$$t^{JP}_{5,8\pm} = \frac{a}{\sqrt{6}}\ \frac{1}{pp'} \left\{ Q^{(z)}_J \begin{bmatrix} \left(-\frac{1}{2}\, p\beta_2 - \frac{\alpha_1 p'E_1}{M^*}\right) + \frac{z}{M^*}(-\beta_1 p'E_1 - \alpha_1 pE_4) \\ \qquad + z^2\left(\frac{1}{2}\, p\beta_2 - \beta_1 \frac{pE_4}{M^*}\right) \\ \left(-\frac{1}{2}\, p\alpha_2 + \frac{\beta_1 p'E_1}{M^*}\right) + \frac{z}{M^*}(\alpha_1 p'E_1 + \beta_1 pE_4) \\ \qquad + z^2\left(\frac{1}{2}\, p\alpha_2 + \frac{\alpha_1 pE_4}{M^*}\right) \end{bmatrix} \right.$$

$$\left. - \delta_{J0} \begin{bmatrix} \frac{1}{M^*}(-\beta_1 p'E_1 - \alpha_1 pE_4) + z\left(\frac{1}{2}\, p\, \beta_2 - \beta_1 \frac{pE_4}{M^*}\right) \\ \frac{1}{M^*}(\alpha_1 p'E_1 + \beta_1 pE_4) + z\left(\frac{1}{2}\, p\, \alpha_2 + \frac{\alpha_1\, pE_4}{M^*}\right) \end{bmatrix} \right\} \qquad J \text{ even}$$

$= 0 \quad J$ odd. (III.27d)

$$t^{JP}_{6,7+} = \frac{a}{\sqrt{6}}\ \frac{1}{pp'}\ \frac{\sqrt{J(J+1)}}{(2J+1)} \left[Q^{(z)}_{J+1} - Q^{(z)}_{J-1}\right] \cdot$$

$$\cdot \left[\left(\frac{-\beta_2 p'E_1}{M^*} + \frac{1}{2}\, p\, \alpha_1\right) + z\left(\frac{\beta_1 p}{2} - \frac{\beta_2 pE_4}{M^*}\right) \right] \qquad J \text{ even}$$

$= 0 \quad J$ odd. (III.27e)

$$t^{JP}_{6,7-} = \frac{-a}{\sqrt{6}} \frac{1}{pp'} \frac{\sqrt{J(J+1)}}{(2J+1)} \Bigg\langle \left[Q^{(z)}_{J+1} - Q^{(z)}_{J-1} \right] \cdot$$

$$\cdot \left[\left(- \frac{\alpha_2 p' E_1}{M^*} - \frac{1}{2} p \beta_1 \right) + z \left(\frac{-\alpha_1 p}{2} - \frac{\alpha_2 p E_4}{M^*} \right) \right] +$$

$$+ \delta_{J1} \left(\frac{-\alpha_1 p}{2} - \frac{\alpha_2 p E_4}{M^*} \right) \Bigg\rangle \quad J \text{ odd}$$

$$= 0 \quad J \text{ even.} \qquad \text{(III.27e)}$$

$$t^{JP}_{2,3+} = \frac{a}{2\sqrt{2}} \frac{1}{p'} \left\{ \left[\frac{J Q^{(z)}_{J+1} + (J+1) Q^{(z)}_{J-1}}{2J+1} \right] \left[-\alpha_2 + \beta_2 z \right] \right.$$

$$\left. + Q_J \left[-\beta_2 + \alpha_2 z \right] - \alpha_2 \delta_{J0} \right\} \quad J \text{ even}$$

$$= 0 \quad J \text{ odd.}$$

$$t^{JP}_{2,3-} = \frac{-a}{2\sqrt{2}} \frac{1}{p'} \left\{ \left[\frac{J Q^{(z)}_{J+1} + (J+1) Q^{(z)}_{J-1}}{2J+1} \right] \left[-\beta_2 + \alpha_2 z \right] \right.$$

$$\left. - \alpha_2 \frac{2}{3} \delta_{J1} + Q^{(z)}_J \left[-\alpha_2 + \beta_2 z \right] \right\} \quad J \text{ odd}$$

$$= 0 \quad J \text{ even .} \qquad \text{(III.27f)}$$

$$t^{JP}_{14,15+} = + \frac{1}{2\sqrt{2}} \frac{a}{p'} \sqrt{(J-1)(J+2)} \cdot$$

$$\cdot \left\{ \left[\frac{-(J+1) Q^{(z)}_{J-2}}{(2J-1)(2J+1)} + \frac{3 Q_J(z)}{(2J-1)(2J+3)} + \frac{J Q_{J+2}(z)}{(2J+1)(2J+3)} \right] \beta_1 \right.$$

$$+ \left[\frac{-Q^{(z)}_{J-1} + Q^{(z)}_{J+1}}{2J+1} \right] \alpha_1 \Bigg\} \qquad J \text{ even}$$

$$= 0 \qquad J \text{ odd.}$$

$$t^{JP}_{14,15-} = + \frac{1}{2\sqrt{2}} \frac{a}{p'} \sqrt{(J-1)(J+2)} \cdot$$

$$\cdot \left\{ \left[\frac{-(J+1)Q^{(z)}_{J-2}}{(2J-1)(2J+1)} + \frac{3\,Q_J(z)}{(2J-1)(2J+3)} + \frac{J\,Q_{J+2}(z)}{(2J+1)(2J+3)} \right] \alpha_1 \right.$$

$$\left. + \left[\frac{-Q_{J-1}(z) + Q_{J+1}(z)}{(2J+1)} \right] \beta_1 \right\} \qquad J \text{ odd}$$

$$= 0 \qquad J \text{ even.} \qquad \text{(III.27g)}$$

$$t^{JP}_{10,11+} = + \frac{a}{\sqrt{6}} \frac{1}{pp'} \left\{ \left[\frac{JQ^{(z)}_{J+1} + (J+1)Q^{(z)}_{J-1}}{2J+1} \right] \left[\left(\frac{1}{2} p\, \alpha_2 - \frac{\beta_1 p' E_1}{M^*} \right) + \right. \right.$$

$$\left. + z \left(\frac{1}{2} p\, \beta_2 - \frac{\beta_1 p E_4}{M^*} \right) \right]$$

$$+ Q^{(z)}_J \left[\left(-\frac{1}{2} p\, \beta_2 - \frac{\alpha_1}{M^*} p' E_1 \right) + z \left(-\frac{1}{2} p\, \alpha_2 - \frac{\alpha_1}{M^*} p E_4 \right) \right]$$

$$\left. + \delta_{J0} \left[\frac{1}{2} p\, \alpha_2 + \frac{\alpha_1 p E_4}{M^*} \right] \right\} \qquad J \text{ even}$$

$$= 0 \quad J \text{ odd.}$$

$$t^{JP}_{10,11-} = + \frac{a}{\sqrt{6}} \frac{1}{pp'} \left\{ \left[\frac{JQ^{(z)}_{J+1} + (J+1)Q^{(z)}_{J-1}}{2J+1} \right] \left[\left(-\frac{1}{2} p\, \beta_2 - \frac{\alpha_1 p' E_1}{M^*} \right) + \right. \right.$$

$$\left. + z \left(-\frac{1}{2} p\, \alpha_2 - \frac{\alpha_1 p E_4}{M^*} \right) \right]$$

$$+ \frac{2}{3}\delta_{J1}\left[\frac{1}{2}\,p\,\alpha_2 + \frac{\alpha_1 p E_4}{M^*}\right]$$

$$+ Q_J^{(z)}\left[\left(\frac{1}{2}\,p\,\alpha_2 - \frac{\beta_1 p' E_1}{M^*}\right) + z\left(\frac{1}{2}\,p\,\beta_2 - \frac{\beta_1}{M^*}\,p\,E_4\right)\right]\Bigg\} \qquad J \text{ odd}$$

$$= 0 \qquad J \text{ even}. \qquad \text{(III.27h)}$$

where

$$a = \frac{-1}{4\pi}\,\frac{2}{3}\,\sqrt{6}\;g\,\frac{G}{M}\,\sqrt{pp'}\,\frac{(E_1 + M)\sqrt{(E_3 + M)(E_4 + M^*)}}{W} \qquad \text{(III.28a)}$$

$$\alpha_{1,2} = \frac{2p}{E_1 + M}\left[1 \pm \frac{p'^2}{(E_3 + M)(E_4 + M^*)}\right] \qquad \text{(III.28b)}$$

$$\beta_{1,2} = 2p'\left[\pm\frac{1}{E_3 + M} + \frac{p^2}{(E_1 + M)^2 (E_4 + M^*)}\right] \qquad \text{(III.28c)}$$

and an i spin factor of $-2/3\ \sqrt{6}$ has been included*) in a.

We have chosen the phases so that our inelastic amplitudes are real (which will make our Born input real and symmetric) and as we shall see later, the results of our dynamical calculation are independent of the sign of the inelastic amplitudes. The partial wave amplitudes listed above are valid for all J and we note that off-shell pieces only appear for J = 0 and 1, and thus are not present in $J = 2^+$,

---

* The i spin amplitude is $(\bar{N}\,\tau_k\,N)\,(\bar{N}_j^*\,\delta_{jk}\,N)$.

the state for which we make dynamical calculations*).

There is another $NN^* \to NN^*$ OPE diagram which we have omitted from our discussion**)

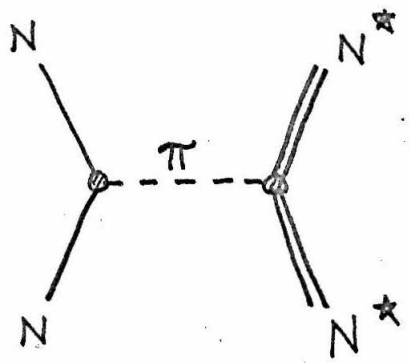

An $N + N^* \to N + N^*$ OPE Diagram which has been Neglected

Fig. 6

The reasons for choosing to calculate the amplitude for the diagram of Fig. 4 but not that of Fig. 6 are principally practical ones with only limited theoretical justification. Probably most important is the fact that we have almost no experimental knowledge of the $\pi N^* N^*$ vertex though we could estimate an effective $\pi N^* N^*$ coupling constant using SU_6.

---

* Our difficulty with off-shell pieces may be related to the phenomenon discussed by S. Mandelstam, Nuovo Cimento 30, 1113 (1963), of extra terms which are present in perturbation amplitudes but which will not be present if sufficient Reggeization, including that of the external particles, is performed.

** Both Fig. 6 and Fig. 4 represent pieces, perhaps partially overlapping, of the complete $NN\pi \to NN\pi$ interaction.

On the theoretical side, since Fig. 6 contains no unstable vertices, there will be no force cut which runs into the physical region*) as there was for Fig. 4, and thus, no opportunity for a Peierls type enhancement (see the Introduction). In any case, in our actual dynamical calculation all elastic forces are omitted so naturally Fig. 6 will also not be included.

Properties of the OPE Amplitudes

Now, let us go back to the OPE partial wave helicity amplitudes we have calculated and briefly discuss their threshold and high-energy behavior. After a great deal of tedious algebra and using the relation

$$Q_\ell(x) \xrightarrow[x \to 1]{} \frac{1}{2} \ell n \frac{2}{x - 1} - \sum_{n=1}^{\ell} \frac{1}{n} \qquad \text{(III.29)}$$

we find for the large W behavior of the $NN^* \to NN^*$ partial wave amplitudes the results summarized in the following table, which gives the energy dependence of the leading term for $W \to \infty$ $(S = W^2)$.

---

* The cut stops at $S = (M^* + M)^2 - \mu^2/2$.

Table II

The Energy Dependence of the Elastic NN^* OPE Amplitudes in the Limit

$W \to \infty \quad (S = W^2)$

	J = 0	J = 1	J = 2	J > 2
T_1^J		Const	Const	Const
T_2^J		$\sqrt{S}$	$\sqrt{S}$	$1/\sqrt{S}$
T_3^J		S	S	$\ell nS/S$
T_4^J			$\sqrt{S}$	$1/\sqrt{S}$
T_5^J			$\sqrt{S}$	$\sqrt{S}$
T_6^J		S	S	Const
T_7^J		$S\sqrt{S}$	$S\sqrt{S}$	$1/\sqrt{S}$
T_8^J		S	S	$\ell nS/S$
T_9^J	S	Const	S	$\ell nS/S$
T_{10}^J		$S\sqrt{S}$	$S\sqrt{S}$	$1/\sqrt{S}$

	J = 0	J = 1	J = 2	J > 2
T_{11}^J			S	Const
T_{12}^J			S	Const
T_{13}^J		$S\sqrt{S}$	$S\sqrt{S}$	$1/\sqrt{S}$
T_{14}^J	S^2	S^2	S^2	$\ell nS/S$
T_{15}^J		S^2	S^2	Const
T_{16}^J			$S\sqrt{S}$	$\sqrt{S}$
T_{17}^J			$\sqrt{S}$	$1/\sqrt{S}$
T_{18}^J		S	S	$\ell nS/S$
T_{19}^J			S	S
T_{20}^J			Const	$\ell nS/S$

In this Table the J = 0, 1, 2 columns correspond to the amplitudes with off-mass-shell terms included. For J > 2 there are no off-shell pieces. (Some of the amplitudes in the J > 2 column may be missing a factor of ℓn S.)

As mentioned earlier we note that the low J off-shell ampli-

tudes tend to violate the unitarity limit ($T^J \sim$ const) very badly while most of the on-shell ($J > 2$) amplitudes are reasonably behaved for large W.*) Before these badly divergent amplitudes could be used in any dynamical calculation one would have to damp them in some way; e.g., by use of a form factor modification at the vertices (although the expressions usually proposed do not seem theoretically justified since they imply the existence of low mass intermediate states which do not exist) or by some Regge-type cutoff.

Now, let us examine the threshold behavior of the elastic $NN^* \to NN^*$ amplitudes and from this make some crude estimate of the sign and strength of the forces in different J^P states.

Using the limit

$$Q_\ell^{(x)} \xrightarrow[x \to 0]{} \frac{\ell!}{(2\ell+1)!!}\left(\frac{1}{x}\right)^{\ell+1} \qquad \text{(III.30)}$$

We evaluated the amplitudes of the matrices representing elastic NN^* scattering for definite J^P states in the limit $q^2 \to 0$, keeping the lowest order term in q^2, and then diagonalized these real symmetric matrices (which are 4×4 for $J \geq 2$). Since we do not usually find high J resonances appearing in elementary particle

---

* It is interesting to note that the $J > 2$ helicity amplitudes obey the heuristic rule $T^J \sim (1/S)\ (\sqrt{S})^{\lambda+\mu}$ for large S (modulo a possible factor of $\ell n S$. The behavior of the low J off-shell amplitudes may also be predicted by determining the u dependence (u = crossed momentum transfer = $(p_3 - p_1)^2$) of the helicity amplitudes before a partial wave expansion is made.

interactions we only examined the OPE forces in lower J states ($J \leq 4$). The results are listed below in Table III, where the momentum dependence of $\frac{1}{q} T^{JP}$ is given in parentheses following the J^P (in this calculation the value $G^2 = 43$ corresponding to $\Gamma_{N^*} = 100$ MeV was used).

Table III

Eigenvalues of the Elastic NN^* OPE Born Amplitudes Evaluated at Threshold for States of Definite J, Parity, and I-Spin

J^P	Eigenvalues I = 2	I = 1	J^P	Eigenvalues I = 2	I = 1
$0^+_{off}(q^4)$	1080	- 359	$0^-_{off}(q^2)$	- 170	56.4
$1^+_{off}(q^2)$	64.7 .00612 - 105	- 21.6 -.00204 34.9	$1^-_{off}(q^2)$	152 20.7 - 2.86	- 50.7 - 6.90 .954
$2^+_{off}(q^2)$	145 .00300 -.0125 - 24.8	- 48.2 -.00100 .00417 8.27	$2^-_{off}(q^2)$	.00474 .000628 1.05×10^{-7} - 79.0	-.00158 -.000209 -3.49×10^{-8} 26.3
$2^+_{on}(q^0)$	8.43 .0659 -.00354 -.0380	- 2.81 -.0220 .00118 .0127	$2^-_{on}(q^2)$	.841 -.0354 -.342 - 79.3	-.280 .0119 .114 26.4
$3^+(q^4)$	213 -.866 - 2.85 - 659	- 70.9 .288 .951 220	$3^-(q^2)$	79.7 .567 -.00452 -.433	- 26.6 -.189 .00150 .144
$4^+(q^4)$	905 6.14 -.0291 - 5.24	- 302 - 2.05 .00969 1.75	$4^-(q^6)$	3750 325 - 106 - 7600	- 1250 - 108 35.2 2540

The subscripts "on" and "off" refer to on- and off-shell amplitudes. It is interesting to note that for $J = 1^+$ and 2^+ the off-shell ampli-

tudes have no L = 0 terms for $q^2 = 0$.

These diagonalized threshold values can be used as a crude qualitative guide to the attraction and repulsion produced by the OPE potential in a way similar to that in which for a single channel case the Born approximation scattering length tells us the sign and approximate magnitude of the phase shift and hence the sign and strength of the potential[34]. (For this connection to be valid, the potential must be relatively weak, at least too weak to produce a bound state.)

In our case where we have more than one elastic channel and thus can have both attractive and repulsive "scattering lengths" for the same J^P, the interpretation becomes much more ambiguous and because of the difficulties associated with off-shell amplitudes the results for low J states are somewhat in doubt. (But note that 2^-_{on} and 2^-_{off} values are quite similar.) With all of these qualifications we may still try to draw some qualitative conclusions from Table III. For the coupled NN, $N\overline{N}^*$ problem we consider only the I = 1 column and look for states with strong attractive forces (with our definitions this corresponds to positive entries in the table). For I = 1 we find possible attraction in the states 0^-, 1^+, 2^-, 3^+, 4^- (note the alternating parities) and repulsion in 0^+, $1^\pm$, 2^+, $3^\pm$, 4^+. (Attraction in I = 1 corresponds to repulsion in I = 2 and vice versa since the signs are opposite*). In those states with sizable

---

* Very crudely, if all attractions indicated a bound state or resonance we might speculate that we have two series of rotational levels; I = 2: 0^+, 2^+, 4^+; I = 1: 0^-, 2^-, 4^- .

attraction, the NN^* OPE elastic force should probably be included in any multichannel calculation. But in states with (mild) repulsion or only weak attraction we might be justified in ignoring this elastic force. This seems to be the case for the $J^P = 2^+$ state in which we are especially interested. Also, some further investigation of the $J = 2^+$, $I = 1$ amplitudes showed that they remained rather small (i.e., much below their unitarity limit) and repulsive in a region above threshold. As discussed in the introduction we tend to concentrate our attention on values of J^P which allow the NN^* to be in an orbital $L = 0$ state since that is when threshold and cusp effects are most prominent. And we look for states in which either or both the elastic $NN^* \to NN^*$ force seems very attractive or the $NN \to NN^*$ amplitudes rise quickly from threshold to a value close to their unitarity limit. Hence, we next examined the threshold behavior of the inelastic amplitude(s). We first verified that our amplitudes (including off-shell pieces) satisfied the usual threshold momentum dependence

$$\frac{1}{\sqrt{pp'}}\, t^{JP} \sim (p)^{(L_{NN})_{min}} (p')^{(L_{NN^*})_{min}} \qquad \text{(III.31a)}$$

which for $J \geq 2$ becomes

$$\frac{1}{\sqrt{pp'}}\, t^{JP} \sim \begin{cases} (pp')^{J-1} & \text{for } P = +(-1)^{J-1} \\ p^J\,(p')^{J-2} & \text{for } P = -(-1)^{J-1} \end{cases} . \qquad \text{(III.31b)}$$

The only states for which the rise of the amplitudes from the inelastic threshold was investigated were $J = 2^+$ and $J = 2^-$.

As is evident from Fig. 7 the four $J = 2^+$ amplitudes rise very quickly to values exceeding the unitarity limit (which is .5 for

Figure 7

The $J = 2^+$ $N + N \rightarrow N + N^*$ inelastic OPE amplitudes

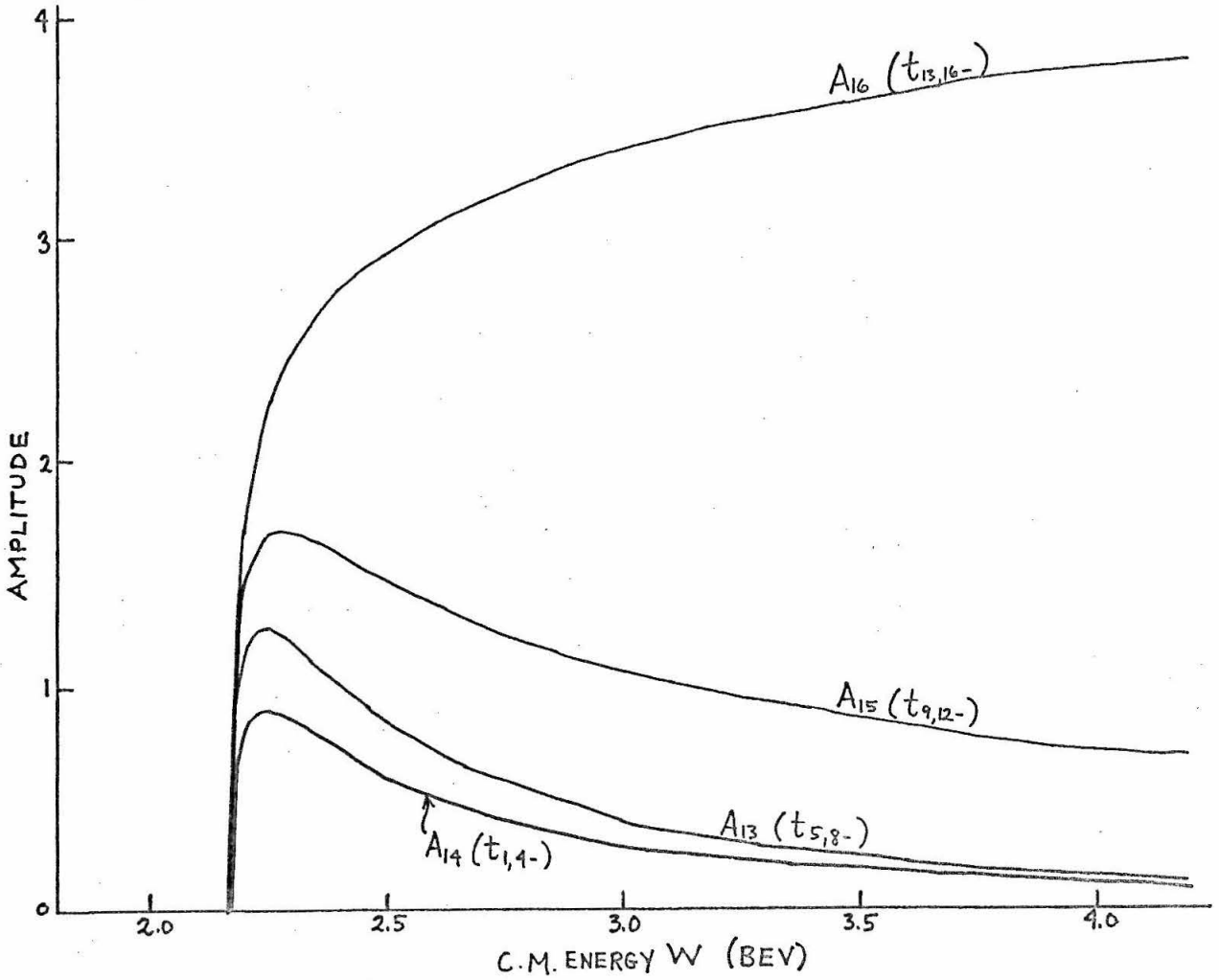
4
3
2
1
0
AMPLITUDE
A_{16} $(t_{13,16-})$
A_{15} $(t_{9,12-})$
A_{13} $(t_{5,8-})$
A_{14} $(t_{1,4-})$
2.0
2.5
3.0
3.5
4.0
C.M. ENERGY W (BEV)

inelastic amplitudes) while the $J = 2^-$ amplitudes (not shown on Figure) rise much more slowly and peak (when they do so) at much higher values of W.

The steep growth of the OPE $J = 2^+$ inelastic amplitudes suggests that since we seem to have all the prerequisites for a Ball-Frazer or cusp type enhancement, we study in detail their effect on the elastic $NN \to NN$ amplitude near the NN^* threshold. And many reasons including the fact that the elastic NN^* OPE potential seems to provide very little attraction in this J^P state plus our desire for a coupled channel problem of not unreasonable complexity, and finally, an interest in studying the mechanism of inelastic coupling in its purest form, all caused us to decide to ignore the elastic forces and use as our sole dynamical input the $J = 2^+$ inelastic amplitudes. With this input and the requirements of analyticity and unitarity (expressed via the multi-channel ND^{-1} dispersion equations) we shall study the coupled NN, NN^* $J = 2^+$ channels.

Now that we have decided on the dynamical problem to be investigated let us redefine and list the four inelastic Born amplitudes.

$$A_{13} = t^{2+}_{5,8-} = + \frac{a}{\sqrt{6}} Q_2^{(z)} \frac{1}{pp'} \left[\left(- \frac{1}{2} p \alpha_2 + \frac{\beta_1 p' E_1}{M^*} \right) + \frac{z}{M^*} (\alpha_1 p' E_1 + \beta_1 p E_4) + z^2 \left(\frac{1}{2} p \alpha_2 + \frac{\alpha_1 p E_4}{M^*} \right) \right] \quad \text{(III.32a)}$$

$$A_{14} = + t^{2+}_{1,4-} = - \frac{a\sqrt{3}}{10} \left[Q_3(z) - Q_1(z) \right] \frac{1}{p'} (\beta_1 + \alpha_1 z) \quad \text{(III.32b)}$$

$$A_{15} = t^{2+}_{9,12-} = -\frac{a}{5}\,(Q_3(z) - Q_1(z))\,\frac{1}{pp'}\left[\left(\frac{\alpha_2 p' E_1}{M^*} + \frac{\beta_1 p}{2}\right) + z\left(\frac{\alpha_1 p}{2} + \frac{\alpha_2 p E_4}{M^*}\right)\right] \qquad \text{(III.32c)}$$

$$A_{16} = t^{2+}_{13,16-} = -\frac{a\sqrt{3}\,\alpha_2}{p'}\left(-\frac{Q_4(z)}{35} + \frac{2Q_2(z)}{21} - \frac{Q_0(z)}{15}\right). \qquad \text{(III.32d)}$$

While we have the amplitudes in front of us let us discuss some of their properties which we shall need later in writing dispersion relations and setting up the ND^{-1} equations.

For $W \to \infty$ we find the asymptotic behavior

$$\begin{aligned} A_{13} &\sim \frac{1}{W^2}\,\ell n\, W \\ A_{14} &\sim \frac{1}{W} \\ A_{15} &\sim \frac{1}{W} \\ A_{16} &\sim \text{const.} \end{aligned} \qquad \text{(III.33)}$$

In the limit $W \to 0$, all the A_{1J}'s $(J = 3, 4, 5, 6) \sim (W)^{-3/2}$. This kinematical singularity will be removed by a proper choice of phase space factors.

The behavior of the $NN \to N\overline{N}^*$ amplitudes under $W \to -W$ is rather interesting. We find

$$\begin{aligned} \frac{A_{13}(-W)}{\sqrt{pp'}} &= -\frac{A_{13}(W)}{\sqrt{pp'}} \\ \frac{A_{14}(-W)}{\sqrt{pp'}} &= +\frac{A_{14}(W)}{\sqrt{pp'}} \end{aligned} \qquad \text{(III.34a)}$$

$$\frac{A_{15}(-W)}{\sqrt{pp'}} = + \frac{A_{15}(W)}{\sqrt{pp'}} \qquad \text{(III.34a)}$$

$$\frac{A_{16}(-W)}{\sqrt{pp'}} = - \frac{A_{16}(W)}{\sqrt{pp'}}$$

i.e., in all cases we have

$$\left| \frac{A_{1J}(-W)}{\sqrt{pp'}} \right| = \left| \frac{A_{1J}(W)}{\sqrt{pp'}} \right| \quad . \qquad \text{(III.34b)}$$

We also examined some of our $NN^* \to NN^*$ OPE amplitudes and the $NN \to NN$ amplitudes of Ref. 28 under the transformation $W \to - W$. And, for all of these examples of fermion-fermion scattering, we find

$$\left| T^{JP}(-W) \right| = \left| T^{JP}(+W) \right| \quad . \qquad \text{(III.35)}$$

Thus, in contrast to the case of boson-fermion (e.g., πN) scattering where we have the MacDowell symmetry

$$\left| T^{JP}(-W) \right| = \left| T^{J(-P)}(+W) \right| \quad ;$$

for 2-fermion scattering amplitudes of the same parity are related. This relation has been noted by Hara[35] who gives a partial proof*)

---

* Perhaps one may argue for a general rule by the following heuristic reasoning: Consider what intermediate states are allowed in the direct (S) channel for the different combinations of two-particle boson (B) and fermion (F) states. For $BF \to BF$ scattering only F intermediate states are allowed. Since the parity of F = - parity of $\bar{F}$ (anti-particle) reversing the sense of W corresponds to changing the parity. But for $BB \to BB$, $FF \to FF$, $BB \to F\bar{F}$, and $F\bar{F} \to F\bar{F}$ the intermediate state must be a boson which has the same parity as the corresponding antiboson. Thus, the same parity amplitudes are related by $W \to - W$. Hence, our general rule would be that if the intermediate state can be a fermion then opposite-parity amplitudes are related by changing the sign of W.

Analytic Structure of the Production Amplitudes

Next, we must investigate the analytic structure of the $NN \to NN^*$ partial wave amplitudes. A more general discussion of the singularities of production amplitudes has been given by Cook and Lee[1], and Ball, Frazer, and Nauenberg[2] and will not be repeated here. As is well-known, because of the presence of an unstable vertex ($N^* N\pi$) our amplitudes will have complex singularities which are treated by an analytic continuation in an external mass[36] (that of the N^* is most convenient). Let σ be the square of the variable external (N^*) mass. The branch points of our production amplitudes are found by setting the argument of the Q functions, z, equal to ± 1. (The Q_ℓ's contain $\ell n \left(\frac{z+1}{z-1}\right)$ which has these branch points.) We find that the branch point lying farthest to the right is given by

$$S_+(\sigma) = \frac{1}{2}(3M^2 + \sigma - \mu^2) \qquad \text{(III.36)}$$

$$+ \frac{1}{2\mu^2}\sqrt{\mu^2(\mu^2 - 4M^2)\left[\sigma - (M+\mu)^2\right]\left[\sigma - (M-\mu)^2\right]} \ .$$

As we increase σ the point S_+ moves to the right and reaches the elastic threshold $S = (2M)^2$ at $\sigma = (M^2 + 2\mu^2)$.

This is the value for which an anomalous threshold develops, since if we give σ a small imaginary part and increase σ further the branch point circles around the point $(2M)^2$ and S_+ moves to the left having gone from the second sheet through the physical cut and onto the physical sheet. When $\sigma = (M+\mu)^2$ the branch point is at $S_+ = M(2M+\mu) = S_-$, and as σ is increased further (the vertex is unstable for $\sigma > (M+\mu)^2$) the branch point moves into the complex

plane. With $\sigma = (M^*)^2$, the complex branch points are given by

$$S_{\pm} = \frac{1}{2}\,(3M^2 + M^{*2} - \mu^2)$$

$$\mp\, i\,\frac{1}{2\mu^2}\,\sqrt{\mu^2\,(4M^2 - \mu^2)\,[M^{*2} - (M + \mu)^2][M^{*2} - (M - \mu)^2]}\ .$$

With our choice for the Q_ℓ functions the branch cut lies on the locus of W (or S) corresponding to a cut in the z plane on the real axis between -1 and +1. We have numerically traced the cut in the W plane and find for our $NN \to NN^*$ amplitudes the singularity structure shown in Fig. 8. Because the complex cut crosses (at W = 2.033) the physical region for elastic NN scattering and thus intersects the elastic unitarity cut, certain difficulties appear which will be discussed later.

Figure 8

Singularities of the OPE production amplitudes in the complex W plane

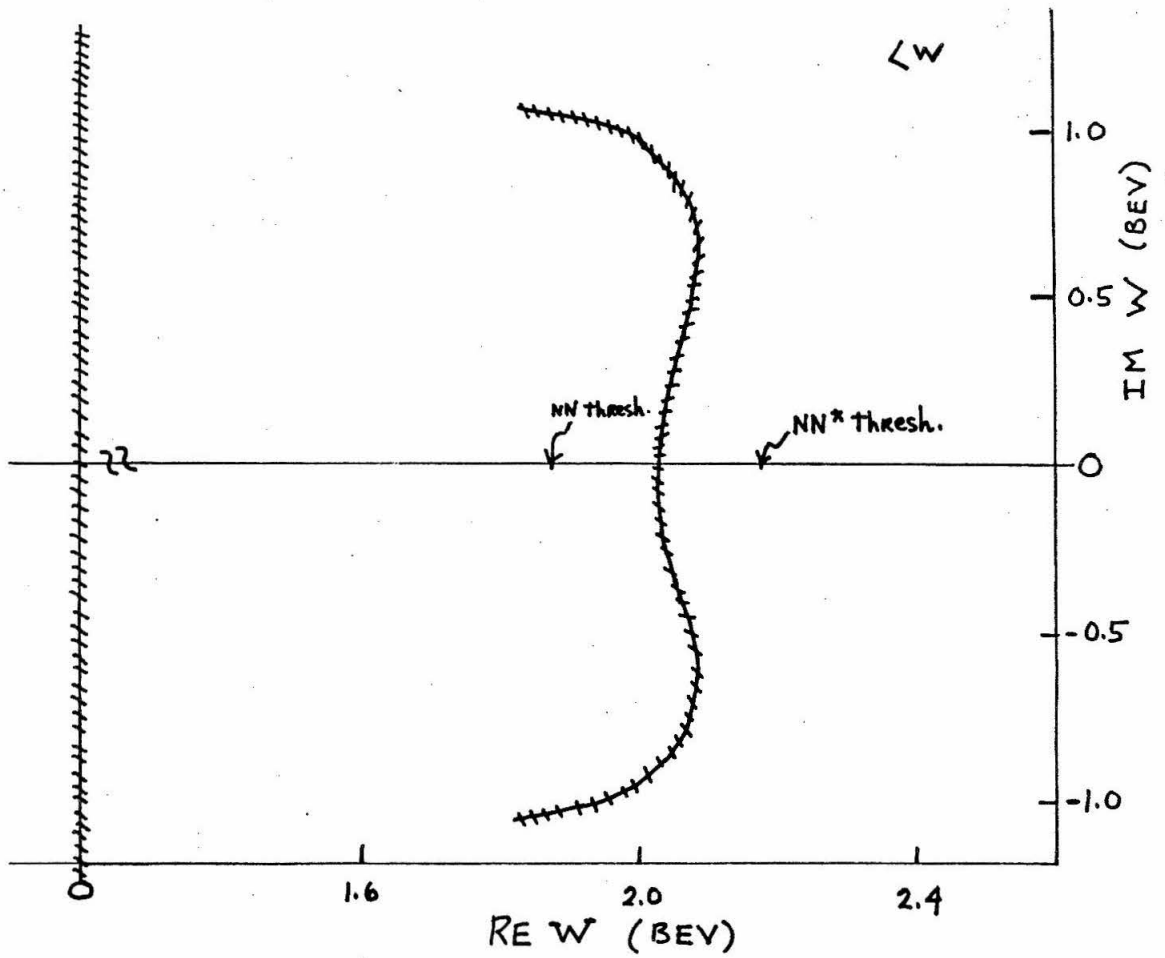
ζW
1.0
0.5
IM W (BEV)
NN' thresh.
NN* thresh.
22
0
-0.5
-1.0
0
1.6
2.0
2.4
RE W (BEV)

IV. UNITARITY OF HELICITY AMPLITUDES IN THE ISOBAR MODEL

The unitarity relations and multi-channel ND^{-1} method with appropriate extensions for three particle states in the isobar approximation have been discussed at length by many authors. Although the details in these treatments do not always agree and some problems remain, we shall not try to give a thorough presentation of the subject here but simply select the pertinent results we shall need from the work of References 1 and 2, who seem to have considered the problem most carefully. Based on Reference 1, Eqs. (19), (26), and (34), and Reference 2, Eqs. (3.8) and (3.9), we may write down the discontinuity equations for partial wave helicity amplitudes (of definite parity). As is usual when fermions are involved, to avoid certain kinematical branch points we choose to work in the W plane. Then, in terms of amplitudes F_{ij} from which the kinematical singularities have been removed (see the next section) the unitarity relations (in the isobar approximation) may be expressed for $W \geq 2M$ by

$$\frac{1}{2i}\left[F_{22}^{JP}(W_+) - F_{22}^{JP}(W_-)\right] = F_{22}^{JP}(W_+)\ \rho_2(W_+)\ F_{22}^{JP}(W_-)$$

$$+ F_{23}^{JP}(W_+,\ \sigma = M^{*2})\,\theta\left[W - (2M + \mu)\right]\ \rho_3(W_+)\ F_{32}^{JP}(W_-,\ \sigma = M^{*2}) .$$

$$\frac{1}{2i}\left[F_{32}^{JP}(W_+,\sigma) - F_{32}^{JP}(W_-,\sigma)\right] = F_{32}^{JP}(W_+,\sigma)\ \rho_2(W_+) \cdot$$

$$\cdot\ F_{22}^{JP}(W_-) + F_{33}^{JP}(W_+,\sigma,\sigma' = M^{*2})\rho_3(W_+)\ \theta\left[W-(2M + \mu)\right]\cdot$$

$$\cdot\ F_{32}^{JP}\ (W_-,\sigma' = M^{*2}) .$$

$$\frac{1}{2i}\left[F_{23}^{JP}(W_+,\sigma) - F_{23}^{JP}(W_-,\sigma)\right] = F_{22}^{JP}(W_+)\rho_2(W_+)\, F_{23}^{JP}(W_-,\sigma)$$

$$+ F_{23}^{JP}(W_+,\sigma' = M^{*2})\, \rho_3(W_+)\, \theta\left[W - (2M + \mu)\right]\, F_{33}^{JP}(W_-,\sigma,\sigma' = M^{*2}).$$

$$\frac{1}{2i}\left[F_{33}^{JP}(W_+,\sigma,\sigma') - F_{33}^{JP}(W_-,\sigma,\sigma')\right] = F_{32}^{JP}(W_+,\sigma)\rho_2(W_+)F_{23}^{JP}(W_-,\sigma')$$

$$+ F_{33}^{JP}(W_+,\sigma,\sigma' = M^{*2})\rho_3(W_+)\, \theta\left[W - (2M + \mu)\right]\, F_{33}^{JP}(W_-,\sigma',\sigma = M^{*2}) \,. \qquad \text{(IV.1)}$$

where $W_\pm = W \pm i\,\epsilon$, θ is the usual step function (equal to one where the argument is positive and zero otherwise) and σ (σ') is the energy square of the πN system (the N^*) in its center-of-mass. The subscripts 2 and 3 refer to the two- and three-particle channels, NN and NNπ respectively, and thus for our case where each "channel" may actually consist of several channels (since for J fixed several L,S states are possible) a summation is implied. (We recall for $J = 2^+$ there is one NN state coupled to four possible NN^* states). These equations are identical in form to the partial wave unitarity relations for stable two-particle channels. The properties of the unstable N^* are entirely contained in $\rho_3(W)$ which is a generalized phase space integral (the integration being over σ, the mass of the unstable particle). Explicit expressions for $\rho_2(W)$ and $\rho_3(W)$ are given in the next section. Since in our approximation we have (pseudo) two-particle channels, the solution to the discontinuity equations may be expressed in terms of the usual multi-channel ND^{-1} method[37] without the full generality to multiparticle reactions as derived by

Blankenbecler[38]. Thus writing

$$F_{ij} = N_{ik}(D^{-1})_{kj} \tag{IV.2}$$

the constraint imposed by the unitarity conditions becomes

$$\text{Im } D_{ij}(W_+) = -\rho_i(W_+)\, N_{ij}(W_+)\, \theta\,(|W| - W_i) \tag{IV.3}$$

where W_i is the threshold energy for channel i.

If F has force cuts with discontinuities disc F, then (in terms of matrices)

$$\text{disc } N = (\text{disc } F)\, D \tag{IV.4}$$

in the region of these cuts. With the matrix B(W) defined as the dispersion integral over the force cuts of the true F

$$B(W) = \frac{1}{2\pi i} \int_{\text{force cuts}} \frac{\text{disc } F(W')dW'}{W' - W} . \tag{IV.5}$$

The basic ND^{-1} equations are

$$N(W) = B(W) + \frac{1}{\pi}\int_U dW' \left[B(W') - \frac{W - W_0}{W' - W_0}\, B(W)\right] \frac{\rho(W')N(W')}{W' - W} \tag{IV.6}$$

$$D(W) = I - \frac{W - W_0}{\pi}\int_U \frac{\rho(W')\, N(W')\, dW'}{(W' - W)(W' - W_0)} , \tag{IV.7}$$

where the contour U is the entire real axis except for $|W| < W_i$ (where the integration for D_{ij} begins depends on the subscript i) and I is the unit matrix. We have assumed that N satisfies an unsubtracted dispersion relation while D requires one subtraction. (We have put the subtraction point at the same place for all channels although this

is not necessary.)

Because the force cut (in the OPE amplitudes) intersects the unitarity cut (see Fig. 21) the integration contour U must be deformed to avoid the protruding singularities. As a result of the anomalous threshold and complex singularities additional integrals will appear in the N and D equations. This problem is discussed quite thoroughly in References 1 and 2 (by performing an analytic continuation in the N^* mass). Although, (for reasons to be given in Section VI) we ignore the presence of the anomalous singularity in our determinental calculations, we shall make some further remarks on the subject in Appendix C.

For a more complete discussion of the ND^{-1} method, including its properties and some examples of how the calculations are performed, the reader is referred to references 37 and 34, and other references which are given there.

V. REMOVAL OF KINEMATICAL SINGULARITIES AND CONTINUATION BELOW THE INELASTIC THRESHOLD

We must now specify in detail the phase space factors $\rho_2(W)$ and $\rho_3(W)$. These factors serve several purposes and must meet certain other requirements[39]. Principally they are chosen to eliminate "kinematical" singularities (which we have assumed are not contained in F) and to guarantee the "correct" threshold behavior**). The partial wave threshold behavior ($\delta_\ell \sim q^{2\ell+1}$ for spinless elastic scattering) will not result from unitarity and analyticity requirements, but does follow from the Mandelstam representation. (In non-relativistic scattering the ordinary threshold behavior can be derived if the potential is suitably restricted.[40] With our approximation for the left hand cut (the "potential") it would be purely accidental if the correct threshold behavior resulted and the amplitude vanished at threshold with the proper momentum dependence. Hence, we divide out the factors of momentum so our new amplitude will just approach a constant at threshold.

We have seen that the inelastic amplitudes $A_{1J}(W)$ $(J = 3,4,5,6)$ behave like $\sim \sqrt{pp'}\, p^2$ at the thresholds $(p \to 0,\ p' \to 0)$. And because of their $W \to -W$ behavior they have the same momentum dependence at the negative W thresholds. Using this and recalling the behavior at $W = 0$ we choose phase space factors

---

** There is no a priori guarantee that a suitable phase space factor exists.

$$\rho_2(W) = \frac{p^5}{W(W+2M)^4} = \frac{(W-2M)^{5/2}}{32W(W+2M)^{3/2}} \qquad (V.1)$$

$$\rho_3(W) = \frac{p'}{W} = \frac{[W^2 - (M^* + M)^2]^{1/2}[W^2 - (M^* - M)^2]^{1/2}}{2W^2} \qquad (V.2)$$

where we have so far assumed the N^* is stable. We now define

$$F_{ij} = t_{ij}/\sqrt{\rho_i \rho_j} \qquad (V.3)$$

(where $t_{ij} = (S_{ij} - \delta_{ij})/2i$).

Because of a desire to have $\rho_2(W) \xrightarrow[W \to \infty]{} \text{const}$ and $\rho_3(W) \xrightarrow[W \to \infty]{} \text{const}$ so that our dispersion integrals will be convergent, we were forced to include a factor $(W + 2M)^{-2}$ in ρ_2 which introduces a kinematical zero at the beginning of the left hand unitarity cut. The placement of this zero is rather arbitrary except for the feeling that it should be reasonably distant from the region of physical interest ($W \sim M + M^*$). Since we decided to ignore the integrations over the negative W unitarity cut (see below) it does not matter that we have disturbed the threshold behavior at the W = - 2M threshold. Aside from this, F_{ij} is expected to have no kinematical zeros and only dynamical singularities throughout the W plane and thus satisfies the dispersion relations given in the previous section.

The Born amplitudes which constitute the dynamical input to our coupled channel problem are thus given by

$$B_{1J}^{(W)} = \frac{A_{1J}(W)}{\sqrt{\rho_2(W)\rho_3(W)}} = B_{J1}^{(W)} \quad J = 3,4,5,6. \qquad (V.4)$$

Although we shall shortly discuss the appropriate modification of ρ_3

to include the width of the N^*, we note that it is correct when forming the B_{1J} to use the ρ_3 given above, assuming a stable N^*, since the A_{1J} were calculated with this assumption.

In the determinental approximation[41] where we replace N_{ij} by the corresponding Born amplitude, those D integrals beginning at the NN threshold (W = 2M) require the evaluation of B_{1J} in the region below the inelastic threshold ($W = M + M^*$). The B_{1J} we have formed are smooth functions at the $N\bar{N}^*$ threshold but they must be rewritten before one can calculate their values for $W < M + M^*$. Using the relations

$$p' \longrightarrow + i \, |p'| \text{ for } p'^2 < 0$$

$$z \longrightarrow \frac{z'}{i} = \frac{2M^2 - \mu^2 - 2E_1E_3}{i \, 2p|p'|} \tag{V.5}$$

and thus,

$$Q_0(z) = \frac{1}{2} \ell n \left(\frac{z+1}{z-1}\right) \longrightarrow \frac{i}{2} \tan^{-1}\left(\frac{2z'}{z'^2 - 1}\right) \equiv iQ_{00}$$

$$Q_1(z) \rightarrow z' \, Q_{00} - 1 \equiv Q_{11}$$

$$Q_2 \rightarrow i\left[\frac{1}{2}(-3z'^2 - 1)Q_{00} + \frac{3}{2} z'\right] \equiv iQ_{22} \tag{V.6}$$

$$Q_3 \rightarrow \frac{5}{3} z' \, Q_{22} - \frac{2}{3} Q_{11} \equiv Q_{33}$$

$$Q_4 \rightarrow i\left[-\frac{7}{4} z' \, Q_{33} - \frac{3}{4} Q_{22}\right] \equiv i \, Q_{44} \, ,$$

we have, for $W < M + M^*$

$$B_{13} = \frac{a' Q_{22}}{\sqrt{6}\sqrt{\rho_2 |\rho_3|}\, p|p'|} \cdot$$

$$\cdot \left[\left(-\frac{1}{2} p \alpha_2 - \frac{\beta_1'|p'|E_1}{M^*}\right) + \frac{z'}{M^*}(\alpha_1|p'|E_1 + \beta_1' p E_4)\right.$$

$$\left. - z'^2\left(\frac{1}{2} p \alpha_2 + \frac{\alpha_1 pE_4}{M^*}\right)\right] \qquad \text{(V.7a)}$$

$$B_{14} = -\frac{a'\sqrt{3}}{10\sqrt{\rho_2|\rho_3|}\,|p'|}(Q_{33} - Q_{11})(\beta_1' - \alpha_1 z') \qquad \text{(V.7b)}$$

$$B_{15} = -\frac{a'(Q_{33} - Q_{11})}{5\sqrt{\rho_2|\rho_3|}\, p|p'|}\left[\left(\frac{\alpha_2|p'|E_1}{M^*} + \frac{\beta_1' p}{2}\right)\right.$$

$$\left. - z'\left(\frac{\alpha_1 p}{2} + \frac{\alpha_2 pE_4}{M^*}\right)\right] \qquad \text{(V.7c)}$$

$$B_{16} = -\frac{a'\sqrt{3}\,\alpha_2}{\sqrt{\rho_2|\rho_3|}\,|p'|}\left(\frac{-Q_{44}}{35} + \frac{2Q_{22}}{21} - \frac{Q_{00}}{15}\right), \qquad \text{(V.7d)}$$

where a prime on any quantity refers to the unprimed quantity evaluated with p' replaced by $|p'|$. (a, α, β are defined in Eq. (III.28)).

In Fig. 9 we have graphed the amplitudes B_{1J} in the region near the $N\bar{N}^*$ threshold.

In Figs. 10(a) and 10(b) we display the continued amplitudes B_{1J} over the whole region between the elastic and inelastic thresholds ($2M \leq W \leq M + M^*$). The rather troubling behavior near W = 2.033 is a result of the fact that the branch cut joining the complex

Figure 9

The $NN \rightarrow NN^*$ input Born amplitudes

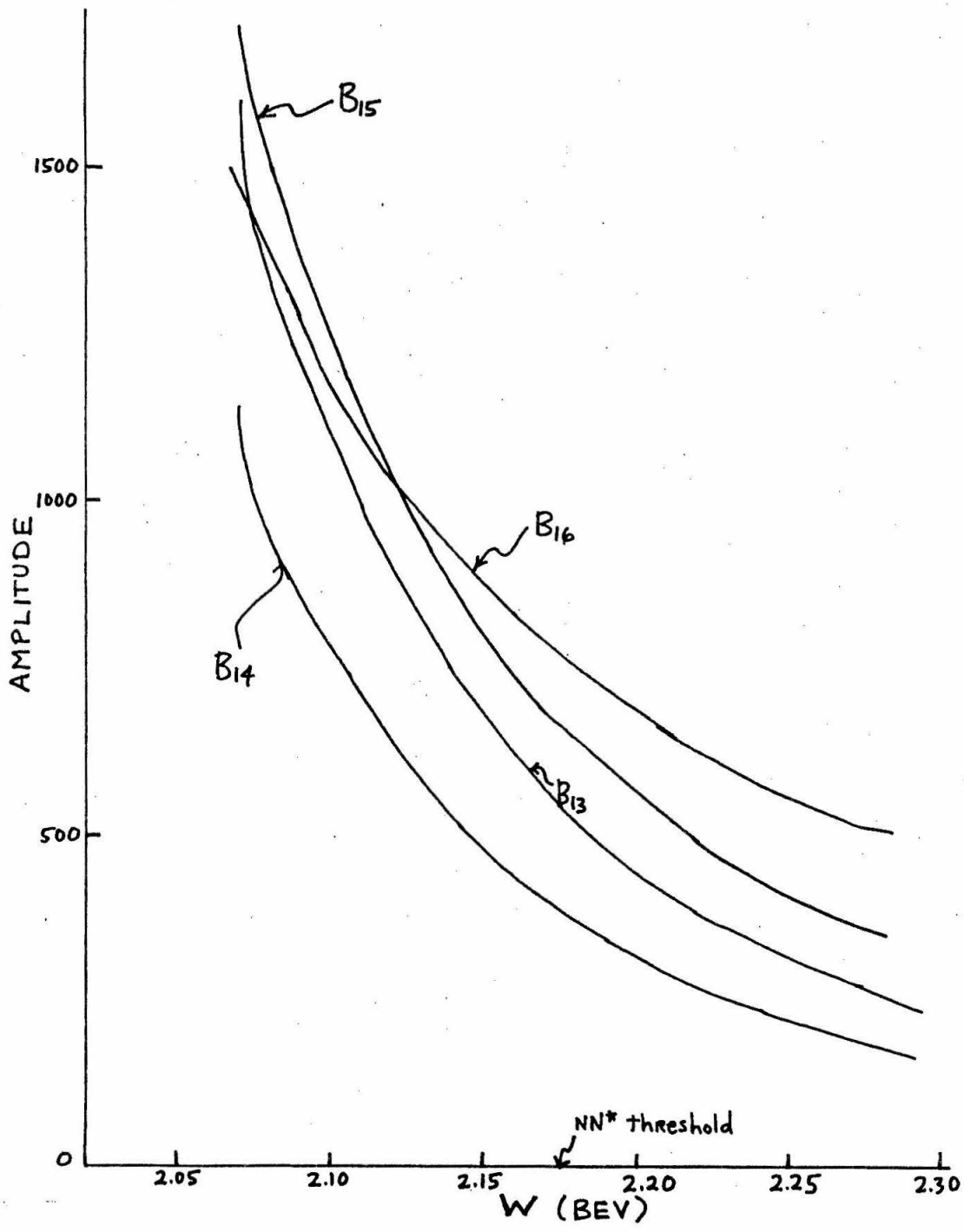
B15
B16
B14
B13
1500
1000
500
0
AMPLITUDE
NN* threshold
2.05
2.10
2.15
2.20
2.25
2.30
W (BEV)

Figure 10

The $NN \rightarrow NN^*$ input Born amplitudes in the region between the elastic and inelastic thresholds

(a) $B_{14}(W)$ and $B_{15}(W)$ (b) $B_{13}(W)$ and $B_{16}(W)$

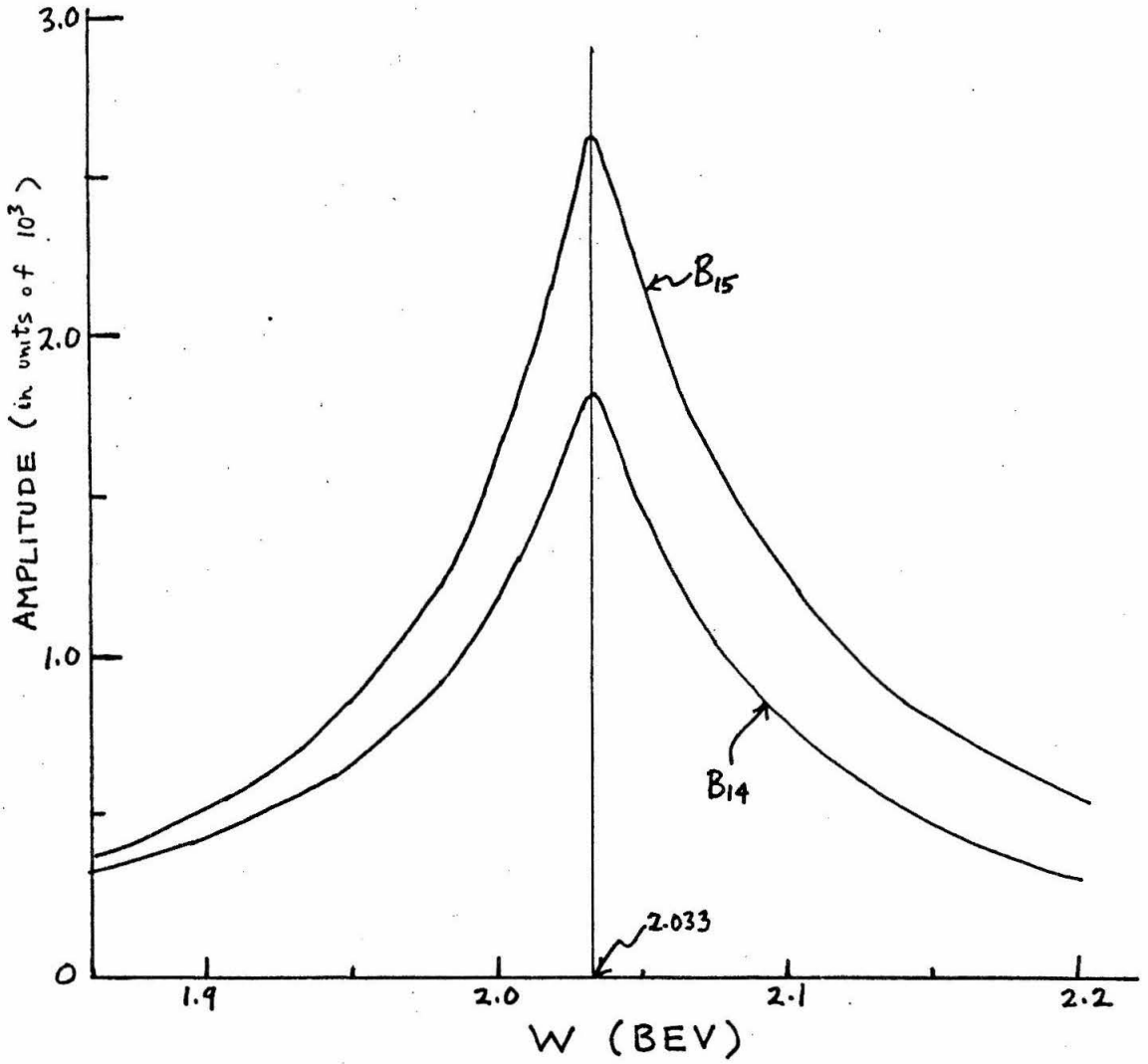
3.0
2.0
1.0
0
AMPLITUDE (in units of 10^3)
B_{15}
B_{14}
2.033
1.9
2.0
2.1
2.2
W (BEV)

(a)

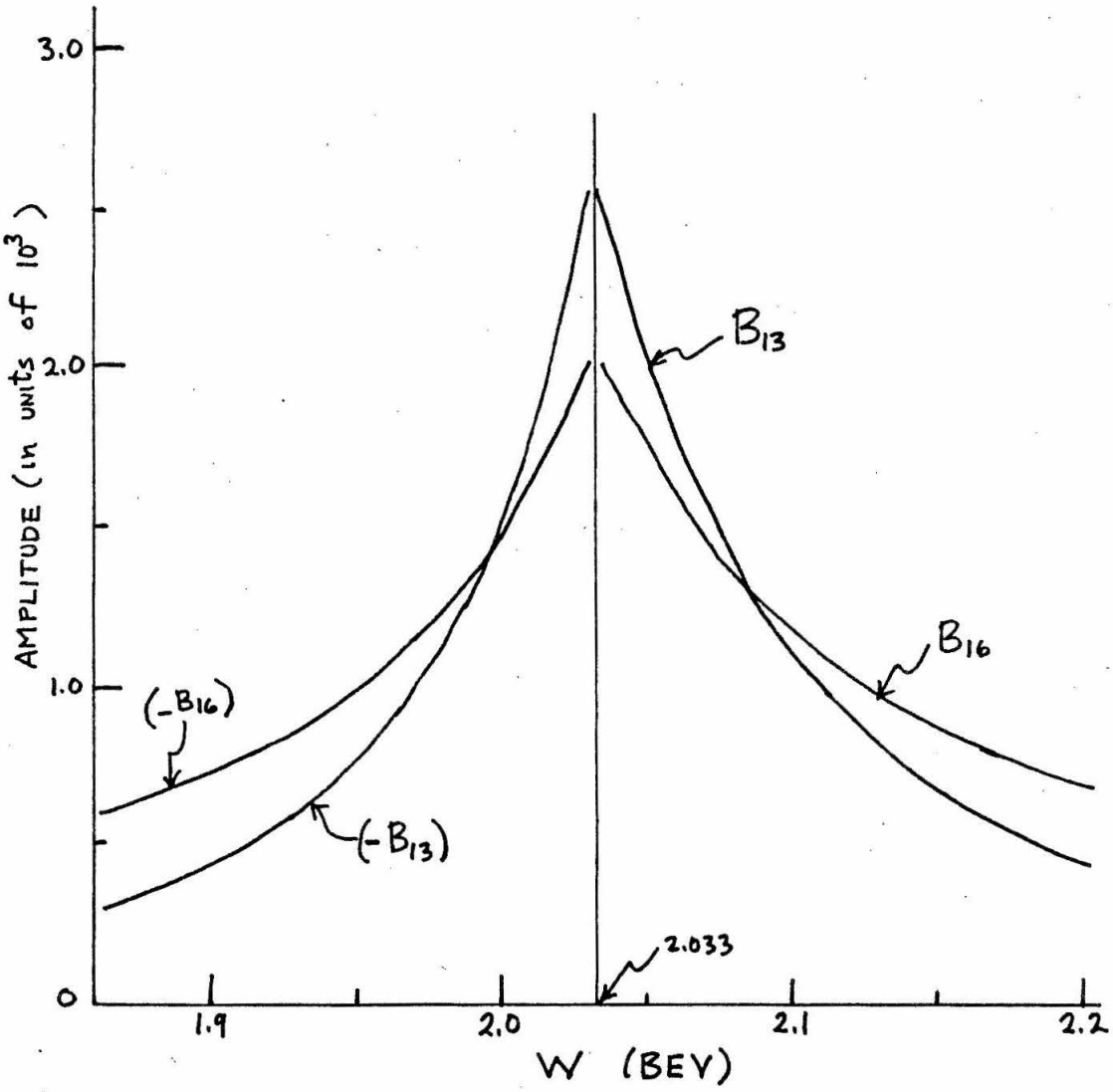
3.0
2.0
1.0
0
AMPLITUDE (in units of 10^3)
B_{13}
B_{16}
$(-B_{16})$
$(-B_{13})$
2.033
1.9
2.0
2.1
2.2
W (BEV)

(b)

singularities crosses the real W axis at this point. This strong peaking of the Born amplitudes is reflected in a corresponding peaking in the elastic NN amplitudes which we calculate via the determinental approximation. But for several reasons we felt justified in ignoring such peaks. W = 2.033 corresponds to $T_{lab} \simeq$ 330 MeV and thus lies essentially in the purely elastic scattering region. But in our calculation we center our attention on the region close to the inelastic threshold ($T_{lab} \simeq$ 646 MeV) and in fact believe the results are only valid for energies not too far from W = 2.176. (When the dynamical calculations were repeated using B_{1J}'s cut flat for $W \leq 2.176$; i.e., B_{1J} (W < 2.176) = B_{1J} (2.176), the results near the inelastic threshold changed very little.) We also believe that a more exact treatment of the NNπ state and a proper continuation of the dynamical equations past the anomalous singularities would tend to eliminate any spurious behavior.

Now, let us include the instability of the N^* by modifying $\rho_3(W)$ to take into account the width of the resonant Nπ state[42]. To do this we replace p' in $\rho_3(W)$ by

$$\frac{1}{\pi}\int_{(M+\mu)^2}^{(W-M)^2} d\sigma \left\{ \frac{\left\{[\sigma - (W+M)^2][\sigma - (W-M)^2]\right\}^{1/2}}{2W} \cdot \frac{2M^*(\Gamma/2)}{(\sigma - M^{*2})^2 + (2M^*\frac{\Gamma}{2})^2} \right\} \equiv p'_u \qquad \text{(V.8)}$$

where

$$\Gamma(\sigma) = \frac{1}{3\pi}\left(\frac{G}{M}\right)^2 \frac{q^3(E_N + M)}{\sqrt{\sigma}} = \text{the width of the } N^*$$

$$q^2 = \frac{[\sigma - (M+\mu)^2][\sigma - (M-\mu)^2]}{4\sigma}$$

$$E_N = \sqrt{q^2 + M^2}\ ,$$

and σ is again the energy square of the Nπ state in the Nπ center of mass. To verify this replacement and understand how it is derived note that in the limit $\Gamma \to 0$

$$p_u' \xrightarrow[\Gamma \to 0]{} \int p'(s,\sigma)\,\delta(\sigma - M^{*2})\,d\sigma \qquad (V.9)$$

$$= p' \text{ (for stable } N^*).$$

Thus, we have just a two-particle momentum distribution weighted by a "finite width delta-function"*).

The limits on the integral for p_u' are the smallest and largest "mass" square of an Nπ state which is part of a total NNπ state with c.m. energy W.

Following the method used by Nauenberg and Pais[11] and Baz[11] we can derive an approximate expression for p_u' the case of very small width (width/mass of resonance $\ll 1$).

---

*) Heuristically, to understand the finite width δ-function, one can note that since $1/(\omega - \omega_0 - i\epsilon) = P/(\omega - \omega_0) + i\pi\delta(\omega - \omega_0)$ as $\epsilon \to 0$, then it is reasonable to say
$\text{Im}\ 1/(\omega - \omega_0 - i\,\gamma/2) \cong \pi\,\delta(\omega - \omega_0)$ or $\delta(\omega - \omega_0) \cong (\gamma/2\pi)/[(\omega - \omega_0)^2 + \gamma^2/4]$ for γ finite. We also used the relations $\delta(\sigma - M^{*2}) = \frac{1}{2M^*}[\delta(\sqrt{\sigma} - M^*) + \delta(\sqrt{\sigma} + M^*)]$ with $\sqrt{\sigma} + M^* \approx 2M^*$.

With a very narrow width nearly all the contribution to the integral comes from a very small region around $\sigma = M^{*2}$. We thus may extend the limits so that the integration runs along the whole Re σ axis and then we can perform a contour integral by closing the contour in the lower-half σ plane enclosing the pole at $\sigma = M^{*2} - i M^{*} \Gamma$, where Γ is the constant obtained by evaluating $\Gamma(\sigma)$ for $\sigma = M^{*2}$. Although the integral is formally divergent it is to be interpreted in the sense that only the contribution of the N^{*} peak is to be included. Performing the contour integral using Cauchy's Residue Theorem and evaluating for $W \approx M^{*} + M$ we find

$$p_u' \rightarrow p_u'' = \left[p'^2 + i \frac{M^{*} M \Gamma}{M^{*} + M} \right]^{1/2} . \qquad \text{(V.10)}$$

The real part of p_u'' gives an approximate description of three-body phase space when two of the final three particles form a narrow width resonance and we are not too far from the resonance energy. The imaginary part of p_u'' results from that part of the extended integration $(W - M)^2 < \sigma < (W + M)^2$ corresponding to $\sqrt{\sigma} - M < W < \sqrt{\sigma} + M$ (below the inelastic threshold) and is a useful expression when some type of effective range (or K matrix) approximation is being made.

However, for widths much larger than a few MeV graphical comparison shows that p_u'' is not a very good representation of the true p_u' especially if one is interested in the region close to the NN^{*} threshold. In general, p_u'' is larger and flatter than p_u'; while even for rather large widths p_u' rises steeply upwards in a short range around the inelastic threshold.

At larger energies ($W \geq 2.5$ BeV) all expressions for p', p_u', p_u'' give very similar numerical values. For this reason, and because of the computing time (and hence expense) of doing an integral for each different value of W we used p_u'' in our expressions for $\rho_3(W)$ when they occurred in integrals (viz. for Re D_{ij}), but used p_u' when no integrals were involved (e.g., Im D_{ij}).

In Fig. 11 we have graphed $\rho_3(W) = \frac{p_u'}{W}$ for several different values of the N^* width. This shows clearly that the broader the width the slower and flatter the rise of ρ_3. As we shall see later this is reflected in the shape and height of the peaks produced by the inelastic amplitudes.

Figure 11

The NN^* phase space factor ρ_3, for different values of the N^* width

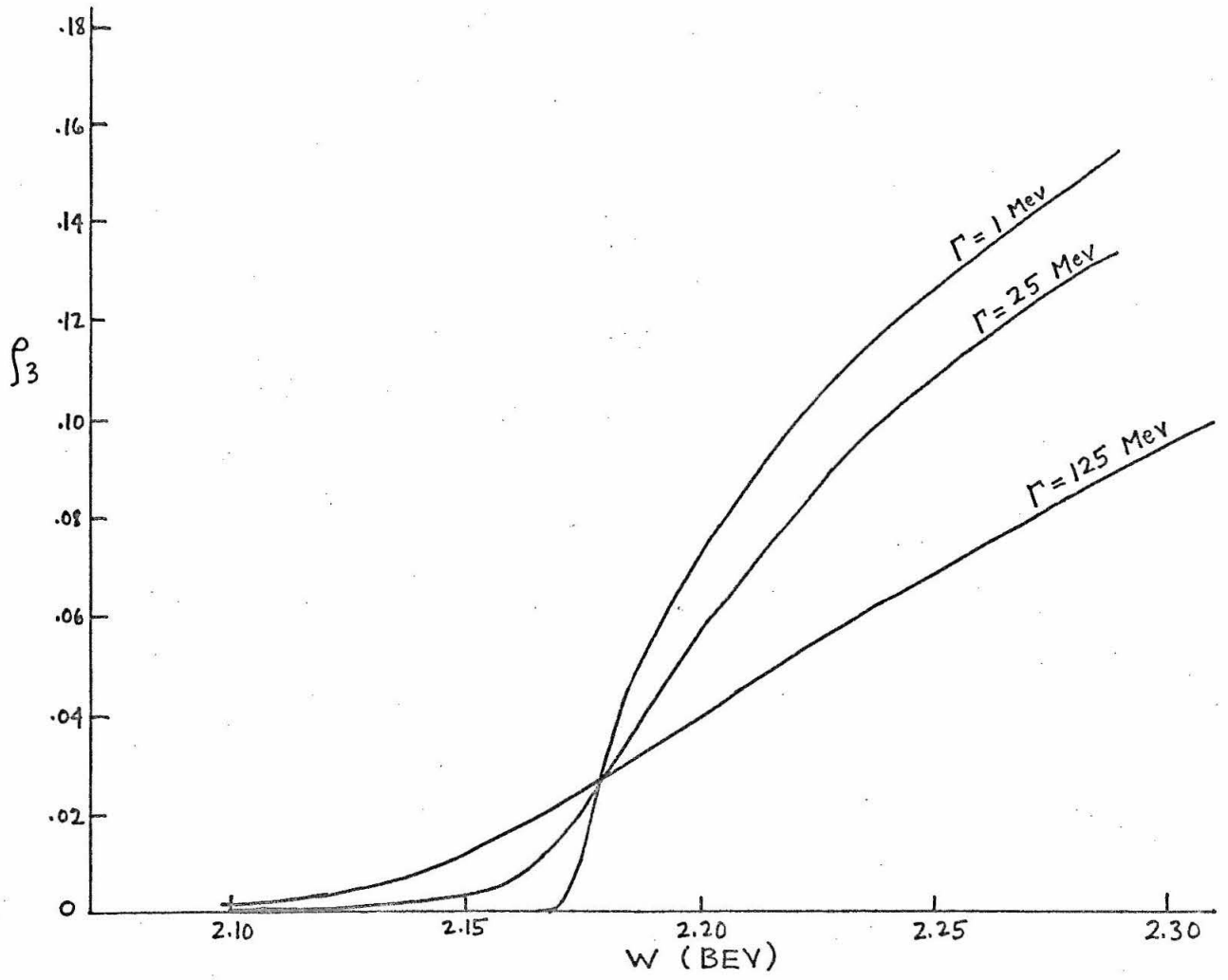
.18
.16
.14
.12
.10
.08
.06
.04
.02
0
ρ_3
Γ = 1 Mev
Γ = 25 Mev
Γ = 125 Mev
2.10
2.15
2.20
2.25
2.30
W (BEV)

VI. DETAILS OF THE CALCULATION AND GENERAL PROPERTIES OF THE SOLUTIONS

In this section we shall describe the details of our approximate calculation. The numerical results and conclusions are given in the next section.

Rather than solve the set of full ND^{-1} equations we decided to employ the lowest order determinental method[37] in which the integral equation for N, (IV.6), is simply replaced by the approximation $N(W) = B(W)$ and then D is calculated from N by the dispersion relation Eq. (IV.7). Of course, in our calculation, as in any calculation of finite size, B(W) is approximated by including only that part of the potential due to the exchange of certain particles, usually the lightest mass ones (corresponding to the longest range part of the potential) or exchanges which have features such as form or strength of coupling, or singularities, which are of special interest. As discussed earlier, we chose to keep only the OPE force. Primarily, we used the determinental method because we did not want our calculation to become excessively involved and costly (= much computer time). But, in fact, considering the other approximations made in the problem (e.g., for B), it is not clear that the full ND^{-1} calculation would necessarily be superior or the results more "accurate", or at least be that much better to justify the greatly increased complexity of the method. In problems which have been solved both by the ND^{-1} and determinental methods the general features of the results usually are very similar[43]. In a sense it is misleading to just call the determinental method an <u>approximation</u> to the ND^{-1} equations. Rather

it should be thought of as a different method, with special properties of its own, which may or may not be a useful or accurate method for any particular problem. Several of its features are undesirable, especially the dependence of results on choice of subtraction point and the lack of symmetry ($F_{ij} \neq F_{ij}$) of the solutions. The ND^{-1} method does not have these troubles and in that sense is superior.

We thus have the following set of equations to solve (note that we are changing some of our earlier conventions)

$$F_{ij} = B_{ik}(D^{-1})_{kj} \tag{VI.1}$$

$$D_{ij} = \delta_{ij} - \frac{(W - W_0)}{\pi} \int_{W_i}^{\infty} \frac{\rho_i \, B_{ij} \, dW'}{(W' - W)(W' - W_0)} - \frac{(W - W_0)}{\pi} \int_{-W_i}^{-\infty} \frac{\rho_i \, B_{ij} \, dW'}{(W' - W)(W' - W_0)} \tag{VI.2}$$

where W_i is the threshold energy for channel i.

With our approximations (neglecting all but the inelastic amplitudes) $B_{ij} = 0$ except for $B_{13} = B_{31}$, $B_{14} = B_{41}$, $B_{15} = B_{51}$ and $B_{16} = B_{61}$, and these are given by the OPE amplitudes of Section V. Writing these as B_{1J}, with J = 3,4,5,6 only (subscript 1 refers to NN state and subscript J = 3,4,5,6 to NN^* state), we have

$$D_{1J} = -\left(\frac{W - W_0}{\pi}\right) \left\{ \int_{W_{NN}=2M}^{\infty} + \int_{-W_{NN}}^{-\infty} \right\} \frac{\rho_2 \, B_{1J} \, dW'}{(W' - W - i\epsilon)(W' - W_0)} \tag{VI.3}$$

$$D_{J1} = -\left(\frac{W - W_0}{\pi}\right)\left\{ \int_{W_{NN^*}}^{\infty} + \int_{-W_{NN^*}}^{-\infty} \right\} \frac{\rho_3 \, B_{1J} \, dW'}{(W' - W - i\epsilon)(W' - W_0)} \tag{VI.4}$$

where ρ_2 and ρ_3 are the phase space factors for the (two-particle) NN and (three-particle) NN^* channels, respectively, discussed in Section IV.

Allowing for the instability of the N^*, $W_{NN^*} = 2M + \mu$.

The only other non-zero D_{ij} are those for which $i = j$ and then $D_{ij} = D_{ii} = \delta_{ii} = 1$. Thus, our matrix D may be represented in the form

$$D = \begin{pmatrix} 1 & D_{13} & D_{14} & D_{15} & D_{16} \\ D_{31} & 1 & 0 & 0 & 0 \\ D_{41} & 0 & 1 & 0 & 0 \\ D_{51} & 0 & 0 & 1 & 0 \\ D_{61} & 0 & 0 & 0 & 1 \end{pmatrix} \tag{VI.5}$$

In writing the equations for D_{1J} and D_{J1} we have ignored any possible deformations of the contour of integration along the unitarity cut to avoid intersecting the force cut crossing the physical region. (The intersection occurs between W_{NN} and W_{NN^*} and thus only D_{1J} (and D_{11}) need be modified.) We shall try to discuss this further in Appendix C but we can remark here that because we are using the determinental method our integrands contain B_{1J} and thus we are

including some of the effects of the complex singularities. And, of course, with a proper treatment of the three-particle NNπ state such anomalous cuts may not even be present[44].

Before we further discuss the calculation of D_{1J} and D_{J1} let us look at the form of the solutions for F_{ij}.

The elastic NN scattering amplitude

$$F_{11} = B_{1J} \, (D^{-1})_{J1} \tag{VI.6}$$

sum over J = 3,4,5,6. Using the relation

$$(D^{-1})_{J1} = \frac{\text{cof } D_{1J}}{\det D} \tag{VI.7}$$

and the matrix for D, Eq. (VI.5), given above, we find

$$F_{11} = \frac{- B_{1J} \, D_{J1}}{1 - D_{1J} \, D_{J1}} \tag{VI.8}$$

with a sum over J implied. The off-diagonal inelastic amplitudes turn out to be

$$F_{J1} = \frac{B_{1J}}{\det D} = \frac{B_{1J}}{1 - D_{1J} \, D_{J1}} \tag{VI.9}$$

and

$$F_{1J} = B_{1J} + D_{1J} \left(\frac{B_{1K} \, D_{K1}}{\det D} \right) = B_{1J} - D_{1J} \, F_{11} \, . \tag{VI.10}$$
(sum over K)

In general, $F_{1J} \neq F_{J1}$, but it is interesting to note that if we had only one inelastic channel we would have the symmetric solutions $F_{1J} = F_{J1}$.

As will be mentioned in the next section, our numerical results were not very symmetric. Of course, this could have been avoided if we had used the full ND^{-1} equations.

Several further approximations were made in calculating D_{1J} and D_{J1}. The integral over the left-hand unitarity cut, $\int_{-W_i}^{-\infty}$, was neglected because for W in the region of physical interest, the denominator (W' - W) remains almost constant and is never near zero (as it can be for the integral on the right cut); thus the integral $\int_{-W_i}^{-\infty}$ will show little variation with W and is considerably smaller than the similar integral over the right-hand cut. So we are essentially neglecting a probably small constant piece in the integrals for D_{1J} and D_{J1}. And of course we are neglecting much other singularity structure (e.g., due to other particle exchanges) so the neglect of this cut which is rather distant from the physical region is not a further drastic approximation.

The choice of subtraction point, W_0, is a difficult matter. Usually in the determinental method (recall with the full ND^{-1} that the results are independent of W_0) the subtraction point is chosen to insure some approximate degree of crossing symmetry[41] and thus W_0 is placed near or at the right-hand edge of the force cut (near the place of maximum discontinuity) due to the exchanged particle. At the subtraction point, $W = W_0$, we have $D_{ij} = \delta_{ij}$ and hence $F_{ij} = B_{ij}$. We expect the Born approximation to be a fair representation of the true amplitude over that part of the force cut where the diagram being considered provides the only or major discontinuity. In our case,

where the right-most part of the OPE cut lies in the complex plane and intersects the physical region the selection of W_0 is not so easy. The decision was largely made by considering the singularity structure of perhaps the next most important part of the potential which we have omitted, that due to ρ-exchange (Fig. 12),

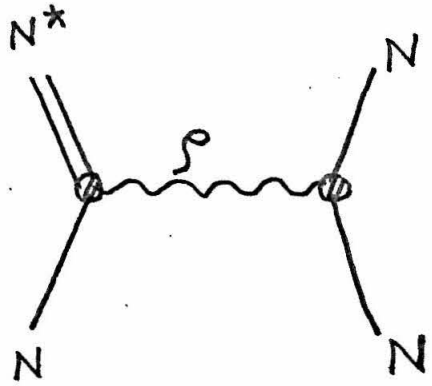

Rho Meson Exchange Interaction in $N + N \rightarrow N + N^*$

Fig. 12

where we assume the ρ is a stable particle with mass = 763 MeV. Now no vertices are unstable ($M^* < M + m_\rho$) and thus, no complex singularities are present. The partial wave amplitudes have a force cut on the right half plane which runs from S_- to S_+ where

$$S_\pm = \frac{1}{2}(3M^2 + M^{*2} - m_\rho^2) \pm \frac{1}{2}\left[(3M^2 + M^{*2} - m_\rho^2)^2 - (M^{*2} - M^2)^2 \cdot \frac{4M^2}{m_\rho^2}\right]^{1/2} . \qquad \text{(VI.11)}$$

In the W plane the right edge of this cut lies at $W \cong 1.84$ BeV.

Since we are omitting this part of the potential, we decided to place our subtraction point between W = 1.84 and W = 1.88, the beginning of the physical region for elastic NN scattering. So we chose $W_0 = 1.86$ as a reasonable location. In our numerical work W_0 was varied between $W_0 = 1.60$ and $W_0 = 1.86$ and we found that the results (viz., location and height of peaks) were rather sensitive to the value of W_0. This seems to be one of the most undesirable features of the determinental method.

By making one subtraction in our dispersion relations for D all integrals are convergent since in the worst case $\rho B_{16} \sim$ const. as $W \to \infty$. Nevertheless, the calculation was made with a (variable) cutoff on all integrals. One may ask why use a cutoff or make subtractions when they are not needed? Because we know that we have omitted much physics from our problem - e.g., other particle exchanges, other channels, possible Reggeistic damping of amplitudes - and by having some parameters which can be varied we can get some feeling for how our solutions depend on the physics we have left out. Using a cutoff, for example, gives us a way to study the possible effect higher energy channels and modified high energy behavior of amplitudes would have on our results.

Let us now rewrite the expressions for D_{1J} and D_{J1} separating out the real and imaginary parts.

$$D_{1J} = -\frac{(W - W_0)}{\pi} P \int_{W_{NN}}^{W_c} \frac{\rho_2 \, B_{1J} \, dW'}{(W' - W)(W' - W_0)} - i \, \rho_2 \, B_{1J} \, \theta(W - W_{NN})$$

$$\equiv D_{1J}^R + i \, D_{1J}^I \qquad \text{(VI.12)}$$

$$D_{J1} = -\frac{(W - W_0)}{\pi} P \int_{W_{NN\pi}}^{W_c} \frac{\rho_3 \, B_{1J} \, dW'}{(W' - W)(W' - W_0)} - i \, \rho_3 \, B_{1J} \, \theta(W - W_{NN\pi})$$

$$= D_{J1}^R + i \, D_{J1}^I \, , \qquad \text{(VI.13)}$$

where P signifies that the principal value is taken when W lies in the range of integration and W_c is the cutoff energy.

In the integrals for D_{J1}^R, $\rho_3 = \frac{p'_u}{W}$ was approximated by $\mathrm{Re}\,\frac{p''_u}{W}$ since the time for numerical integration would have been greatly increased if we had to calculate p'_u (which involves an integration) for each mesh point in the Simpson sum. The value of Γ used in p''_u was chosen in each case so that Re p''_u resembled as closely as possible the actual p'_u. The error made by this approximation is negligible since the shape of the (cusp) peak is determined primarily by the ρ_3 in D_{J1}^I and here the true $\rho_3 = \frac{p'_u}{W}$ was used.

Numerically, the principal value integrals were performed by subtracting out the singular point

$$P \int \frac{\rho(W') \, B(W') \, dW'}{(W' - W)(W' - W_0)} = P \int \frac{[\rho(W')B(W') - \rho(W)B(W)]dW'}{(W' - W)(W' - W_0)} +$$

$$+ \rho(W)B(W) \; P \int \frac{dW'}{(W' - W)(W' - W_0)} \, , \qquad \text{(VI.14)}$$

where the second integral on the RHS can be done analytically. To do the numerical integration, Simpson's rule was used, after a change of variable was made, $W' = \frac{W_{thresh}}{Y}$.

Increased accuracy was achieved by using the Aitken convergence procedure[45] in which Simpson sums for 4n, 2n, and n intervals are

combined according to the formula

$$\text{SUM(4n)} - \left\{ \frac{[\text{SUM(4n)} - \text{SUM(2n)}]^2}{[\text{SUM(4n)} + \text{SUM(n)} - 2\ \text{SUM(2n)}]} \right\} = \text{SUM} .$$

General Properties of the Solutions

Let us rewrite our solution for the elastic NN $J = 2^+$ amplitude and note some of its properties. We have

$$\rho_2\ F_{11} = \text{"}e^{i\delta_{NN}} \sin \delta_{NN}\text{"} = \frac{-\rho_2\ B_{1J}\ D_{J1}}{1 - D_{1J}\ D_{J1}} \qquad \text{(VI.15a)}$$

$$\text{or } \rho_2\ F_{11} = \frac{D^I_{1J}(D^R_{J1} + i\ D^I_{J1})}{(1 - D^R_{1J}\ D^R_{J1} + D^I_{1J}\ D^I_{J1}) - i\ (D^R_{1J}\ D^I_{J1} + D^I_{1J}\ D^R_{J1})} \qquad \text{(VI.15b)}$$

(a sum over J is always implied).

If we are above the threshold for inelastic scattering we must remember that δ_{NN}, in general, will be complex and then we have

$$\rho_2\ F_{11} = \left(\frac{e^{2i\delta} - 1}{2i}\right) = \left(\frac{\eta\ e^{2i\delta_R} - 1}{2i}\right) \qquad \text{(VI.16)}$$

where $\eta = e^{-2\delta_I}$ and $\delta = \delta_R + i\ \delta_I$.

One of the first things to note is that our result for F_{11} is independent of the sign of the inelastic amplitudes. Whether positive or negative the effect of the inelastic amplitudes is attractive in the elastic channel. Even the relative signs between the different B_{1J}'s are unimportant.

If there were a resonance in the elastic scattering amplitude we would have near the resonance energy

$$\rho_2 \, F_{11} = \left\{ \frac{-(\Gamma_1/2)}{(W - W_R) + i\,\Gamma/2} \right\} \qquad \text{(VI.17)}$$

where Γ is the total width (at half-maximum) of the supposed resonance (not to be confused with the width of the N^*) and Γ_1 is the partial width for decay of the resonance into channel 1.

($\Gamma = \sum_i \Gamma_i$, where the sum is over all accessible channels).

Defining

$$\left\{ \frac{(D^I_{1J}\, D^R_{J1}) + i(D^I_{1J}\, D^I_{J1})}{(1 - D^R_{1J}\, D^R_{J1} + D^I_{1J}\, D^I_{J1}) - i(D^R_{1J}\, D^I_{J1} + D^I_{1J}\, D^R_{J1})} \right\} \equiv \left[\frac{a_R + i\, a_I}{d_R + i\, d_I} \right] \qquad \text{(VI.18)}$$

we can write

$$\rho_2 \, F_{11} = \frac{a_R + i\, a_I}{d_R + i\, d_I} = \frac{(a_R^{\,2} + a_I^{\,2})}{(a_R d_R + a_I d_I) + i(a_R d_I - a_I d_R)} \qquad \text{(VI.19a)}$$

or

$$\rho_2 \, F_{11} = \frac{(a_R d_R + a_I d_I) - i(a_R d_I - a_I d_R)}{d_R^{\,2} + d_I^{\,2}} \, . \qquad \text{(VI.19b)}$$

Equation (VI.19a) is useful for comparison with the form of Eq. (VI.17) and (VI.19b) is convenient if we wish to examine the real and imaginary parts of $\rho_2 \, F_{11}$.

Comparing Eqs. (VI.19a) and (VI.17) we see that <u>at resonance</u>

$(\delta_R = \pi/2)$

$$a_R d_R + a_I d_I = 0 \qquad \text{(VI.20a)}$$

or

$$(a_R/a_I = - (d_I/d_R) \qquad \text{(VI.20b)}$$

and thus using (VI.20)

$$(\rho_2 F_{11})_{res.} = + i \left(\frac{\Gamma_1}{\Gamma}\right) = + i \left(\frac{a_I}{d_R}\right) = - i \left(\frac{a_R}{d_I}\right) = + i \frac{(1 + \eta)}{2} . \qquad \text{(VI.21)}$$

In terms of the elements of D_{ij}

$$\eta = \frac{D^I_{1J} D^R_{J1} - D^R_{1J} D^I_{J1}}{D^I_{1J} D^R_{J1} + D^R_{1J} D^I_{J1}} \qquad \text{(VI.22)}$$

$$\frac{\Gamma}{\Gamma_1} = 1 + \frac{D^R_{1J} D^I_{J1}}{D^I_{1J} D^R_{J1}} . \qquad \text{(VI.23)}$$

Above the threshold for inelastic scattering $\eta < 1$, and so $|\rho_2 F_{11}| \leq \frac{1 + \eta}{2} < 1$, $|d_I| > |a_R|$, $\Gamma > \Gamma_1$. The presence of inelastic scattering will cause the elastic amplitude to decrease above the inelastic threshold.

For energies below or close to the inelastic threshold (so that $\rho_3 \approx 0$), we have $D^I_{J1} \approx 0$ $(a_I \approx 0)$ and we may write

$$\rho_2 F_{11} \cong \left\{ \frac{(D^I_{1J} D^R_{J1})}{(1 - D^R_{1J} D^R_{J1}) - i(D^I_{1J} D^R_{J1})} \right\} . \qquad \text{(VI.24)}$$

Now, the resonance condition is

$$\text{Re det } D = d_R = 0 = 1 - D^R_{1J} D^R_{J1} = \det (\text{Re } D) \tag{VI.25}$$

and the unitarity limit is

$$|\rho_2 F_{11}| \leq 1. \tag{VI.26}$$

Clearly, (VI.22) and (VI.23) reduce to

$$\eta = 1 \tag{VI.27}$$

$$\frac{\Gamma}{\Gamma_1} = 1 \tag{VI.28}$$

as they should for energies below the inelastic threshold.

For reasonably narrow N^* widths ρ_3 is small for $W < W_{NN^*} = M + M^*$ (see Fig. 11) and hence any resonances below the inelastic threshold are essentially given by Eq. (VI.25).

Since the product $D^R_{1J} D^R_{J1}$ is positive, increasing the $N^*N\pi$ coupling constant, G, will bring us closer to satisfying the resonance condition and thus increase the height of any peaks (or cusps) present. The factor D^R_{J1}, defined by the principal valve integral in Eq. (VI.13), has a cusp (at the NN^* threshold) whose shape is controlled by the phase space factor ρ_3. The cusp is sharpest and most pronounced when ρ_3 rises most steeply and quickly, and this occurs when the width is narrowest and the orbital angular momentum of the NN^* state is lowest. (In our case, for $J = 2^+$, $L_{NN^*} = 0$.) For higher angular momenta or broad widths ρ_3 rises more slowly and thus shifts the

effects of the integral to higher energies, where its value is reduced.

From the resonance condition, Eq. (VI.25), it is also easy to note that the effect of each inelastic channel (J = 3,4,5,6) is additive - each one adds to the attraction and increases the likelihood of a resonance.

We can briefly observe a few other general properties of our solution.

From Eq. (VI.15) we see that for very large coupling constant the 1 in det D may be neglected and $\rho_2 F_{11}$ becomes independent of the magnitude of G with $|\rho_2 F_{11}|$ near its unitarity limit if $|D^R_{1J}| \ll |D^I_{1J}|$ for all J. The inelastic amplitude (see Eq. (VI.9)) $F_{J1} \to 0$ like $\frac{1}{G}$ as $G \to \infty$. When such strong coupling is present there is a decoupling between the NN and NN^* channels and the transition between the two- and three-particle states will not be a permanent (asymptotic) one. However, we must be a little cautious in drawing simple general conclusions about the large G limit because it is well-known from the study of several soluble models[13,12] that ghost poles will appear for G sufficiently large.

In the weak coupling limit: $G \to 0$, and both F_{1J} and $F_{J1} \to B_{1J} \propto G$ and $F_{11} \to - B_{1J} D_{J1} \propto G^2 \to 0$.

VII. RESULTS AND CONCLUSIONS

Our numerical results are summarized in Figures 13 - 20. Usually what has been plotted is the square of the elastic NN scattering amplitude, $|\rho_2 F_{11}|^2$, versus c.m. energy so that the unitarity limit (below the inelastic threshold) for the elastic channel is 1.

In Figures 13, 14, 15, we show the dependence of $|\rho_2 F_{11}|^2$ on the $N^*N\pi$ coupling constant for three different values of the N^* width Γ = 1, 25, and 125 MeV. The quantity A is directly proportional to the coupling constant G. For $A \gtrsim 1$ the curves become rather flat; we seem by then to have saturated the elastic amplitude with inelastic forces. The peaking seems to move to somewhat lower energies and there is a possibility "ghosts" have appeared in our solution (see further comments later in this section). From these figures we note the general features that increasing the coupling constant causes cusps to grow and become more prominent until they become rather flat and near the unitarity limit below the inelastic threshold but fall off rather sharply above that point. For small widths the peaks display a definite asymmetry as the lower energy side grows to the unitarity limit with increasing coupling constant but the high energy side approximately maintains its shape. As the width of the N^* becomes larger the cusps become less distinct - they are "woolier" (more rounded).

Also now the loss of symmetric shape with increasing coupling constant, though still present, is less noticeable. In comparing these figures one should remember that the width of the N^* and the

Figure 13

The elastic NN scattering amplitude squared with an N^* width of 1 MeV for different values of the πNN^* coupling constant. For these curves $W_0 = 1.86$ BeV and $W_c = 500$ BeV

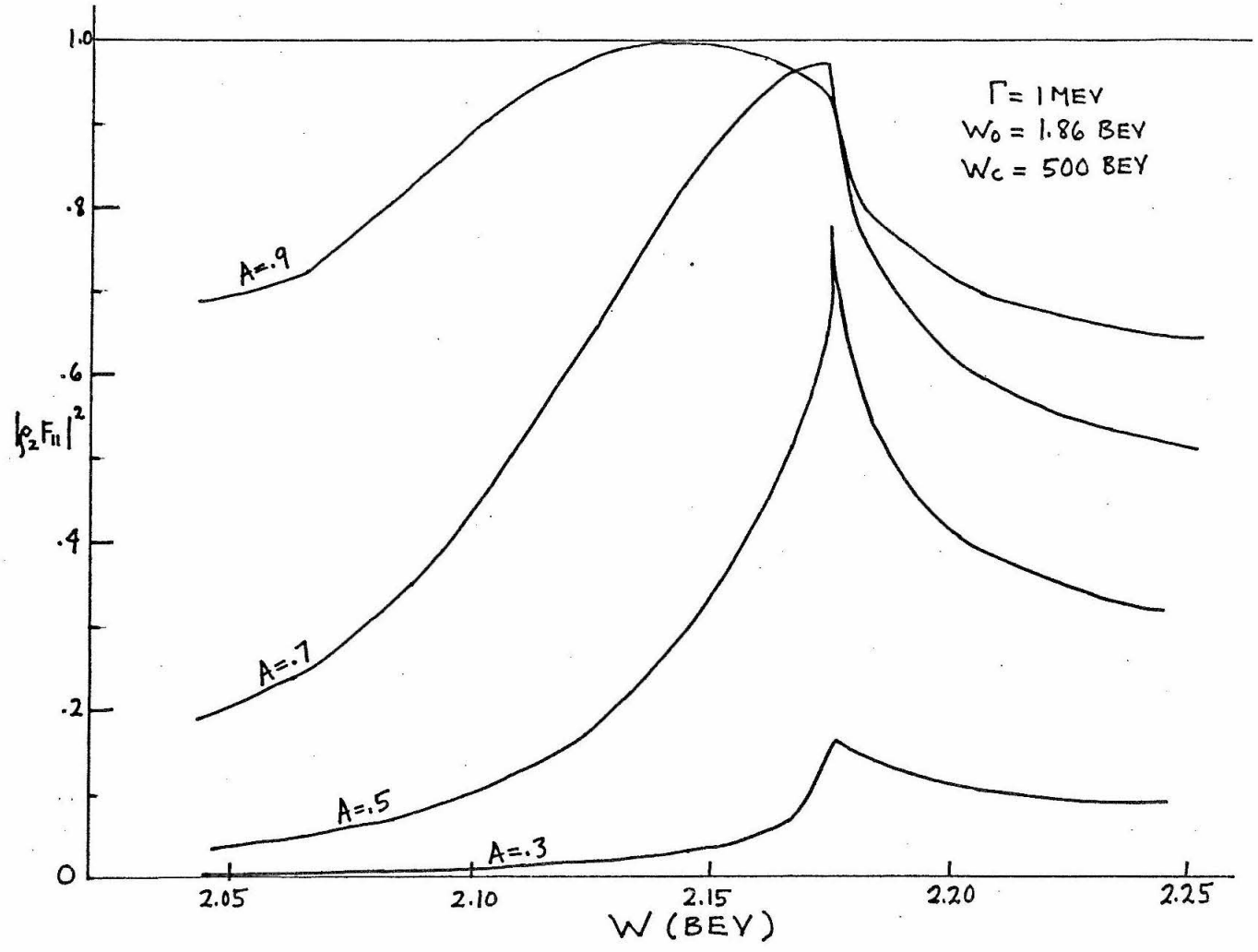
1.0
.8
.6
.4
.2
0
$|\rho_2 F_{11}|^2$
A=.9
A=.7
A=.5
A=.3
Γ= 1 MEV
W_0 = 1.86 BEV
W_c = 500 BEV
2.05
2.10
2.15
2.20
2.25
W (BEV)

Figure 14

The elastic NN scattering amplitude squared with an N^* width of 25 MeV for different values of the πNN^* coupling constant. For these curves

$$W_0 = 1.86 \text{ and } W_c = 500$$

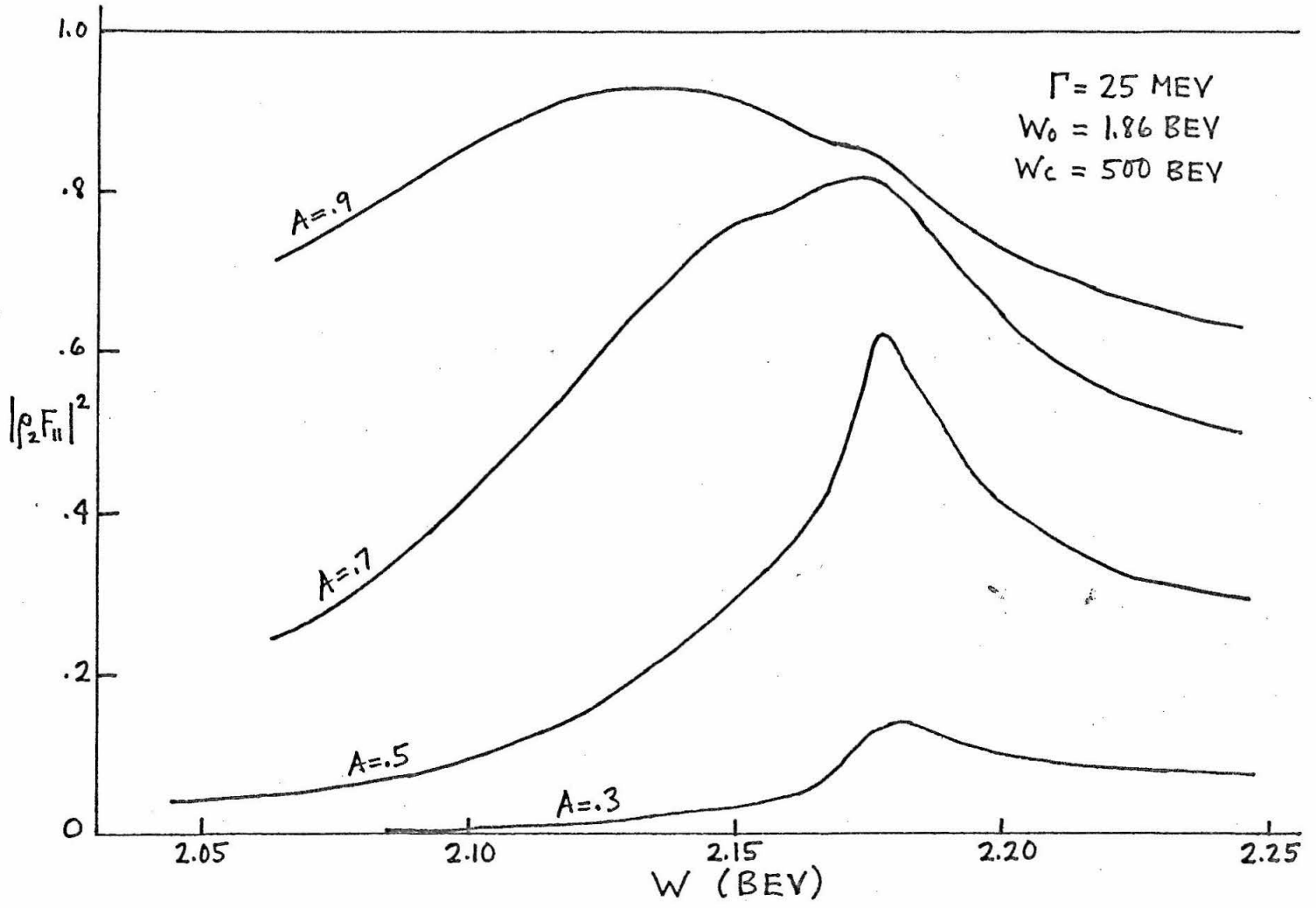
Γ = 25 MEV
W₀ = 1.86 BEV
Wc = 500 BEV
A=.9
A=.7
A=.5
A=.3
1.0
.8
.6
.4
.2
0
$|f_2 F_{11}|^2$
2.05
2.10
2.15
2.20
2.25
W (BEV)

Figure 15

The elastic NN scattering amplitude squared with an N^* width of 125 MeV for different values of the πNN^* coupling constant. For these curves

$$W_0 = 1.86 \text{ and } W_c = 500$$

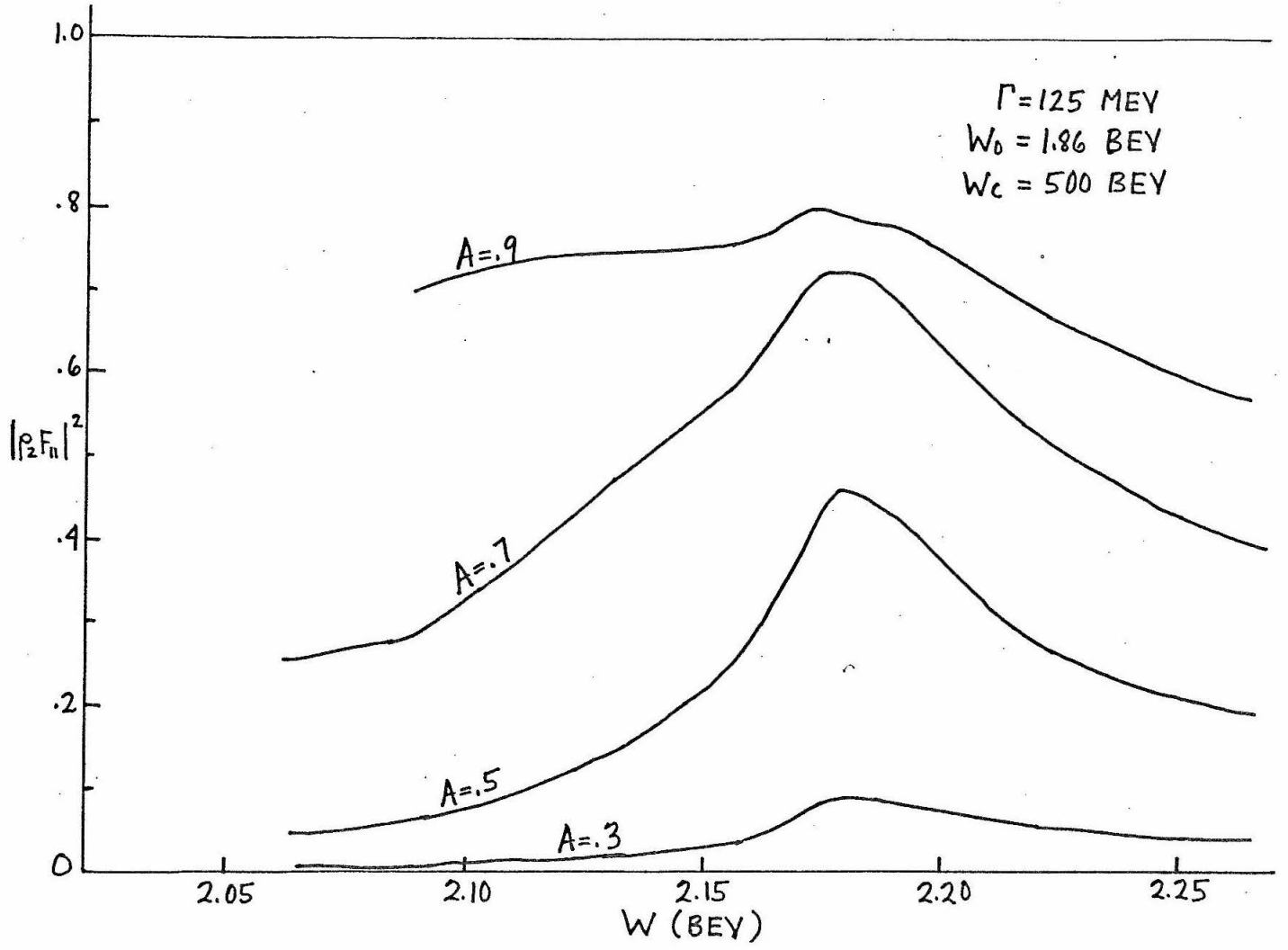
1.0
.8
.6
.4
.2
0
$|p_2 F_{11}|^2$
Γ = 125 MEV
W_0 = 1.86 BEV
W_c = 500 BEV
A=.9
A=.7
A=.5
A=.3
2.05
2.10
2.15
2.20
2.25
W (BEV)

Figure 16

The elastic NN scattering amplitude squared with input Born amplitudes assumed constant (equal to their value at the $N\overline{N}^*$ threshold) for energies below the inelastic threshold. For these curves $\Gamma(N^*) = 1$ MeV, $W_0 = 1.86$ BeV, $W_c = 500$ BeV. Compare with Figure 13.

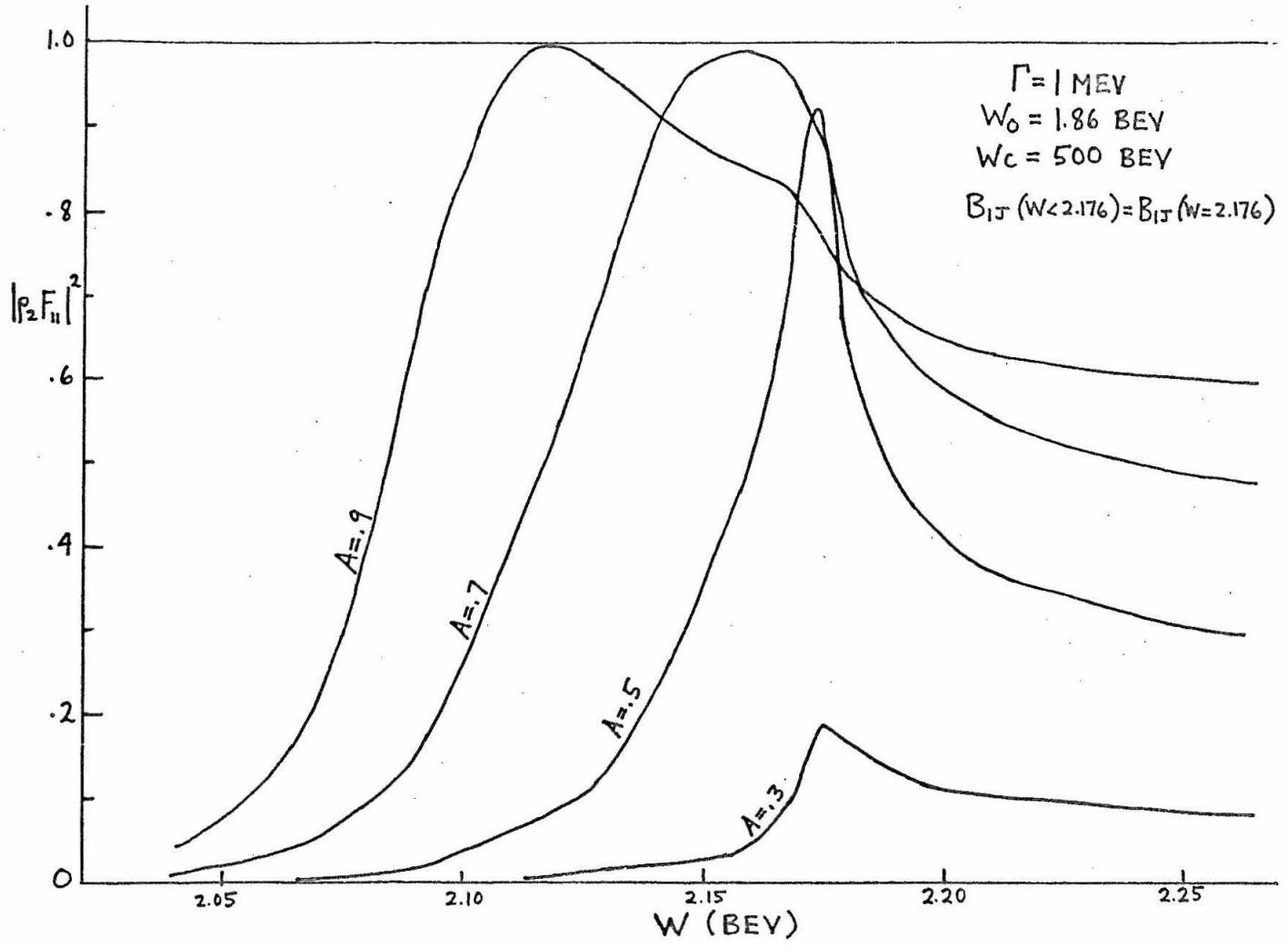
Γ = 1 MEV
W0 = 1.86 BEV
Wc = 500 BEV
B1J (W<2.176) = B1J (W=2.176)
|P2F11|2
1.0
.8
.6
.4
.2
0
A=.9
A=.7
A=.5
A=.3
2.05
2.10
2.15
2.20
2.25
W (BEV)

Figure 17

The elastic NN scattering amplitude squared with an N^* width of 1 Mev and coupling constant A = .5 for different values of the subtraction point. For these curves $W_c = 500$.

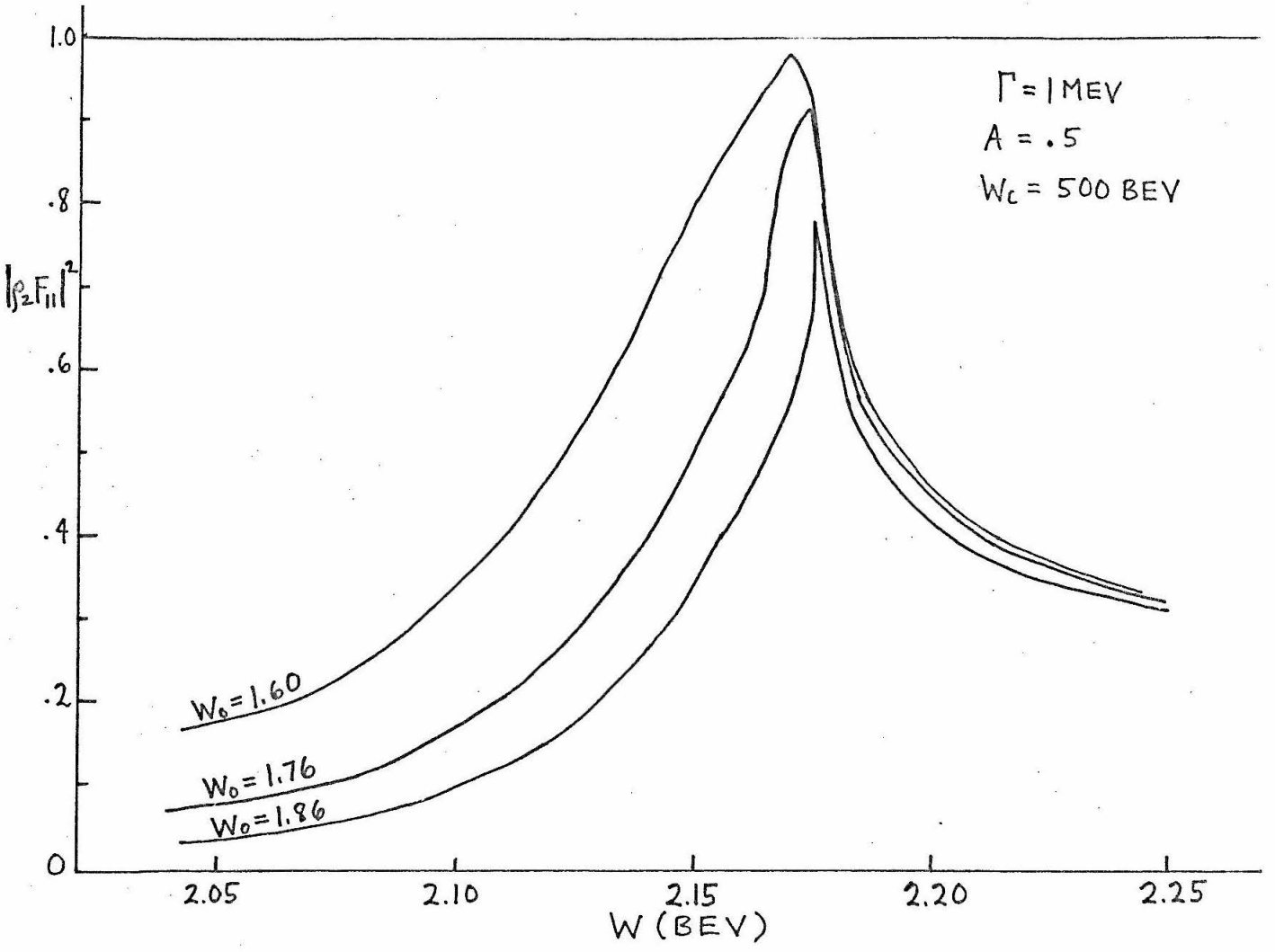
1.0
.8
.6
.4
.2
0
$|\rho_2 F_{11}|^2$
$\Gamma = 1$ MEV
$A = .5$
$W_c = 500$ BEV
$W_0 = 1.60$
$W_0 = 1.76$
$W_0 = 1.86$
2.05
2.10
2.15
2.20
2.25
W (BEV)

Figure 18

The elastic NN scattering amplitude squared with an N^* width of 1 MeV and coupling constant A = .7 for different values of the subtraction point. For these curves $W_c = 500$.

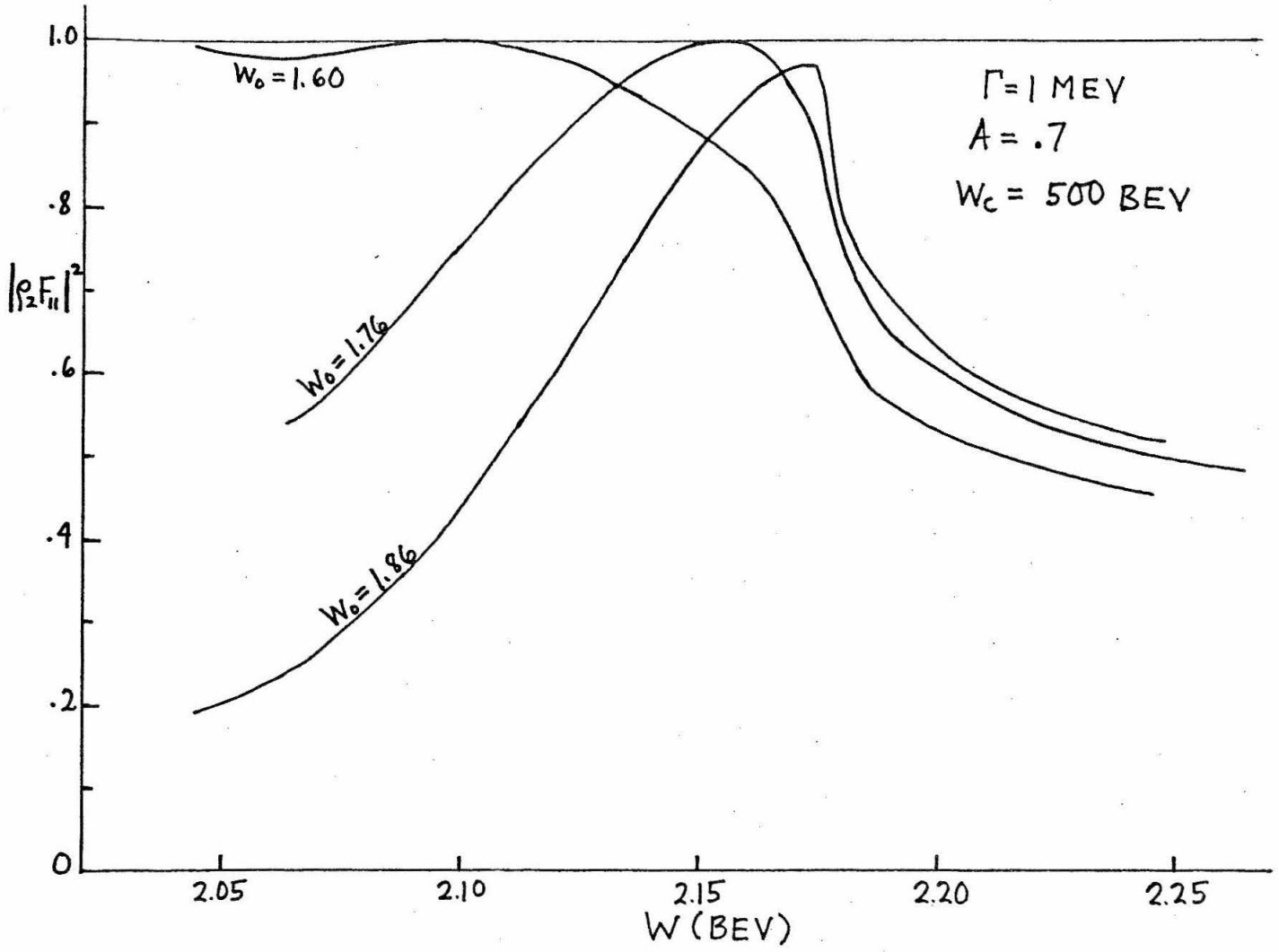
1.0
.8
.6
.4
.2
0
$|p_2 F_{11}|^2$
$W_0 = 1.60$
$W_0 = 1.76$
$W_0 = 1.86$
$\Gamma = 1$ MEV
$A = .7$
$W_c = 500$ BEV
2.05
2.10
2.15
2.20
2.25
W (BEV)

Figure 19

The elastic NN scattering amplitude squared with an N^* width of 125 MeV and coupling constant A = .7 for different values of the subtraction point. For these curves $W_c = 500$.

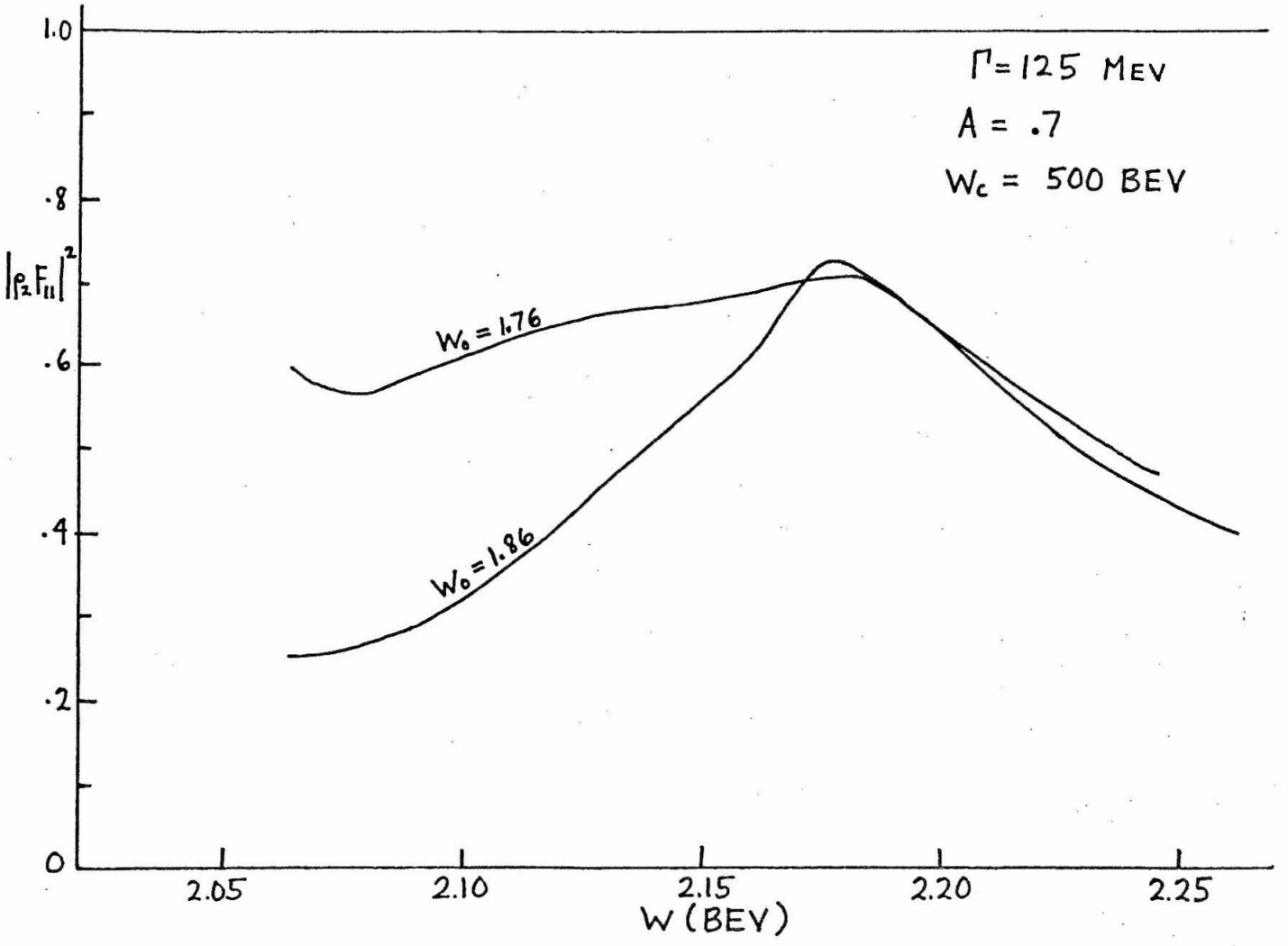
1.0
.8
.6
.4
.2
0
$|p_2 F_{11}|^2$
Γ = 125 MEV
A = .7
W_c = 500 BEV
W_0 = 1.76
W_0 = 1.86
2.05
2.10
2.15
2.20
2.25
W (BEV)

Figure 20

The elastic NN scattering amplitude squared with an N^* width of 1 MeV for different values of the cutoff energy. For these curves $W_0 = 1.86$ and $A = .7$.

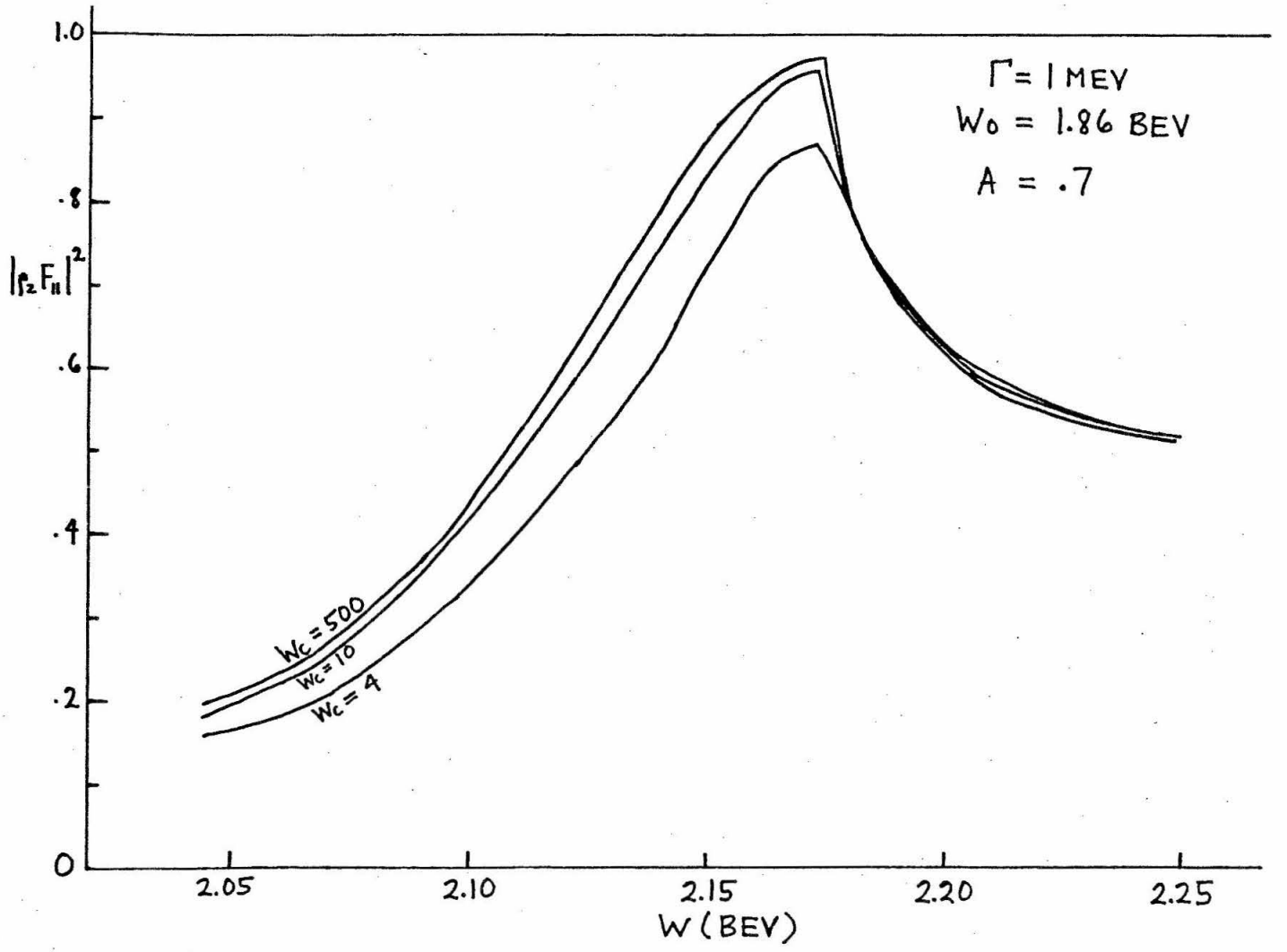
1.0
.8
.6
.4
.2
0
$|p_2 F_{11}|^2$
Γ = 1 MEV
W₀ = 1.86 BEV
A = .7
Wc = 500
Wc = 10
Wc = 4
2.05
2.10
2.15
2.20
2.25
W (BEV)

effective $N^*N\pi$ coupling are not independent quantities. From Eq. (III.15) we see that $\Gamma \propto (G)^2$ so that it is not perfectly proper to compare curves corresponding to different widths but the same A(G). Using the experimental width $\Gamma = 125$, the effective G derived from (III.15) corresponds to $A \cong 1.7$. For a smaller width A must be reduced correspondingly.

In Section V we discussed the behavior of the Born amplitude near W = 2.033 where the anomalous cut crosses the physical region. This does produce some erratic points in the elastic scattering amplitude near this energy which we have ignored for the reasons given in Section V. But, in order to get some quantitative idea of the size of the effects, we recalculated the elastic scattering amplitude using as input Born amplitudes which are constant for $W < M + M^*$; i.e., the B_{1J}'s are cut flat below the inelastic threshold with $B_{1J}(W < 2.176) = B_{1J}(W = 2.176)$. For large widths most of the differences are hidden because the peaks are so broad and flat. But in Fig. 16 we show the results for the $\Gamma = 1$ MeV case. Comparing with Fig. 13 we see that the curves are rather similar in the neighborhood of the $N\bar{N}^*$ threshold for smaller coupling constants, but as A increases the corresponding peaks for the flat B_{1J} input are slightly higher, more symmetrical, and occur at lower energies.

For the calculations represented by Figs. 13 - 16, the subtraction point is at $W_0 = 1.86$ BeV and the cutoff energy is $W_c = 500$ BeV. This value for W_c gives results essentially identical to those for $W_c \to \infty$ but for numerical reasons we could not, in practice, use

higher values for W_c.

Figures 17, 18, and 19 show the sensitivity of our results to the choice of subtraction point. Again for broad widths (Fig. 19) the effect is not so noticeable but for very narrow N^* widths (Γ = 1 MeV) the elastic scattering amplitude is clearly fairly sensitive to a variation in subtraction point. In general, the effect of reducing W_0 seems to be roughly equivalent to increasing the magnitude of the coupling constant while keeping W_0 constant; for example, the curves for $W_0 = 1.60$, A = .7 and $W_0 = 1.86$, A = 1.0 are rather similar. Reducing W_0 tends also to move the location of the peaks to slightly lower energies (see Fig. 17). As discussed in Section VI we have no very convincing argument for the placement of W_0. Recall that we did however decide a priori that $1.84 \leq W_0 \leq 1.88$ was perhaps the most reasonable region.

One feature of our results seems also to support that choice; viz., with $W_0 = 1.86$ the cusps in Figs. 17 and 18 occur at the NN^* threshold and not at lower energies as they do for $W_0 = 1.60$*). But again we must admit that the rather strong dependence of the solutions on the value of W_0 is a fairly severe weakness of the determinental method.

In Fig. 20 we illustrate the fact that our results are essentially independent of the cutoff. This is no doubt true because of the rapid convergence of the integrals for D^R_{1J} and D^R_{J1}. Only for quite low cutoffs, e.g., $W_c \leq 4$, do we start to see any change in the

---

* However, since lowering W_0 seems to be equivalent to increasing G it is not surprising that peaks move to lower energies.

solutions and then just a small reduction in the height of the peaks. We can probably conclude from this that modifying the high energy behavior of the input amplitudes (for example, a la Reggeism) would have very little effect on our results.

The inelastic amplitudes are too numerous to graph, but we can make a few general observations (based mainly on the $\Gamma = 1$ MeV case). With more than one inelastic amplitude as input, $F_{J1} \neq F_{1J}$, i.e., the determinental solution is not symmetric. (It is most symmetric for small values of the coupling constant.) What we find is that $|\sqrt{\rho_2\rho_3}\ F_{J1}|$ reach their maximum value ($\lesssim .4$) for $A \approx .5$ at $W \approx 2.20$ BeV and decrease for higher energies or larger values of the $N^*N\pi$ coupling constant. They are generally well below the unitarity limit ($|\sqrt{\rho_2\rho_3}\ F_{J1}| \leq .5$) and show no peaking at the NN^* threshold. In contrast we find that the $|\sqrt{\rho_2\rho_3}\ F_{1J}|$'s seem to steadily increase with increasing W (at least up to W = 2.32 BeV) or increasing coupling constant, and do eventually violate the unitarity limit (for $A \gtrsim .5$) although they also do not display any peaking behavior.

Based on the work of Reference 3 our results for the inelastic amplitudes suggest the possible presence of "ghosts" for coupling constant corresponding to $A \gtrsim .5$ (at least for very narrow widths). The problem of "ghosts", or spurious singularities which develop to allow the ND^{-1} equations to satisfy unitarity, cannot be properly examined without studying the properties of our solutions in a much larger region of the W plane (e.g., for $W < W_0$) than was computationally feasible for the present problem. As a result of their

work with some simple models and a similar type calculation, Ball and Thurnauer[3] suggest that any approximation which ignores the existence of complex singularities may be haunted by "ghosts".

Our numerical results also verified the increased effective attraction due to there being more than one inelastic channel.

We now may briefly summarize the conclusions to be drawn from our calculations. The $NN \rightarrow NN^*$ OPE amplitudes clearly may act to produce a cusp in the elastic NN scattering amplitude near the NN^* threshold. We found that the shape and features of this cusp-type enhancement depend in a reasonable way on the assumed width of the N^* and the $N^*N\pi$ effective coupling constant. But for the known experimental value of Γ_{N^*} the curves of Fig. 15 indicate that the cusp is so "wooly" that the resulting "peak" is likely to be too broad and flat to be experimentally prominent. The rather large width of the N^* means that there is much inelasticity present near the N-stable N^* threshold (W = 2.176 BeV) and this necessarily reduces the height of the elastic peak even for resonant-like real phase shifts. Naturally, we would be unjustified in drawing <u>quantitative</u> experimental predictions from these approximate calculations since we have omitted so much of the true complexity of the problem (including all elastic NN, NN^* forces, other channels, etc.).

In fact, if present experimental evidence (cited in Section I) is confirmed, it is likely that the <u>magnitude</u> of the real part of the phase shift in this energy region near the inelastic threshold can be adequately explained solely by the elastic NN one-boson-exchange (OBE)

forces of Scotti and Wong*). Our model predicts real phase shifts close to 90°**) and therefore, we must conclude that we have omitted significant repulsive forces from our calculation, perhaps those due to OPE in the elastic NN^* channel and forces due to particles besides the pion being exchanged. However, when more detailed experimental results are available we may find that the detailed <u>shape</u> of the $^1D_2$ NN phase shift near the NN^* threshold is influenced by the $NN \rightarrow NN^*$ production amplitudes. And certainly some inelasticity is needed to damp the elastic amplitude at higher energies.

The total computer time expended for this project excluding that wasted in programming errors was about one and a half hours. All calculations were done on the CIT IBM 7040-7094 computer system.

We should briefly mention two other papers which have also considered the influence of the NN^* channel on elastic NN scattering. The work of Leung[26] is rather similar to our own but the following

---

* This can be seen from the dashed curve in the figures of reference 27 which show that with the Scotti-Wong elastic NN OBE forces (reference 24) as sole dynamical input, real phase shifts on the order of 13° (at 600 MeV lab energy) are obtained. The author is indebted to Professor Scotti for a discussion of this point.

** Writing $(\rho_2 F_{11})$ in the form of Eq. (VI.16) one can show that $\eta^2 = 1 - 4[\mathrm{Im}(\rho_2 F_{11}) - |\rho_2 F_{11}|^2]$ and $\sin^2 \delta_R = \frac{1}{2}[1 + \frac{2\mathrm{Im}(\rho_2 F_{11})-1}{\eta}]$. Using our numerical results for $\mathrm{Im}(\rho_2 F_{11})$ and $|\rho_2 F_{11}|^2$ we can thus extract values for η and δ_R. When this is done for values of $A \geq .6$ we find (even for broad widths) that δ_R exceeds 80° for some energies close to the NN^* threshold. But the present experimental values of δ_R lie in the range 8° - 15°.

differences may be noted:

1. He calculates no elastic $NN^* \to NN^*$ forces;
2. His inelastic $NN \to NN^*$ OPE amplitudes do not agree with ours; e.g., he has $B_{16} \equiv 0$, and some of his amplitudes seem to have incorrect threshold behavior;
3. In performing the dynamical calculation he combines all of the (four) inelastic amplitudes into one "averaged" amplitude;
4. His calculation consists of a modified pole approximation to the ND^{-1} equations;
5. He does not vary the N^* width;
6. From his Fig. 6 it seems that the input averaged inelastic amplitude has been cut flat for $W < M + M^*$.

Coulter, Scotti, and Shaw[27] use the single channel N/D equations modified to take into account inelastic processes by means of the factor $\eta (= e^{-2\delta_I})$. The elastic NN forces due to multi-meson exchanges (calculated by Scotti and Wong[24]) are included but the inelasticity factor η is taken from experiment for lab energies < 800 MeV with several different asymptotic forms assumed for η at high energy. They find that δ_{1D_2} generally peaks at 400 - 500 MeV (with $\delta \sim 16^o$) and goes negative for $T_{lab} \gtrsim 1$ BeV. However, we note that recent work by several authors[46] indicates that one must be cautious in using the one channel N/D method with inelastic unitarity instead of the more correct multi-channel ND^{-1} equations.

There are many obvious ways in which our calculation could be improved or extended. We could include elastic NN and NN^* forces*) and interactions arising from other than pion exchange. Instead of the determinental method we could solve the full ND^{-1} equations. Other channels (e.g., π^+D) might be added. And of course, there are many J^P states besides 2^+ which could be studied[47].

---

* The model calculations of Frazer and Hendry, Ref. 12, indicate that an attractive elastic $NN^* \rightarrow NN^*$ force has the reasonable effect of increasing the strength of attraction in the elastic NN channel.

VIII. IMPLICATIONS OF SU_3 SYMMETRY

The results presented in the last section indicate an enhancement in the I = 1, $^1D_2$ NN state near the NN^* threshold ($\approx$ 2175 MeV c.m. energy). Because of the broad width of the N^*, our model predicts any peaking would not tend to be experimentally prominent and this seems to be in agreement with the data. But aside from the detailed predictions of any particular approximate model it is interesting to investigate what the implications of the Eightfold Way symmetry scheme[48,49] are, assuming some such NN $^1D_2$ enhancement exists and corresponds to a bound or resonant state.

In SU_3 we have the following decompositions into irreducible representations:

$$8 \times 8 = 1 + 8 + 8 + \overline{10} + 10 + 27$$

$$8 \times 10 = 8 + 10 + 27 + 35$$

$$10 \times 10 = \overline{10} + 27 + 28 + 35$$

The nucleon is assumed to belong to an octet (8) and the N^* isobar to a decuplet (10). Only the 27 multiplet has a Y = 2, I = 1 piece (which could correspond to the NN $^1D_2$ state) and is contained in 8 x 8, 8 x 10, and 10 x 10[50].

Thus, if SU_3 were an exact symmetry, we would expect all of the other members of the 27 to exist in nature as $J = 2^+$, B = 2 bound or resonant states of mass $\sim$ 2175 MeV. The 27 contains the following states

$Y = 2;\ I = 1$

$Y = 1;\ I = 1/2,\ 3/2$

$Y = 0;\ I = 0,1,2$

$Y = -1;\ I = 1/2,\ 3/2$

$Y = -2;\ I = 1$

However, it is well-known that SU_3 is not exact and thus the masses will not all be equal. Assuming octet breaking of SU_3 *), the masses will be given by the Gell-Mann - Okubo mass formula

$$M = a + bY + c[I(I + 1) - Y^2/4]$$

or, for J = 2 states since they are formally bosons

$$M^2 = \alpha + \beta Y + \gamma[I(I + 1) - Y^2/4] \ .$$

In Table IV we have listed the predicted octet splitting for each member of the 27.

---

* We expect octet breaking to be dominant with maybe a small amount of 27, 64, and other representations present.

(Y,I)	$M = a + bY + c[I(I+1) - Y^2/4]$	$M^2 = \alpha + \beta Y + \gamma[I(I+1) - Y^2/4]$
(2, 1)	$a + 2b + c$	$\alpha + 2\beta + \gamma$
(1, 3/2)	$a + b + 7/2\ c$	$\alpha + \beta + 7/2\ \gamma$
(1, 1/2)	$a + b + 1/2\ c$	$\alpha + \beta + 1/2\ \gamma$
(0, 2)	$a + 6\ c$	$\alpha + 6\ \gamma$
(0, 1)	$a + 2\ c$	$\alpha + 2\ \gamma$
(0, 0)	a	α
(-1, 1/2)	$a - b + 1/2\ c$	$\alpha - \beta + 1/2\ \gamma$
(-1, 3/2)	$a - b + 7/2\ c$	$\alpha - \beta + 7/2\ \gamma$
(-2, 1)	$a - 2b + c$	$\alpha - 2\beta + \gamma$

Table IV

Octet Breaking of the 27

Gerstein[51] has given the expansion of the 27 in terms of baryon-baryon states for each Y, I, I_z state.

What is the experimental evidence concerning possible manifestations of the proposed 27? Except for the pp $^1D_2$ cusp-type enhancement[52] the experimental data is rather meager. Besides NN the only two-baryon states which have been studied to any extent are ΣN and ΛN. And here the best evidence seems to be a possible Λp peak at 2360 MeV[53]. There is also a possible $\Lambda^o n$ peak (Y = 1, I = 1/2) at 2098 MeV[54]. Several other low energy Λp peaks have been seen but these are probably S-wave interactions and thus not $J = 2^+$ states.

On the basis of our dynamical model for NN $^1D_2$ enhancement we expect other members of the 27 to also be associated with thresholds for the inelastic reaction $8 + 8 \rightarrow 8 + 10$. Therefore we make the following table:

(Y,I)	Allowed 8 + 8 states (and c.m. threshold)	Coupled 8 + 10 states (c.m. threshold)
(2,1)	NN(1876)	NN^*(2176)
(1, 3/2)	ΣN (2131)	NY_1^*(2323), ΛN^*(2353), ΣN^*(2431)
(1, 1/2)	ΣN(2131), Λ N (2053)	NY_1^*(2323), ΣN^*(2431)
(0,2)	$\Sigma\Sigma$(2386)	ΞN^*(2555), ΣY_1^*(2578)
(0,1)	ΞN (2255), $\Lambda\Sigma$(2308), $\Sigma\Sigma$(2386)	$N\Xi^*$(2468), ΣY_1^*(2578), ΛY_1^*(2500), ΞN^*(2555)
(0, 0)	ΞN (2255), $\Lambda\Lambda$(2230), $\Sigma\Sigma$(2386)	$N\Xi^*$(2468), ΣY_1^*(2578)
(-1, 1/2)	$\Lambda\Xi$ (2432), $\Sigma\Xi$ (2510)	N Ω^-(2613), $\Lambda\Xi^*$(2645), $\Sigma\Xi^*$(2723), ΞY_1^*(2702)
(-1, 3/2)	$\Sigma\Xi$ (2510)	$\Sigma\Xi^*$(2723), ΞY_1^*(2702)
(-2,1)	$\Xi\Xi$ (2634)	$\Sigma\Omega^-$(2868), $\Xi\Xi^*$(2847)

Table V

Allowed B = 2, 8 + 8, 8 + 10 states in the 27

If we make the assumption that the masses of the members of the 27 will lie near one of the thresholds for the coupled 8 + 10 states, then we can use this table to get approximate values for the constants (a,b,c or α,β,γ) appearing in the Gell-Mann - Okubo (GMO) mass formula. Let us choose three values and then predict the others. We pick the three by looking for (Y,I) states where the allowed 8 + 10 thresholds have a narrow energy spread and then use the average of the inelastic threshold energies. We decided to use the following three (Y,I) states.

$(2,1)$: $a + 2b + c = 2176$ or $\alpha + 2\beta + \gamma = (2176)^2$

$(0,2)$: $a + 6c = 2565$ or $\alpha + 6\gamma = (2565)^2$

$(-2,1)$: $a - 2b + c = 2857$ or $\alpha - 2\beta + \gamma = (2857)^2$

Solving, we find $a = 2507$, $b = -170$, $c = 9.7$; and $\alpha = 6.42 \times 10^6$, $\beta = -.857 \times 10^6$, $\gamma = .0261 \times 10^6$. With these values the GMO formulae predict the masses given in Table VI.

(Y,I)	M(linear GMO formula)	M(quadratic GMO formula	Experimental 8 + 10 threshold energies
(1, 3/2)	2372	2378	2323, 2353, 2431
(1, 1/2)	2342	2362	2323, 2431
(0, 1)	2526	2544	2468, 2578, 2500, 2555
(0, 0)	2507	2534	2468, 2578
(-1, 1/2)	2682	2700	2613, 2645, 2723, 2702
(-1, 3/2)	2712	2714	2723, 2702

Table VI.

Predicted octet mass splitting of the 27 assuming three members lie near to inelastic $8 + 8 \rightarrow 8 + 10$ thresholds

It is not very surprising that the predicted masses lie close to the 8 + 10 inelastic thresholds since the masses M_8 and M_{10} are themselves known to follow the pattern of octet splitting.

The results of our dynamical calculation suggest that it might be worthwhile to do a similar calculation using other members of the 8 and 10 multiplets; for example, if the experimental evidence for a 2360 Λp peak becomes convincing it would be interesting to look at the ΛN, NY_1^*, ΣN^* coupled channel problem. Aside from differences in i-spin factors some of the amplitudes are the same as those for the NN, NN^* problem.

Among the other work which has been done on the two-baryon system and SU_3 is that of Gerstein[51] on the $^1S_0$ NN virtual state as part of a 27 and that of Oakes[55] on the deuteron as part of a $\overline{10}$. Dyson and Xuong[56] have looked at Y = 2 states in SU_6 theory.

Appendix A. NOTATION AND KINEMATICS

We define the scalar product

$$x \cdot y = x_0 y_0 - \vec{x} \cdot \vec{y} = x_\mu \delta_{\mu\nu} y_\nu = x_\mu y_\mu \tag{A.1}$$

with metric tensor $\delta_{\mu\nu} = 0$ for $\mu \neq \nu$ and

$$\delta_{00} = - \delta_{11} = - \delta_{22} = - \delta_{33} = 1. \tag{A.2}$$

Then

$$\gamma_\mu \gamma_\nu + \gamma_\nu \gamma_\mu = 2\delta_{\mu\nu} \tag{A.3}$$

$$\gamma_0^{\,2} = - \gamma_1^{\,2} = - \gamma_2^{\,2} = - \gamma_3^{\,2} = 1 \tag{A.4}$$

where

$$\gamma_0 = \begin{pmatrix} 1 & 0 \\ 0 & -1 \end{pmatrix} \quad , \vec{\gamma} = \begin{pmatrix} 0 & \vec{\sigma} \\ -\vec{\sigma} & 0 \end{pmatrix} \quad , \quad \gamma_5 = \gamma_1\gamma_2\gamma_3\gamma_0 = + \begin{pmatrix} 0 & i \\ i & 0 \end{pmatrix} \tag{A.5}$$

with

$$\sigma_1 = \begin{pmatrix} 0 & 1 \\ 1 & 0 \end{pmatrix} \quad , \sigma_2 = \begin{pmatrix} 0 & -i \\ i & 0 \end{pmatrix} , \quad \sigma_3 = \begin{pmatrix} 1 & 0 \\ 0 & -1 \end{pmatrix} . \tag{A.6}$$

We define $\not{a} = a_\mu \gamma_\mu$ for any four vector a_μ. We use the following symbols and numerical values

μ = pion mass = 139 MeV

M = nucleon mass = 938 MeV

M^* = N^* mass = 1238 MeV

W = total c.m. energy

$S = W^2$

g = πNN coupling constant ($g^2/4\pi \cong 15.$)

G = effective πNN^* coupling constant

q = c.m. momentum for elastic NN^* scattering

p,p' = c.m. momentum of NN, NN^* states, respectively, for

$N + N \rightarrow N + N^*$ scattering.

$E_i = \sqrt{p_i^2 + m_i^2}$ = energy of particle i in c.m.

θ = c.m. scattering angle.

I. For $N + N^* \rightarrow N + N^*$ scattering in the c.m. we have

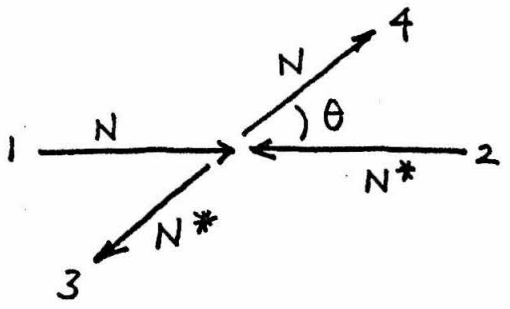

$$p_1 = (E_1, 0, 0, q) \tag{A.7a}$$

$$p_2 = (E_2, 0, 0, -q) \tag{A.7b}$$

$$p_3 = (E_3, -q \sin\theta, 0, -q \cos\theta) \tag{A.7c}$$

$$p_4 = (E_4, +q \sin\theta, 0, +q \cos\theta) \tag{A.7d}$$

where

$$E_1 = E_4 = \sqrt{q^2 + M^2} = \frac{W^2 + M^2 - M^{*2}}{2W} \tag{A.8}$$

$$E_2 = E_3 = \sqrt{q^2 + M^{*2}} = \frac{W^2 + M^{*2} - M^2}{2W} \tag{A.9}$$

$$W = E_1 + E_2 = E_3 + E_4 \tag{A.10}$$

$$S = W^2 = (p_1 + p_2)^2 = (p_3 + p_4)^2 \tag{A.11}$$

$$q^2 = \frac{[W^2 - (M^* + M)^2][W^2 - (M^* - M)^2]}{4W^2} \tag{A.12a}$$

$$= \frac{[(W + M)^2 - M^{*2}][(W - M)^2 - M^{*2}]}{4W^2} \tag{A.12b}$$

II. Now consider the reaction $N + N \rightarrow N + N^*$

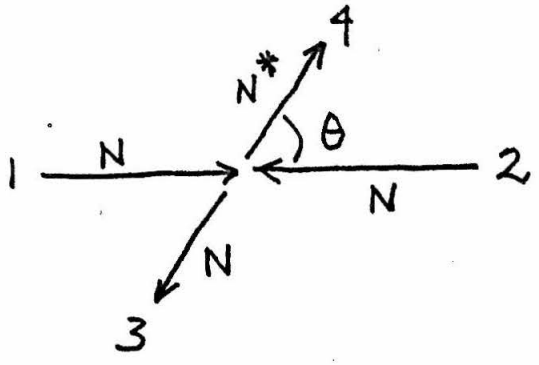

In the c.m.

$$p_1 = (E_1, 0, 0, p) \tag{A.13a}$$

$$p_2 = (E_2, 0, 0, -p) \tag{A.13b}$$

$$p_3 = (E_3, -p' \sin\theta, 0, -p' \cos\theta) \tag{A.13c}$$

$$p_4 = (E_4, +p' \sin\theta, 0, +p' \cos\theta) \tag{A.13d}$$

$$E_1 = E_2 = \frac{W}{2} = \sqrt{p^2 + M^2} \tag{A.14}$$

$$E_3 = \sqrt{p'^2 + M^2} = \frac{W^2 + M^2 - M^{*2}}{2W} \tag{A.15}$$

$$E_4 = \sqrt{p'^2 + M^{*2}} = \frac{W^2 + M^{*2} - M^2}{2W} \tag{A.16}$$

$$W = E_1 + E_2 = E_3 + E_4 \tag{A.17}$$

$$S = W^2 = (p_1 + p_2)^2 = (p_3 + P_4)^2 \tag{A.18}$$

$$p^2 = \left(\frac{W^2}{4} - M^2\right) = \frac{(W + 2M)(W - 2M)}{4} \tag{A.19}$$

$$p'^2 = \frac{[W^2 - (M^* + M)^2][W^2 - (M^* - M)^2]}{4W^2} \tag{A.20}$$

$$E_3 \pm M = \frac{(W \pm M)^2 - M^{*2}}{2W} \tag{A.21}$$

$$E_4 \pm M^* = \frac{(W \pm M^*)^2 - M^2}{2W} \tag{A.22}$$

Appendix B. DESCRIPTION OF HELICITY STATES AND CALCULATION OF THE OPE PARTIAL WAVE HELICITY AMPLITUDES

We write for positive energy spinors

$$u(\pm \tfrac{1}{2}) = \sqrt{\frac{E+M}{2M}} \left(1 + \frac{\vec{\alpha}\cdot\vec{p}}{E+M}\right) \begin{pmatrix} |\pm \frac{1}{2}\rangle \\ 0 \end{pmatrix} \tag{B.1}$$

where

$$\left(1 + \frac{\vec{\alpha}\cdot\vec{p}}{E+M}\right) = \begin{pmatrix} 1 & \frac{\vec{\sigma}\cdot\vec{p}}{E+M} \\ \frac{\vec{\sigma}\cdot\vec{p}}{E+M} & 1 \end{pmatrix} \tag{B.2}$$

and

$$\tfrac{1}{2}\vec{\sigma}\cdot\hat{p}\,|\hat{p},\lambda\rangle = \lambda|\hat{p},\lambda\rangle$$

with

$$\lambda = \pm 1/2 \tag{B.3}$$

so

$$u(\pm \tfrac{1}{2}) = \sqrt{\frac{E+M}{2M}} \begin{pmatrix} |\pm 1/2\rangle \\ \frac{2\lambda p}{E+M}\,|\pm 1/2\rangle \end{pmatrix} \tag{B.4}$$

and

$$\bar{u}(\pm \tfrac{1}{2}) = u^{+}\gamma_0 = \sqrt{\frac{E+M}{2M}} \left(\langle \pm \tfrac{1}{2} | \frac{-2\lambda p}{E+M} \langle \pm \tfrac{1}{2}|\right) . \tag{B.5}$$

For a particle moving in the $\theta,\varphi = 0$ direction

$$|+\tfrac{1}{2}\rangle = \begin{pmatrix} \cos\theta/2 \\ \sin\theta/2 \end{pmatrix} \tag{B.6a}$$

$$|-\tfrac{1}{2}\rangle = \begin{pmatrix} -\sin\theta/2 \\ \cos\theta/2 \end{pmatrix} \tag{B.6b}$$

and if moving in the direction $\pi - \theta$, $\varphi + \pi$ ($\varphi = 0$)

$$|+\tfrac{1}{2}\rangle = \begin{pmatrix} -\sin\theta/2 \\ \cos\theta/2 \end{pmatrix} \tag{B.7a}$$

$$|-\tfrac{1}{2}\rangle = \begin{pmatrix} \cos\theta/2 \\ \sin\theta/2 \end{pmatrix} \tag{B.7b}$$

The spin 1 four-vectors satisfy

$$k_\mu \epsilon_\mu = 0 \tag{B.8}$$

$$\epsilon_\mu^* \epsilon_\mu = -1 \tag{B.9}$$

Writing $\epsilon_\mu = (\epsilon_0, \vec{\epsilon})$, we have

$$\vec{\epsilon}(+1) = \begin{pmatrix} -\cos\theta \\ -i \\ \sin\theta \end{pmatrix} \tag{B.10a}$$

$$\vec{\epsilon}(0) = \begin{pmatrix} \sin\theta \\ 0 \\ \cos\theta \end{pmatrix} \tag{B.10b}$$

$$\vec{\epsilon}(-1) = \begin{pmatrix} \cos\theta \\ -i \\ -\sin\theta \end{pmatrix} \tag{B.10c}$$

for a particle moving in the θ, $\varphi = 0$ direction. If it is moving in the $\pi - \theta$, $\varphi = \pi$ direction the $\vec{\epsilon}$'s are the same with the ± 1 states interchanged.

Using (B.8) and (B.9) we construct four-vectors from the three-vectors of Eq. (B.10)

$$\epsilon_\mu(+1) = \frac{1}{\sqrt{2}} \begin{pmatrix} 0 \\ -\cos\theta \\ -i \\ \sin\theta \end{pmatrix} \tag{B.11a}$$

$$\epsilon_\mu(0) = \frac{1}{M^*} \begin{pmatrix} k \\ E \sin\theta \\ 0 \\ E \cos\theta \end{pmatrix} \tag{B.11b}$$

$$\epsilon_\mu(-1) = \frac{1}{\sqrt{2}} \begin{pmatrix} 0 \\ \cos\theta \\ -i \\ -\sin\theta \end{pmatrix} \tag{B.11c}$$

If we reverse the direction of motion ($\pi - \theta$, $\varphi = \pi$), $\epsilon_\mu(+1)$ and $\epsilon_\mu(-1)$ change places and the time component of $\epsilon_\mu(0)$ changes sign.

We now list some of the quantities which were used in the calculation of the helicity amplitudes.

I. $N + N^* \to N + N^*$ (see Appendix A for kinematical definitions and conventions)

$$\langle \lambda_4 | \lambda_2 \rangle = \begin{cases} \sin\theta/2 & (+\,+) \\ -\sin\theta/2 & (-\,-) \\ \cos\theta/2 & (+\,-) = (-\,+) \end{cases} \tag{B.12}$$

where $(+\,-) = \langle \lambda_4 = +\frac{1}{2} | \lambda_2 = -\frac{1}{2} \rangle$, etc.

$$\langle \lambda_3 | \lambda_2 \rangle = \begin{cases} -\sin\theta/2 & (+\,+) \\ \sin\theta/2 & (-\,-) \\ \cos\theta/2 & (+\,-) = (-\,+) \,. \end{cases} \tag{B.13}$$

Define $\bar{u}(\lambda_4)\, u(\lambda_2)\, \bar{u}(\lambda_3)\, u(\lambda_1) = (\lambda_4\lambda_2\lambda_3\lambda_1)$

Then

$$(+\,+\,+\,+) = (-\,-\,-\,-) = -(-\,-\,+\,+) = -\,(+\,+\,-\,-)$$

$$= -\left(\frac{E_1 + M}{2M}\right)\left(\frac{E_2 + M^*}{2M^*}\right) \sin^2 \theta/2 \quad \left[1 - \frac{q^2}{(E_1 + M)(E_2 + M^*)}\right]^2$$

(B.14a)

$$(+\,-\,+\,+) = (-\,+\,+\,+) = (-\,-\,+\,-) = (-\,-\,-\,+)$$

$$= -\,(+\,-\,-\,-) = -\,(-\,+\,-\,-) = -\,(+\,+\,+\,-\,) = -\,(+\,+\,-\,+)$$

$$= -\left(\frac{E_1 + M}{2M}\right)\left(\frac{E_2 + M^*}{2M^*}\right) \sin \theta/2 \cos \theta/2 \cdot$$

$$\cdot \left[1 - \frac{q^4}{(E_1 + M)^2 (E_2 + M^*)^2}\right]$$

(B.14b)

$$(+\,-\,+\,-) = (-\,+\,+\,-) = (+\,-\,-\,+) = (-\,+\,-\,+)$$

$$= +\left(\frac{E_1 + M}{2M}\right)\left(\frac{E_2 + M^*}{2M^*}\right) \cos^2 \theta/2 \left[1 + \frac{q^2}{(E_1 + M)(E_2 + M^*)}\right]^2$$

(B.14c)

$$\epsilon_\nu^+(1)\ (p_1)_\nu = \frac{1}{\sqrt{2}}\ q \sin \theta \qquad \text{(B.15a)}$$

$$\epsilon_\nu^+(0)\ (p_1)_\nu = -\frac{1}{M^*}\ (q\,E_1 + q\,E_3 \cos \theta) \qquad \text{(B.15b)}$$

$$\epsilon_\nu^+(-1)\,(p_1)_\nu = -\frac{1}{\sqrt{2}}\, q \sin \theta \qquad \text{(B.15c)}$$

$$(p_4)_\mu\ \epsilon_\mu(1) = -\frac{1}{\sqrt{2}}\, q \sin \theta \qquad \text{(B.16a)}$$

$$(p_4)_\mu \, \epsilon_\mu(0) = - \frac{1}{M^*} (q E_4 + q E_2 \cos\theta) \qquad \text{(B.16b)}$$

$$(p_4)_\mu \, \epsilon_\mu(-1) = \frac{1}{\sqrt{2}} q \sin\theta. \qquad \text{(B.16c)}$$

II. $N + N \rightarrow N + N^*$

$$\langle \lambda_4 | \lambda_2 \rangle = \begin{cases} \sin\theta/2 & (+\,+) \\ -\sin\theta/2 & (-\,-) \\ \cos\theta/2 & (+\,-) = (-\,+) \end{cases} \qquad \text{(B.17)}$$

$$\langle \lambda_3 | \lambda_1 \rangle = \begin{cases} -\sin\theta/2 & (+\,+) \\ \sin\theta/2 & (-\,-) \\ \cos\theta/2 & (+\,-) = (-\,+) \end{cases} \qquad \text{(B.18)}$$

$$\langle \lambda_4 | \lambda_1 \rangle = \begin{cases} \cos\theta/2 & (+\,+) = (-\,-) \\ \sin\theta/2 & (+\,-) \\ -\sin\theta/2 & (-\,+) \end{cases} \qquad \text{(B.19)}$$

$$\langle \lambda_3 | \lambda_2 \rangle = \begin{cases} \cos\theta/2 & (+\,+) = (-\,-) \\ -\sin\theta/2 & (+\,-) \\ \sin\theta/2 & (-\,+) \end{cases} \qquad \text{(B.20)}$$

Define $\bar{u}(\lambda_4)\, u(\lambda_2)\, \bar{u}(\lambda_3)\, \gamma_5\, u(\lambda_1) \equiv (\lambda_4\lambda_2\lambda_3\lambda_1)$ and

$\bar{u}(\lambda_4)\, u(\lambda_1)\, \bar{u}(\lambda_3)\, \gamma_5\, u(\lambda_2) \equiv ((\lambda_4\lambda_1\lambda_3\lambda_2))$.

Then, omitting a common factor of $\left\{ i \left(\frac{E_1 + M}{2M}\right) \sqrt{\frac{(E_4 + M^*)}{(2M^*)} \frac{(E_1 + M)}{(2M)}} \right\}$

$$(+\,+\,+\,+) = (+\,+\,-\,-) = -\,(-\,-\,+\,+) = -\,(-\,-\,-\,-)$$

$$= -\sin^2\theta/2 \; F_- G_- \qquad \text{(B.21a)}$$

$$(+\ -\ +\ +\ ) = (-\ +\ +\ +) = (+\ -\ -\ -) = (-\ +\ -\ -)$$

$$= -\ \sin\theta/2\ \cos\theta/2\ F_+G_- \qquad \text{(B.21b)}$$

$$(+\ +\ +\ -\ ) = (-\ -\ -\ +) = -\ (+\ +\ -\ +) = -\ (-\ -\ +\ -)$$

$$= -\ \sin\theta/2\ \cos\theta/2\ F_-G_+ \qquad \text{(B.21c)}$$

$$(+\ -\ +\ -) = (-\ +\ +\ -) = -\ (+\ -\ -\ +) = -\ (-\ +\ -\ +)$$

$$= -\ \cos^2\theta/2\ F_+G_+ \qquad \text{(B.21d)}$$

$$((+\ +\ +\ +)) = ((-\ -\ +\ +)) = -\ ((+\ +\ -\ -)) = -\ ((\ -\ -\ -\ -))$$

$$= \cos^2\theta/2\ F_-G_- \qquad \text{(B.22a)}$$

$$((+\ -\ +\ +)) = ((-\ +\ -\ -)) = -\ ((+\ -\ -\ -)) = -\ ((\ -\ +\ +\ +))$$

$$= \sin\theta/2\ \cos\theta/2\ F_+G_- \qquad \text{(B.22b)}$$

$$((+\ +\ +\ -)) = ((+\ +\ -\ +)) = ((\ -\ -\ +\ -)) = ((\ -\ -\ -\ +))$$

$$= \sin\theta/2\ \cos\theta/2\ F_-G_+ \qquad \text{(B.22c)}$$

$$((+\ -\ +\ -)) = ((+\ -\ -\ +)) = -\ ((\ -\ +\ +\ -)) = -((-\ +\ -\ +))$$

$$= \sin^2\theta/2\ F_+G_+ \qquad \text{(B.22d)}$$

where

$$F_\pm \equiv \left[1 \pm \frac{pp'}{(E_1 + M)(E_4 + M^*)}\right] \qquad \text{(B.23)}$$

$$G_\pm \equiv \left[\frac{p}{E_1 + M} \pm \frac{p'}{E_3 + M}\right]. \qquad \text{(B.24)}$$

Some of the relations used in making the partial wave expansions (both for $NN \to NN^*$ and $NN^* \to NN^*$) are:

a) The well-known recursion relations and symmetry properties of the d functions (See reference 29).

b) Using

$$\frac{1}{2}\int_{-1}^{1} x^n P_J d_x = \begin{cases} 0 \text{ for } n < J \text{ or } n - J \text{ odd} \\ \dfrac{(2\mu + 2;1;J - 1)}{(2\mu + 3;2;J)} \text{ for } n - J = 2\mu \end{cases} \tag{B.25}$$

where $(a;b;c) = a(a + b)(a + 2b) \ldots (a + (c - 1)b)$, and

$$\frac{1}{2}\int_{-1}^{1} \frac{P_k(x)dx}{B - x} = Q_k(B) \tag{B.26}$$

we can show that

$$\frac{1}{2}\int_{-1}^{1} \frac{x\, P_k(x)dx}{B - x} = B\, Q_k(B) - \delta_{k0} \tag{B.27a}$$

$$\frac{1}{2}\int_{-1}^{1} \frac{x^2 P_k(x)dx}{B - x} = B^2 Q_k(B) - B\delta_{k0} - \frac{1}{3}\delta_{k1} \tag{B.27b}$$

$$\frac{1}{2}\int_{-1}^{1} \frac{x^3 P_k(x)dx}{B - x} = B^3 Q_k(B) - (B^2 + \frac{1}{3})\delta_{k0} - \frac{1}{3} B\delta_{k1} - \frac{2}{5}\delta_{k2}. \tag{B.27c}$$

c) $$Q_k(-B) = (-1)^{k-1} Q_k(B) \tag{B.28}$$

$$(\ell + 1)Q^{(B)}_{\ell+1} - B(2\ell + 1)Q_\ell(B) + \ell Q_{\ell-1}(B) = 0 \text{ for } \ell > 0. \tag{B.29}$$

The resultant $NN^* \to NN^*$ partial wave amplitudes of definite parity (calculated according to the procedure outlined in Section II) will now be listed.

Define

$$T^{JP}_{i,k\pm} = T_i{}^J \pm T_k{}^J \tag{B.30}$$

(where $T_i{}^J$ is defined in Section I)

$$A = \frac{M^{*2} + M^2 - \mu^2 - 2E_1E_2}{2q^2}$$

$$R_\pm = \left[1 \pm \frac{q^2}{(E_1 + M)(E_2 + M^*)}\right] \tag{B.31}$$

$$V_0 = \frac{1}{2\pi}\left(\frac{G}{M}\right)^2 \frac{q(E_1 + M)(E_2 + M^*)}{W} \begin{pmatrix} 1 \\ -\frac{1}{3} \end{pmatrix} \begin{matrix} I = 2 \\ I = 1 \end{matrix}$$

Then for $J \geq 3$ we have

1) $P = +(-1)^{J-2}$

$$T_{9,14+} = -\frac{1}{6} V_0 Q_J^{(A)} \left\{ \left[(R_-^2 - R_+^2) - A(R_+^2 + R_-^2)\right] \left[\left(\frac{E_1 + E_3A}{M^*}\right)^2 - \frac{1}{4}(1 - A^2)\right] + 2R_+R_-(1 - A^2)\left(\frac{E_1 + E_3A}{M^*}\right)\right\} \tag{B.32a}$$

$$T_{2,7+} = \frac{V_0}{4\sqrt{3}} \sqrt{\frac{J}{J+1}} \left[Q_{J-1}^{(A)} - A Q_J^{(A)}\right] \left\{ -R_+R_-(1 - A^2) + \left(\frac{E_1 + E_3A}{M^*}\right)\left[(R_+^2 - R_-^2) + A(R_+^2 + R_-^2)\right]\right\} \tag{B.32b}$$

$$T_{10,13+} = -\frac{V_0}{6}\sqrt{\frac{J}{J+1}}\,(AQ_J^{(A)} - Q_{J-1}^{(A)})\left\{2R_+R_-\left[\left(\frac{E_1 + E_3A}{M^*}\right)^2 - \frac{1}{4}(1 - A^2)\right]\right.$$

$$\left. + \frac{(E_1 + E_3A)}{M^*}\left[A(R_+^2 + R_-^2) + (R_+^2 - R_-^2)\right]\right\} \qquad \text{(B.32c)}$$

$$T_{11,12+} = -\frac{V_0}{4\sqrt{3}}\sqrt{\frac{J}{(J-1)(J+1)(J+2)}}\left[2AQ_{J-1}^{(A)} - (A^2 - A^2J + J + 1)Q_J^{(A)}\right]\cdot$$

$$\cdot\left\{-2R_+R_-\left(\frac{E_1 + E_3A}{M^*}\right) - \frac{1}{2}(R_+^2 - R_-^2) - \frac{A}{2}(R_+^2 + R_-^2)\right\} \qquad \text{(B.32d)}$$

$$T_{1,8+} = \frac{1}{8}\frac{V_0}{J+1}\left\{Q_J^{(A)}\left[-(J)(1 - A^2)(R_+^2 - R_-^2) - J(1 - A^2)A(R_+^2 + R_-^2)\right.\right.$$

$$\left. - (1 + A^2)(R_+^2 - R_-^2) - 2A(R_+^2 + R_-^2)\right]$$

$$\left. + Q_{J-1}\left[(R_+^2 + R_-^2)(1 + A^2) + 2A(R_+^2 - R_-^2)\right]\right\} \qquad \text{(B.32e)}$$

$$T_{3,6+} = -\frac{V_0}{4\sqrt{3}(J+1)}\left\{Q_J^{(A)}\left[2R_+R_-\left(\frac{E_1 + E_3A}{M^*}\right)J(1 - A^2) + 2R_+R_-\frac{(E_1 + E_3A)}{M^*}\right.\right.$$

$$\left. + \frac{1}{2}(1 - A^2)(AJ)(R_+^2 + R_-^2) + \frac{1}{2}(1 - A^2)(1 + J)(R_+^2 - R_-^2)\right]$$

$$\left. + Q_{J-1}^{(A)}\left[-2A\,R_+R_-\frac{(E_1 + E_3A)}{M^*} + \frac{1}{2}(1 - A^2)(R_+^2 + R_-^2)\right]\right\} \qquad \text{(B.32f)}$$

$$T_{4,5+} = \frac{V_0}{4}\frac{R_+R_-}{(J+1)\sqrt{(J-1)(J+2)}}\left\{Q_{J-1}^{(A)}\left[(2 - J^2 - J) + A^2(J^2 + J + 2)\right]\right.$$

$$\left. + Q_J^{(A)}\left[-A^3J(J - 1) + A(J^2 - J - 4)\right]\right\} \qquad \text{(B.32g)}$$

$$T_{15,18+} = \frac{V_0}{6(J+1)} \left\{ Q_J^{(A)} \left[-2 R_+ R_- \left(\frac{E_1 + E_3 A}{M^*} \right) J(1 - A^2) \right.\right.$$

$$+ \left(\frac{E_1 + E_3 A}{M^*} \right)^2 \left(AJ(R_+^2 + R_-^2) + (J+1)(R_+^2 - R_-^2) \right) - 2R_+R_- \left(\frac{E_1 + E_3 A}{M^*} \right)$$

$$+ \frac{1}{4} J A (1 + A^2) (R_+^2 + R_-^2) + \frac{A^2}{2} J (R_+^2 - R_-^2)$$

$$\left. + \frac{1}{4} (J+1) (1 + A^2) (R_-^2 - R_+^2) - \frac{A}{2} (J+1) (R_+^2 + R_-^2) \right]$$

$$+ Q_{J-1}^{(A)} \left[2A R_+ R_- \frac{\left(E_1 + E_3 A \right)}{M^*} + \left(\frac{E_1 + E_3 A}{M^*} \right)^2 (R_+^2 + R_-^2) \right.$$

$$\left.\left. + \frac{1}{4} (1 + A^2) (R_+^2 + R_-^2) + \frac{A}{2} (R_+^2 - R_-^2) \right] \right\} \qquad \text{(B.32h)}$$

$$T_{16,17+} = - \frac{V_0}{4\sqrt{3}\ (J+1)\sqrt{(J-1)(J+2)}} \left\{ Q_{J-1}^{(A)} \left[R_+ R_- \left(J(J+1)(1 - A^2) - 2(1+A^2) \right) \right.\right.$$

$$\left. + \left(\frac{E_1 + E_3 A}{M^*} \right) \left((R_+^2 - R_-^2)(2 - J^2 - J) - A(R_+^2 + R_-^2)(J^2 + J + 2) \right) \right]$$

$$+ Q_J \left[R_+ R_- \left(A^3 J(J-1) + A(4 - J^2 - J) \right) \right.$$

$$\left. \left. + \left(\frac{E_1 + E_3 A}{M^*} \right) \left((R_+^2 - R_-^2) A(J+2)(J-1) + (R_+^2 + R_-^2) \cdot \right.\right.\right.$$

$$\left.\left.\left. \cdot \left(A^2 J(J-1) + 2(J+1) \right) \right) \right] \right\} \qquad \text{(B.32i)}$$

$$T_{19,20+} = \frac{V_0}{8(J-1)(J+1)(J+2)} \left\{ 4 Q_{J-1}^{(A)} \left[(R_+^2 + R_-^2) \left(A^2 (J^2 + J + 1) \right.\right.\right.$$

$$\left.\left.\left. - (J-1)(J+2) \right) \right.\right.$$

$$- 3A\ (R_+^2 - R_-^2)\Big] + Q_J^{(A)}\Big[(R_+^2 + R_-^2)\ \Big(A^3 J(J-1)^2 + A(-J^3+2J^2-J-12)\Big)$$

$$- (R_+^2 - R_-^2)\ \Big(-A^2(J-1)^2(J+4) + (J^2+J-8)(J+1)\Big)\Big]\Big\}$$

(B.32j)

2. $P = -(-1)^{J-2}$

$$T_{9,14-} = -\frac{1}{6} V_0\ Q_J^{(A)} \left\{(R_+^2 + R_-^2) + A(R_+^2 - R_-^2)\right\}\left\{\left(\frac{E_1 + E_3 A}{M^*}\right)^2 + \left(\frac{1 - A^2}{4}\right)\right\}$$

(B.33a)

$$T_{2,7-} = -\frac{V_0}{4\sqrt{3}} \sqrt{\frac{J}{J+1}} \left(\frac{E_1 + E_3 A}{M^*}\right) \left\{(R_+^2 + R_-^2) + A(R_+^2 - R_-^2)\right\}$$

$$\left\{Q_{J-1}^{(A)} - A Q_J^{(A)}\right\} \qquad \text{(B.33b)}$$

$$T_{10,13-} = 0 \qquad \text{(B.33c)}$$

$$T_{11,12-} = +\frac{1}{8\sqrt{3}}\ V_0 \sqrt{\frac{J}{(J-1)(J+1)(J+2)}}\ \left\{(R_+^2 + R_-^2) + A(R_+^2 - R_-^2)\right\} \cdot$$

$$\cdot \left\{2A Q_{J-1}^{(A)} - (A^2 - A^2 J + J + 1) Q_J^{(A)}\right\} \qquad \text{(B.33d)}$$

$$T_{1,8-} = \frac{1}{8} V_0 \left(\frac{1}{J+1}\right) \Big\{ - \Big[Q_{J-1}^{(A)} + A\ J\ Q_J^{(A)}\Big]\Big[(1 + A^2)(R_+^2 - R_-^2)$$

$$+ 2A(R_+^2 + R_-^2)\Big]$$

$$+ (J+1) Q_J^{(A)}\Big[(1 + A^2)(R_+^2 + R_-^2) + 2A(R_+^2 - R_-^2)\Big]\Big\} \qquad \text{(B.33e)}$$

$$T_{3,6-} = + \frac{V_0}{4\sqrt{3}(J+1)} \left\{ + (Q_{J-1}^{(A)} + AJQ_J^{(A)}) \left[2R_+R_- \left(\frac{E_1 + E_3A}{M^*} \right) + \frac{1}{2}(1 - A^2) \cdot \right. \right.$$

$$\left. \cdot (R_+^2 - R_-^2) \right]$$

$$\left. - (J + 1) Q_J^{(A)} \left[2AR_+R_- \frac{(E_1 + E_3A)}{M^*} - \frac{1}{2}(1 - A^2)(R_+^2 + R_-^2) \right] \right\} \qquad \text{(B.33f)}$$

$$T_{4,5-} = - \frac{V_0}{2} \frac{R_+R_-}{(J+1)\sqrt{(J-1)(J+2)}} \left\{ -2AQ_{J-1}^{(A)} + Q_J^{(A)} \left[(J + 1) - A^2(J - 1) \right] \right\} \qquad \text{(B.33g)}$$

$$T_{15,18-} = \frac{1}{6} V_0 \frac{1}{(J + 1)} \left\{ (AJQ_J^{(A)} + Q_{J-1}^{(A)}) \left[-2R_+R_- \frac{(E_1 + E_3A)}{M^*} \right. \right.$$

$$+ (R_+^2 - R_-^2) \left(\frac{E_1 + E_3A}{M^*} \right)^2 + \frac{1}{4}(1 + A^2)(R_-^2 - R_+^2) - \frac{A}{2}(R_+^2 + R_-^2) \Big]$$

$$+ (J + 1) Q_J^{(A)} \left[2A R_+R_- \frac{(E_1 + E_3A)}{M^*} + (R_+^2 + R_-^2) \left(\frac{E_1 + E_3A}{M^*} \right)^2 \right.$$

$$\left. \left. + \frac{1}{4}(1 + A^2)(R_+^2 + R_-^2) + \frac{A}{2}(R_+^2 - R_-^2) \right] \right\} \qquad \text{(B.33h)}$$

$$T_{16,17-} = - \frac{V_0}{4\sqrt{3}(J+1)\sqrt{(J-1)(J+2)}} \left\{ Q_{J-1}^{(A)} \left[4AR_+R_- + \left(\frac{E_1 + E_3A}{M^*} \right) \cdot \right. \right.$$

$$\cdot (R_+^2 + R_-^2)(2 - J^2 - J) - (R_+^2 - R_-^2)A(J^2 + J + 2) \left(\frac{E_1 + E_3A}{M^*} \right) \Big]$$

$$+ Q_J^{(A)} \Big[- 2R_+R_- J(1 - A^2) - 2R_+R_- (1 + A^2)$$

$$+ \frac{(E_1 + E_3A)}{M^*} (R_+^2 + R_-^2) A(J + 2)(J - 1) + \frac{(E_1 + E_3A)}{M^*} (R_+^2 - R_-^2) \cdot$$

$$\left. \left. \left(A^2 J(J - 1) + 2(J + 1) \right) \right] \right\} \qquad \text{(B.33i)}$$

$$T_{19,20-} = -\frac{V_0}{8(J-1)(J+1)(J+2)}\left\{4Q_{J-1}^{(A)}\left[3A(R_+^2+R_-^2)\right.\right.$$

$$+ (R_+^2 - R_-^2)\left((J-1)(J+2) - A^2(J^2+J+1)\right)\Big]$$

$$+ Q_J^{(A)}\Big[(R_+^2+R_-^2)\left(A^2(J-1)^2(J+4) + (J^2+J-8)(J+1)\right)$$

$$\left.\left. + (R_+^2 - R_-^2)\left(A(J^3 - 2J^2 + J + 12) - A^3J(J-1)^2\right)\right]\right\}. \qquad \text{(B.33j)}$$

Using the obvious relation that $d^J_{\lambda\mu}(\theta) = 0$ for $J < |\max(\lambda,\mu)|$ one can determine that for $J = 0$ only $T_9{}^J$ and $T_{14}{}^J$ are non-zero, ($T^{JP}_{9,14\pm} \neq 0$) and for $J = 1$: $T_4{}^J$, $T_5{}^J$, $T_{11}{}^J$, $T_{12}{}^J$, $T_{16}{}^J$, $T_{17}{}^J$, $T_{19}{}^J$, $T_{20}{}^J$ are all zero

$$(T^{J=1}_{4,5\pm} = T^{J=1}_{11,12\pm} = T^{J=1}_{16,17\pm} = T^{J=1}_{19,20\pm} = 0) \quad .$$

When $J \geq 2$ all twenty amplitudes are present (except $T^{JP}_{10,13-}$ which vanishes for all J).

Appendix C. THE COMPLEX SINGULARITIES

In this section we add a few details to our discussion in Section IV (see also Section VI) of how the ND^{-1} equations are modified due to the presence of a complex singularity intersecting the unitarity cut. As stated before, the question is an involved and difficult one and our remarks are not to be taken as either complete or absolutely rigorous. In addition, we shall only discuss the modifications appropriate to our determinental method calculation and not those required in the full ND^{-1} equations.

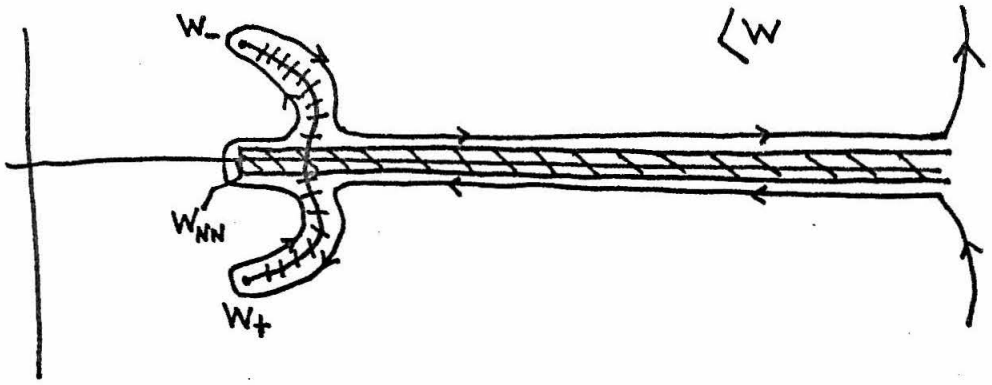

The Deformed Contour of Integration around the Unitarity Cut Beginning at the Elastic NN Threshold

Fig. 21

In Fig. 21 we have symbolically indicated how the integration contour around the unitarity cut beginning at W_{NN} must be deformed to avoid the protruding singularities of the $NN \to NN^*$ Born amplitudes. (Naturally, a symmetrical situation exists in the left hand W plane but we are omitting integrals over the left-hand unitarity cut.)

Note that for integrals beginning at the $N\bar{N}^*$ threshold (viz., D^R_{J1}) no modifications are required since they begin to the right of the complex cut.

Let us denote the contribution of the contour (call it C) around the anomalous cuts by ΔD_{ij}.

Furthermore define

$$\frac{1}{2i} (\text{disc } B_{ij}(W)) = \text{Abs. } B_{ij}(W) \equiv \alpha_{ij}(W) \tag{C.1}$$

and choose the branch cuts of $\alpha(W)$ and $\rho_2(W)$ such that

$$\rho_2(W^*) = -\rho_2^*(W) \tag{C.2}$$

$$\alpha(W^*) = -\alpha^*(W). \tag{C.3}$$

Using some of the results of references 1 and 2, we find the lowest order modification in the determinental approximation to be

$$\Delta D_{1J}^{(W)} = -\frac{i}{\pi} \int_C \frac{\rho_2(W')\ \alpha_{1J}(W')\ dW'}{W' - W} \tag{C.4}$$

where we have omitted the subtraction for brevity. Expanding (C.4) and using Eqs. (C.2) and (C.3) we can write

$$\begin{aligned}
\Delta D_{1J}(W) &= -\frac{i}{\pi} \left\{ \int_{W_-}^{W_R} \frac{\rho_2\ \alpha_{1J} dW'}{W' - W} - \int_{W_+}^{W_R} \frac{\rho_2\ \alpha_{1J} dW'}{W' - W} \right\} \\
&= -\frac{i}{\pi} \left\{ \int_{W_-}^{W_R} \left[\frac{\rho_2(W')\ \alpha_{1J}(W')}{W' - W} - \frac{\rho_2(W'^*)\ \alpha_{1J}(W'^*)}{W'^* - W} \right] dW' \right\} \\
&= -\frac{2}{\pi} \int_{W_R} \text{Im} \left(\frac{\rho_2\ \alpha_{1J}}{W' - W} \right) dW'
\end{aligned} \tag{C.5}$$

where W_R is the point where the anomalous cut crosses the Real W axis (W_R = 2.033 BeV). We note that ΔD_{1J} only contributes to D^R_{1J}.

Evaluating Eq. (C.5) for the four inelastic amplitudes would be a formidable undertaking. Instead we shall merely make a few observations and a crude guess at the order of magnitude of ΔD_{1J} for one value of J.

Using the relation

$$\text{Abs } Q_\ell(z) = \pi/2 \; P_\ell(z) \tag{C.6}$$

we find for the inelastic amplitudes

$$\alpha_{13} \propto P_2 = \frac{1}{2}(3z^2 - 1) \tag{C.7a}$$

$$\alpha_{14} \propto (P_3 - P_1) = 5/2 \; z(z^2 - 1) \tag{C.7b}$$

$$\alpha_{15} \propto (P_3 - P_1) \sim z(z^2 - 1) \tag{C.7c}$$

$$\alpha_{16} \propto (z^2 - 1)^2 \; . \tag{C.7d}$$

Recall that the anomalous contour is the locus of points for which $-1 \leq z \leq 1$ with $z^2 = 1$ corresponding to the end points $W_\pm$ and $z = 0$ the point $W = W_R$. Then we see that α_{14} and $\alpha_{15} = 0$ at the end points of the integrals for ΔD_{14} and ΔD_{15}.

Let us now look at ΔD_{16} in slightly more detail (only because α_{16} has a relatively simple form).

$$\alpha_{16} = \frac{\pi}{2} \; \frac{a\sqrt{3}\,\alpha_2}{\sqrt{\rho_2\rho_3}\; p'} \left(\frac{P_4}{35} - \frac{2P_2}{21} + \frac{P_0}{15}\right) \tag{C.8}$$

where ρ_3 here refers to the stable ($\Gamma_{NN^*} = 0$)NN^* phase space factor. ($\rho_3 = p'/W$).

After a good deal of algebra we can write

$$\rho_2 \alpha_{16} = - \frac{2\sqrt{2}}{(16)^2} g \frac{G}{M} (z^2 - 1)^2 \cdot \cdot \frac{(W - 2M)^2}{W} \frac{(M + M^*)}{\sqrt{W^2 - (M + M^*)^2}} . \qquad (C.9)$$

We then can observe that the integrand of ΔD_{16}, $\mathrm{Im}\left[\frac{\rho_2 \alpha_{16}}{W' - W}\right]$, takes on its maximum value at or near $W' = W_R$. This is plausible because a) the factor $(z^2 - 1)^2$ has its maximum at $z = 0$ ($W' = W_R$) and falls off quickly for larger z; (b) $(W' - W)$ increases as we move up along the anomalous contour away from the real axis and, (c) at $W' = W_R$ $[\rho_2 \alpha_{16}/(W' - W)]$ is pure imaginary.

Taking $W \cong 2.15$ as a typical (interesting) value of the energy we evaluate the integrand at $W' = W_R = 2.033$. We find

$$\mathrm{Im}\,[\rho_2 \alpha_{16}/(W' - W)]_{\substack{W' = W_R \\ W = 2.15}} \approx .3 . \qquad (C.10)$$

To make a very crude estimate for ΔD_{16}, replace the integral with one whose integrand = .3 at W_R and goes linearly to 0 at $|W_-|$ (Since $\alpha_{16} = 0$ at $z = 1$). Then we would have

$$\Delta D_{16} \sim - \frac{2}{\pi} \cdot 1 \cdot \frac{1}{2} (.3) \sim - .1 \qquad (C.11)$$

(Unfortunately) this value is comparable in magnitude to that for D_{16}^R at the same energy.

The work in this section must be regarded as inconclusive. But certainly it does not seem obvious as some authors have concluded (Leung[26], Meiere[7]) that the anomalous contour contributions to the integrals are negligible. What is needed is a much more satisfactory treatment of the three-particle nature of the NN^* state and a more accurate evaluation of the integrals over such complex singularities when they are present*).

---

* Such integrals have been included in the work of Ball and Thurnauer, Ref. 3.

REFERENCES

1. L.F. Cook and B.W. Lee, Phys. Rev. 127, 283 and 297 (1962).

2. J.S. Ball, W.R. Frazer and M. Nauenberg, Phys. Rev. 128, 478 (1962).

3. J.S. Ball and P. Thurnauer, Phys. Rev. 136, B529 (1964).

4. J.S. Ball and W.R. Frazer, Phys. Rev. Letters 7, 204 (1961).

5. P.G. Federbush, M. Grisaru and M. Tausner, Ann. Phys.(N.Y.) 18, 23 (1962).

6. S. Mandelstam, J.E. Paton, R.F. Peierls, and A.Q. Sarker, Ann. Phys. (N.Y.) 18, 198 (1962).

7. F.T. Meiere, Phys. Rev. 136, B1196 (1964).

8. K. Meetz, Phys. Rev. 125, 714 (1962).

9. For more discussion of these mechanisms see references 1 and 2 and also,
S. Barshay, Ann. Phys. (N.Y.) 21, 383 (1963);
Y. Fujii, Progr. Theoret. Phys. (Kyoto) 29, 71 (1963; and
Y. Fujii and M. Uehara, Progr. Theoret. Phys. (Kyoto) Suppl. 21, 138 (1962).

10. Ordinary cusps are discussed by E. Wigner, Phys. Rev. 73, 1002 (1948); and
R. Newton, Ann. Phys. (N.Y.) 4, 29 (1958).

11. Wooly cusps are discussed in M. Nauenberg and A. Pais, Phys. Rev. 126, 360 (1962); and
A. Baz', Soviet Physics JETP 13, 1058 (1961).

12. W.R. Frazer and A.W. Hendry, Phys. Rev. 134, B 1307 (1964).

13. R.H. Dalitz, Phys. Rev. Letters 6, 239 (1961).

14. J.J. Sakurai, Phys. Rev. Letters 7, 355 (1961).

15. R.M. Sternheimer and S.J. Lindenbaum, Phys. Rev. 123, 333 (1961).

16. R.F. Peierls, Phys. Rev. Letters 6, 641 (1961).
Also see the discussion by T. Fulton in Elementary Particle Physics and Field Theory-1962 Brandeis Lectures Vol. 1 (W.A. Benjamin, Inc., New York, 1963), pp. 75-78.

17. R. Wilson, The Nucleon-Nucleon Interaction (Interscience, New York, 1963).

18. For an example, see H.P. Stapp, T.J. Ypsilantis, and N. Metropolis, Phys. Rev. 105, 302 (1957).

19. For a more complete discussion of the nucleon-nucleon problem see the review articles by L. Wolfenstein, Ann. Rev. Nucl. Sci. Vol. 6, 43 (1956); and
M.H. MacGregor, M.J. Moravcsik, and H.P. Stapp, Ann. Rev. Nucl. Sci. Vol. 10, 291 (1960); and also reference 17.

20. L.S. Azhgirei, N.P. Klepikov, Y.P. Kumekin, M.G. Meshcheryakov, S.B. Nurushev, and G.D. Stoletov, Soviet Physics JETP 18, 810 (1964) and 19, 728 (1964). Also see
L.S. Azhgirei, Soviet Physics JETP 18, 1365 (1964).

21. Reported by L. Lapidus at the 1962 International Conference on High-Energy Physics at CERN, pp. 726-736.

22. R. Zul'karneev and I. Silin, Soviet Physics JETP 17, 745 (1963).

23. B.M. Golovin, V.P. Dzhelepov, R.Y. Zul'karneev and Tsui, Soviet Physics JETP 17, 98 (1963).

24. A. Scotti and D.Y. Wong, Phys. Rev. 138, B 145 (1965); and Phys. Rev. Letters 10, 142 (1963).

25. See Reference 1, p. 309.

26. Y. Leung, Phys. Rev. 135, B 732 (1964).

27. P.W. Coulter, A. Scotti and G.L. Shaw, Phys. Rev. 136, B 1399 (1964).

28. See, for example, M.L. Goldberger, M.T. Grisaru, S.W. MacDowell, and D.Y. Wong, Phys. Rev. 120, 2250 (1960).

29. M. Jacob and G.C. Wick, Ann. Phys. (N.Y.) 7, 404 (1959).

30. See Reference 29, Eq. (47).

31. Our conventions usually agree with those of S.S. Schweber, An Introduction to Relativistic Quantum Field Theory (Row, Peterson and Company. Evanston, 1961).

32. This is nicely summarized in E. Marx-Oberländer, California Institute of Technology, thesis (unpublished), Appendix F, who gives other references. Also see Reference 5.

33. L. Durand and Y.T. Chiu, Phys. Rev. Letters 12, 399 (1964); 13, 45 (1964); Phys. Rev. 137, B 1530 (1965); 139, B 646 (1965). J.S. Ball and W.R. Frazer, Phys. Rev. Letters 14, 746 (1965).

34. This is briefly discussed in E. Abers and C. Zemach, Phys. Rev. 131, 2305 (1963).

35. Y. Hara, Phys. Rev. 136, B507 (1964). I also wish to thank Dr. Hara for some correspondence on this matter.

36. S. Mandelstam, Phys. Rev. Letters 4, 84 (1960).

37. A nice summary of the ND^{-1} method is given in B. Kayser, Phys. Rev. 138, B1244 (1965). Also see F. Zachariasen and C. Zemach, Phys. Rev. 128, 849 (1962); J.D. Bjorken and M. Nauenberg, Phys. Rev. 121, 1250 (1961).

38. R. Blankenbecler, Phys. Rev. 122, 983 (1961).

39. For a good discussion in a specific case see S.C. Frautschi and J.D. Walecka, Phys. Rev. 120, 1486 (1960). Compare with references 34 and 37. Also see A.W. Martin and J. Uretsky, Phys. Rev. 135, B803 (1964).

40. See L.D. Landau and E.M. Lifshitz, Quantum Mechanics (Pergammon Press Ltd., London, 1958), p. 405.

41. See Zachariasen and Zemach, reference 37.

42. Also see References 2, 3, 11, and 12.

43. See, for example, the calculations in References 7 and 34.

44. G.N. Fleming, Phys. Rev. 135, B551 (1964).

45. I wish to thank Dr. R. Gerbracht for suggesting this.

46. For example, see M. Bander, P.W. Coulter and G.L. Shaw, Phys. Rev. Letters 14, 270 (1965); J.B. Hartle and C.E. Jones, Phys. Rev. Letters 14, 801 (1965); and Phys. Rev. (to be published).

47. One interesting state might be $J = 2^-$ since the $\delta(^3P_2)$ NN phase shift seems to be about 20° at 657 MeV (see Reference 20).

48. M. Gell-Mann, California Institute of Technology Synchrotron Laboratory Report CTSL-20 (1961); Phys. Rev. 125, 1067 (1962).

49. Y. Ne'eman, Nuclear Phys. 26, 222 (1961).

50. J.J. de Swart, Rev. Mod. Phys. 35, 916 (1963).

51. I.S. Gerstein, Nuovo Cimento, 32, 1707 (1964).

52. This enhancement may also be visible in the reaction $\pi + d \rightarrow p + p$. See M.A. Abolins, D.D. Carmony, R.L. Lander, and Ng-H. Xuong, Phys. Rev. Letters 15, 125 (1965); B.S. Neganov and L.B. Parfenov, Soviet Physics JETP 7, 528 (1958); M.G. Meshcheriakov and B.S. Neganov, Dokl. Akad. Nauk SSSR 100, 677 (1955).

53. P.A. Piroue, Physics Letters 11, 164 (1964).

54. H.O. Cohn, K.H. Bhatt, and W.M. Bugg, Phys. Rev. Letters 13, 668 (1964).

55. R.J. Oakes, Phys. Rev. 131, 2239 (1963).

56. F.J. Dyson and Ng.-H. Xuong, Phys. Rev. Letters 13, 815 (1964) and erratum Phys. Rev. Letters 14, 339 (1965.